A PEER REVIEWED AND REFEREED JOURNAL

Volume 13, Issue 2, 2022

ISSN : 0976-4534

DOI 10.53390

INTERNATIONAL JOURNAL ON ENVIRONMENTAL SCIENCES

Published by

NATIONAL ENVIRONMENTAL SCIENCE ACADEMY

206, Raj Tower -I , Alaknanda Comm. Centre, New Delhi - 110 019

Tel.: 011-2602 3614 • E-mail: nesapublications@gmail.com; nesapub@yahoo.co.in

Website : www.nesa-india.org

Volume 13, Issue 2, 2022

ISSN : 0976-4534
DOI 10.53390

JOURNAL INDEXED IN INDIAN CITATION INDEX

INTERNATIONAL JOURNAL ON ENVIRONMENTAL SCIENCES

Published by

NATIONAL ENVIRONMENTAL SCIENCE ACADEMY

206, Raj Tower -I , Alaknanda Comm. Centre, New Delhi - 110 019
Tel.: 011-2602 3614 • E-mail: nesapublications@gmail.com; nesapub@yahoo.co.in
Website : www.nesa-india.org

International Journal on Environmental Sciences

Volume - 13 | Issue : 2 | *July-December, 2022*

Editorial Board

National Advisory Board

International Advisory Board

International Journal on Environmental Sciences

Volume - 11 | Issue : 2 | *July-December, 2022*

CONTENTS

National Environmental
Science Academy
206 Raj Tower - I
Alaknanda Comm. Centre,
New Delhi - 110 019

Incharge Publication
Gian Chand
nesapublications@gmail.com
infonesa88@gmail.com

Incarge-Accounts
Rakesh Kumar Roy
nesapub@yahoo.co.in

Annual Subscription

Members	Rs. 2000.00
Individual	Rs. 2400.00
Institutional	Rs. 3600.00

Other Countries

Members	$ 50.00
Individual	$ 80.00
Institutional	$ 135.00

www.nesa-india.org • E-mail: nesapublications@gmail.com
International Journal on Environmental Sciences

International Journal on Environmental Sciences 13 (2) Pp.57-65, ***July-December 2022***
ISSN No.: 0976-4534
https://doi.org/10.53390/ijes.v13i2.1

MUNICIPAL SEWAGE MANAGEMENT IN URBAN CENTRES OF MAHARASHTRA; AN APPROACH FOR BETTERMENT OF URBAN DEVELOPMENT A REVIEW

Vijay R. Rakte and Sanjaykumar R. Thorat

School of Environmental and Earth Science
Kavayitri Bahinabai Chaudhari North Maharashtra University, Jalgaon, Maharashtra

Review Article

Received: **15.07.2022** Accepted: **27.07.2022** Published: **10.08.2022**

ABSTRACT

In the present study review has been quoted to know the total scenario of sanitary waste management in State of Maharashtra. This state is the second largest state in India both in terms of population and geographical area (11.23 Cr. and 3.08 lakh sq. km. respectively). The State is highly urbanized with 42 % people residing in urban areas. The state has 255 statutory towns and 279 census towns, it generates the maximum sewage throughout Maharashtra in India is around 13% with 8,143 MLD as against treatment of 5,160.36 MLD through sewage treatment plants (STPs) at least 3,000 million liters of sewage and industrial effluents flow into rivers, water bodies or percolate into the ground every day. (Management of Municipal Solid Waste and Sewage, CPCB, 2004.) As per the overviews on status of sewage management we understood that, such mismanagement of sewage can cause adverse environmental impacts, public health risk. Which will be useful guide for improved waste management services. The idea of this overview will be benefitted to the competent authorities, policy makers who are responsible for municipal sewage management to prepare more resourceful strategies to implement it in the state of Maharashtra.

Keywords: Sewage, Wastewater management, Sewage treatment plant and Maharashtra.

INTRODUCTION

Sewage is a type of wastewater that is produced by a community of people. Sewage is also known as domestic wastewater or municipal wastewater. It is characterized by chemical and toxic constituents, and its bacteriologic status. It consists mostly grey water i.e. water discharged from sinks, bathtubs, showers dishwasher and cloth washers etc. and also black water i.e. water used in toilets. Sewage may contain organic contents like particle of waste food from dish washer; toilet papers etc. as well as Inorganic chemicals which are mostly found in detergents and other domestic cleaners. Sewage encompasses micro and macro pollutants incorporate municipal solid waste and industrial solid waste. Proper collection and scientific disposal of the liquid waste is the necessity in an urbanized, industrialized society**.** Rapid Increase in Urbanization creates several challenges before government and municipal administration. Whereas one troublesome challenge before administration is to manage sewage waste generated by this massive population. Sewage generation could be a regularly growing drawback at international, regional and native level.

A remarkable increase in municipal solid waste generation was observed during the study especially in Maharashtra, India with rapid industrialization and urbanization since 1980. Thereafter effective solid waste management become a major social and environmental concern in the state of Maharashtra. As our review shows until 1990 the most serious problem was disposal of solid waste to uncontrolled dumping sites. That

*Corresponding author: *raktevijay777@gmail.com*

were not properly regulated. The study conducted shows only 31 ULBs have an underground sewerage network with varying degrees of household coverage and connections (Jonnalagadda V.R. Murty, 2011). About 15 ULBs have secondary STPs, and the average state wastewater treatment capacity is only 35 %. This implies that even in the best conditions, only about 35 % sewage is being treated and the remaining 65 % wastewater is into nature without any treatment (MPCB, 2020: Annual report 19-20).

In this study an attempt was made to provide a comprehensive document for the present scenario of waste management in Maharashtrian cities (i.e. Nagar panchayats, Municipal Council and Municipal Corporations). We have also noticed that the evolution, the status and identify the problems of sewage management among to 279 census towns only 16 highly polluted cities compare to 36 district in Maharashtra which is having 91 sewage treatment plant all over Maharashtra. It was also observed that many small, medium polluted cities are unable to treat their sewage and releasing national rivers, streams as well as open land. When we have gone through literature limited number of studies are available on sewage management because of difficulties in collection of representative samples from non-homogeneous landfill (Ramnath k. Sonawane and Sanjaykumar R. Thorat, 2010).

PRESENT SCENARIO OF MUNICIPAL SEWAGE GENERATION IN MAHARASHTRA

Present status of Sewage generation: The population of Maharashtra as per 2011 census is about 11.23 crores, which comprises 5.08 crore in Urban population. There are 383 urban local bodies (ULBs) in the state. This includes 27 Municipal Corporations, 226 Municipal Councils, 7 Cantonment Boards and 123 Nagar Pachayats /capita/ day sewage generation is around 80 to 100 liters. About 42% of the state's population 9.69 crores lives in urban areas. The waste water generated from Municipal Corporations is approximately 45, 62,680 (As per table no.1 and 2) (As per Annual report 19-20: MPCB, 2020). Most of the wastewater which is discharged into the streams and rivers without appropriate treatment affects on micro and macro biota. To know these issues use of low-cost biological treatment systems which has been studied by the many researcher in several years (Dutta, 2003)**.** About 14 ULBs have secondary STPs and the average state wastewater treatment capacity is only 35% (as per fig no.2) This implies that even in the best conditions, only about 35 % sewage is being treated and the remaining 65% sewage is disposed into nature without any treatment.

Table 1: Showing sewage generation in MLD and disposal at source in Maharashtra.

Sr No	Name of Municipal Corporation	Class	District	River / creek	Seawage Generation MLD	Sewage Treatment MLD	Percentage Treatment (%)	Disposal
1	Amravati	D	Amravati	Pedhi/Purna	95	44	46.31%	Pedhi/Purna
2	Akola	D	Akola	Morna \ puna	45	0	0.00%	Morna \ puna
3	Mumbai	A	Mumbai	Arabian sea	2727	1850	67.84%	Arabian sea
4	Navi Mumbai	A	Thane	Divale and Vashi creek	205	205	100.00%	Divale and Vashi creek
5	Nashik	B	Nashik	Godavari	300	270	90.00%	Godavari river
6	Malegaon	B	Malegaon	Mousam	15	0	0.00%	Released into Mousam river without treatment.
7	Ahmednagar	D	Ahmednagar	Pravara	60	0	0.00%	Pravara
8	Dhule	D	Dhule	Panjara	36	0	0.00%	Panjara
9	Jalgaon	D	Jalgaon	Girna	48	0	0.00%	Girna
10	Thane	C	Thane	Thane creek	336	152	45.23%	Thane creek
11	Mira-Bhayandar	C	Thane	Creek	108	56.5	52.31%	creek
12	Vasai-Virar City	C	Palghar	Creek	105	0	0.00%	creek

13	Nagpur	A	Nagpur	Nag	450	230	51.11%	Nag
14	Kolhapur	D	Kolhapur	Panchaganga	96	72	52.00%	Agriculture and others.
15	Kupwad Miraj Sangli	D	Sangli	Krishna	82.2	36.2	43.90%	Krishna river
16	Chandrapur	C	Chandrapur River	Irai and Jharapata	41	0	0.00%	Irai and Jharapata River
17	Bhiwandi	D	Thane	Kamavari creek	90	30	33.33%	Kamavari creek
18	KalyanDombivali	D	Thane	Ulhas Creek	216	48	22.22%	Ulhas Creek
19	Ulhasnagar	C	Thane	Salt water area near Ulhas river	64	0	0.00%	Waldhuni
20	Aurangabad	A	Aurangabad	Sukhna, Kham	107	107	100.00%	Sukhna, Kham
21	Nanded Waghala	D	Nanded	Godavari	48	48	100.00%	Godavari
22	Latur	D	Latur	Manjara	24	0	0.00%	Local nalla to Manjara river
23	Parbhani	D	Parbhani	Purna Godavari	10	0	0	Godavari river
24	Pune	B	Pune	Mula-Mutha	1222	567	46.39%	Mula-Mutha
25	Pimpri-Chinchwad	C	Pune	Mula, Pawana and indrayani	312	265	84.93%	Setup of Domestic sewage treatment system
26	Solapur	D	Solapur	Sina	100	100	100.00%	Sina
27	Panvel	D	Raigad	Panvel / Kamothe Creek	164	156	95.12%	Panvel / Kamothe Creek

(Central Pollution Control Board (CPCB), 2015: National inventory of sewage treatment plants).

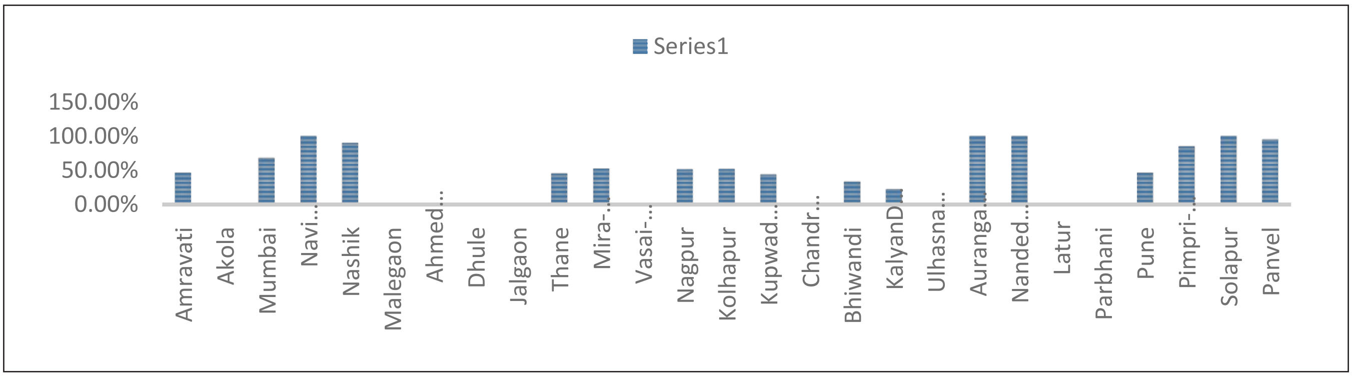

Fig 1: Showing percent treatment of sewage in Municipal Corporation.

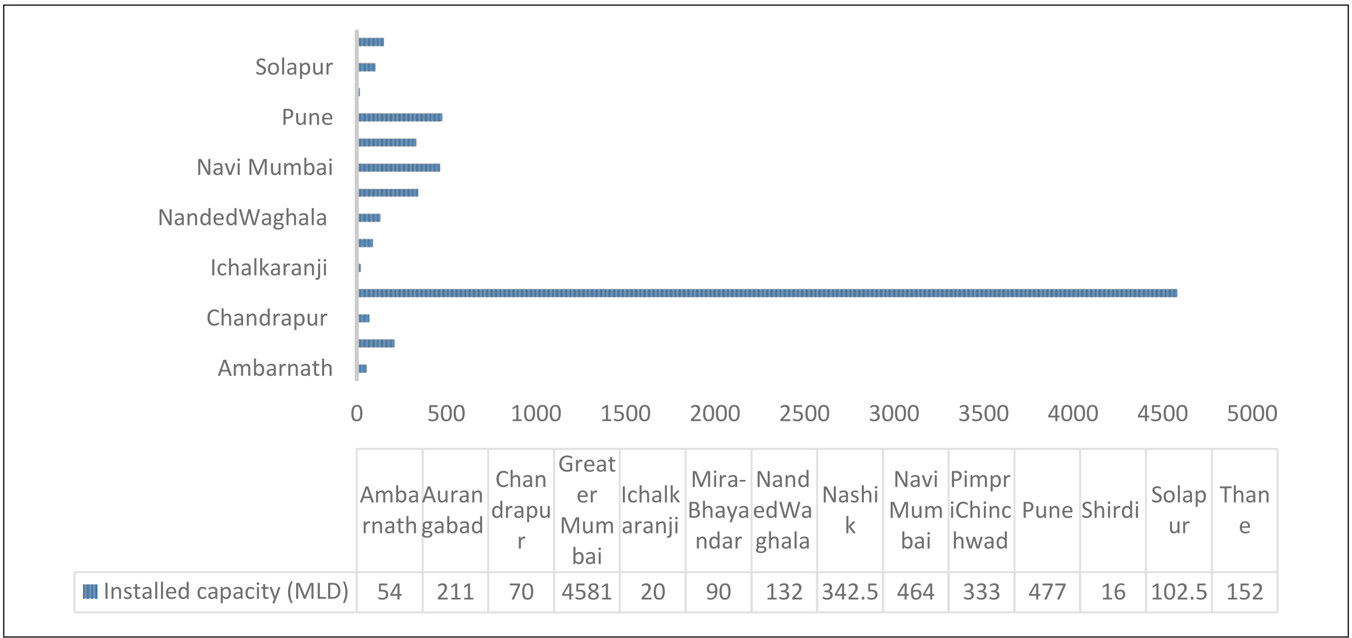

Fig 2: Showing installed capacity of STPs in state.

(Source: National Inventory of sewage Treatment Plant, 2021 CPCB)

Table 2: Region wise details of Effluent generation in Maharashtra state.

Sr. No	Region	No. of Councils	Total Population	Qty. of Water Consumption MLD	Qty. of Effluent Generated MLD
1	Aurangabad	52	2697002	157.85	130.02
2	Nagpur	30	1336096	346.01	215.79
3	Amravati	38	1588810	148.28	120.03
4	Thane	7	576169	51	37.6
5	Kalyan	2	306000	48	39
6	Raigad	10	310858	116.6	72.15
7	Kolhapur	22	545932	65.58	49.09
8	Nashik	38	2769737	285.074	192.7
9	Pune	31	1177306	158.86	123.89
10	Navi Mumbai	1	25000	3	2.1
	Total	**231**	**11332910**	**1380.254**	**982.37**

1.2 Sewage waste management practices in Maharashtra: The state is too much neglected and seriousness about treatment and management is not seen. The area in state has not received any attention because of poor understanding of sewage, lack of finance, inadequate resources and skills and lack of proper technical guidance. As per MPCB Annual report 2020 report. Only 32 cities have at least a partial conventional underground sewerage system out of 383 cities. Hence, state of Maharashtra mostly relies on on-site sanitation systems such as single pit and twin-pit or septic tank based toilets. As per Census 2011, in Maharashtra, around 70% of households have individual toilets of which 53 % are connected to sewer network, 40 % to septic tanks and around 7% to pits and other systems. The toilets that are

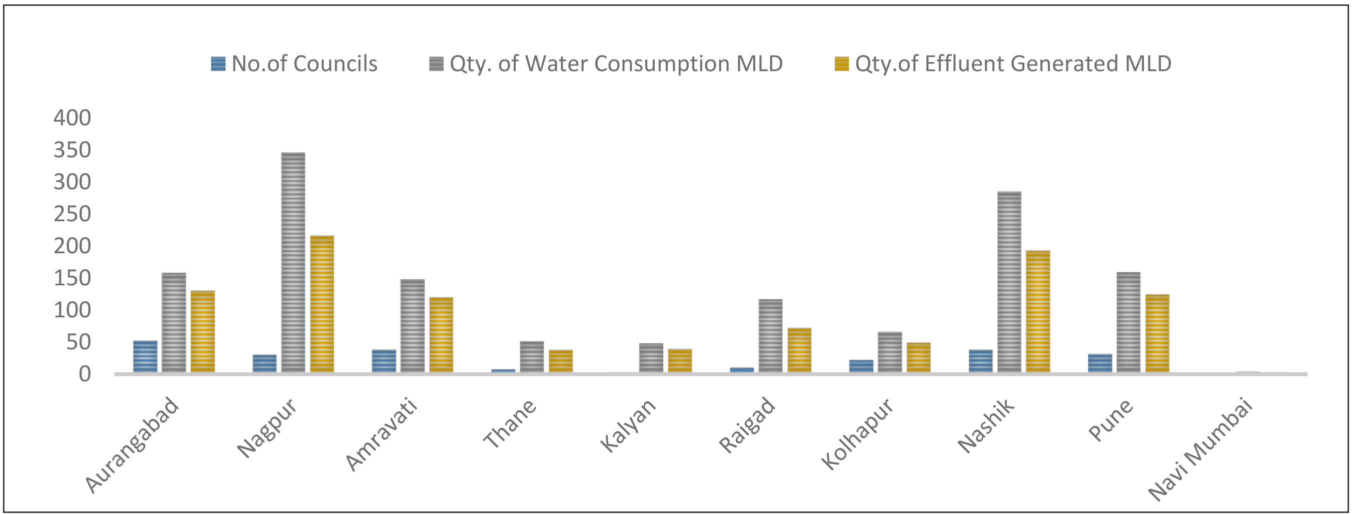

Fig 3: Showing graphical presentation of effluent generation in Maharashtra.

connected to septic tanks/ pits often discharge the effluent into road side open drains. As per Central Public Health & Environmental Engineering Organization (CPHEEO) norms septic tanks need to be cleaned periodically at an interval of 2-3 years. However according to survey conducted in a few cities of Maharashtra suggest that septic tanks/pits are emptied only once in 8 to 10 years and only when they overflow. The Prohibition of Employment as Manual Scavengers (and their rehabilitation) Act, 2013, prohibited manual cleaning/emptying of pit toilets and septic tanks is. Every ULB should adopt mechanical processes for cleaning of pits/septic tank. Most ULBs in Maharashtra provide mechanized cleaning. However, since the tanks are emptied only once in 8 to 10 years, the sludge that is solidified at the bottom of the pit/septic tank is hard to remove with the conventional emptier that is typically used. As a result, the pits/tanks are not emptied properly. Currently there is a lack of adequate infrastructure for adequate fecal sludge treatment in most Municipal councils. Even in cities that have sewerage network and functional sewage treatment plants, only 6 ULBs treat sewage at the STPs, On the whole, sludge treatment the situation in Maharashtra is quite bad. (Guidelines for septage management in Maharashtra: February 2016)

Sewage management Issues

Safe disposal of municipal wastewater is essential for the realization of the right to sanitation. However, it continues to pose a major challenge in Maharashtra where rudimentary disposal practices are common. In major cities sewage often causes problems when people flush chemical, pharmaceutical substances down the toilet and many more. These all substances combining cause complex and harmful sewage which directly mixed with potable water and also percolates into the ground.

CONFIGURATION OF SEWAGE FOR THE TREATMENT:

The configuration of sewage mainly depends upon /capita consumption of water and varies from place to place and season to season. The composition of sewage can be classified as follows

Configuration of Chemical Composition

Roughly, the sewage consists of approximately 99% water and 1% inorganic and organic matter in suspended and soluble forms. Lignocellulose, cellulose, proteins, fat and various inorganic particulate matters exist in suspended state, whereas sugars, fatty acids, alcohols, amino acids and inorganic ions constitute the soluble forms.

However, on an average, the sewage of cities in state contains about 350 ppm biodegradable organic matter, 52 ppm N2, 45 ppm potassium and 16 ppm phosphorus. Salts of heavy metals such as Zn, Cr, Ni, Pb, etc. are also present above the permissible limit of sewage. (https://en.wikipedia.org/wiki/Sewage)

Configuration microbial activity: The microbial population /milli.liter may ranges from few lacs to uncountable numbers. Various types of microorganisms, e.g., micro-fungi, bacteria and protozoa, collectively called 'sewage fungus', are known to grow profusely in sewage. In addition to that viruses and many micro-algal genera have also been recorded from sewage. Bacteria occurring in sewage are mainly fecal and soil inhabiting and their common types are coliforms, streptococci, Clostridia, micrococci, Proteus, Pseudomonas, and lactobacilli.

Sewage mainly classified into two types i.e. Domestic and Industrial sewage and all household liquid waste and excrete constitute domestic sewage, whereas liquid waste coming out from industries is constitute industrial sewage. Since, industrial consists some complex chemicals, may be highly alkaline such as soda wastes, some highly acidic such as acid-mine drainage, and others toxic because of presence of heavy metals and highly contaminated such as antibiotics, pesticides, etc., hence the treatment of industrial sewage is more complicated than domestic sewage as per our observation.

CHARACTERISTICS OF SEWAGE

Biochemical Oxygen Demand (BOD) and Chemical Oxygen Demand (COD) values are extremely high in sewage. The sewage organic matter undergoes anaerobic or partial decomposition resulting in the production of obnoxious gases, namely, CH_3, CO and H_2S due to anoxic condition. Besides being toxic, these gases react with water and produce acids. Production of acids in large quantity makes the sewage more acidic thus it is unfit for life. Concentration of heavy metals present in sewage is generally higher than permissible limits. All these characteristics of sewage, such as anoxic condition, high acidity, high heavy metal concentration, and reduced photosynthetic rate due to poor illumination cause death of oxygen-dependent organisms such as aerobic microorganisms, plants and animals in sewage.

DISPOSAL STRATEGIES OF SEWAGE

Sewage disposal is major part now days it creates unpleasant environment for living being. Untreated sewage is generally disposed of into water reservoirs without taking its pros and cons into account. It is so because we never take its hazardous nature in account the general thought is that the large amount water will accumulate the sewage in it. Self-cleaning property of nature will suffice for it. However, we cannot rely on this self-cleaning property as it is limited and can't prevent whole water being safe for human and other living orgasm hence it is necessary to adopt safe disposal method of sewage. Disposal of sewage in such wrong way, generally leads to following consequences: Frequent dissemination of water-borne disease causing microorganisms in large number. Depiction of dissolved oxygen in water leading to anoxic (oxygen-less) condition which may ultimately kill O_2 dependent aquatic life. Creation of offensive odour and debris-accumulation due to which value of property decreases.

METHODS FOR SEWAGE TREATMENT

Objectives behind the sewage treatment would be to reduce toxicity, to reduce anoxic nature of water, to kill pathogens and to utilize it for domestic purpose etc. When these objectives are achieved by the way of treating the sewage, the conditions prevailing in a natural water reservoir are induced in sewage water and the latter can be reused. Sewage treatment processes work on different technique and varied. We will discuss only those sewage treatment processes which are generally applied in municipal sewage treatment.

Municipal Treatment Processes: Municipal sewage treatment systems carry out different steps involved. These steps are, namely, primary (or physical) treatment, secondary (biological/ chemical) treatment, and tertiary treatment.

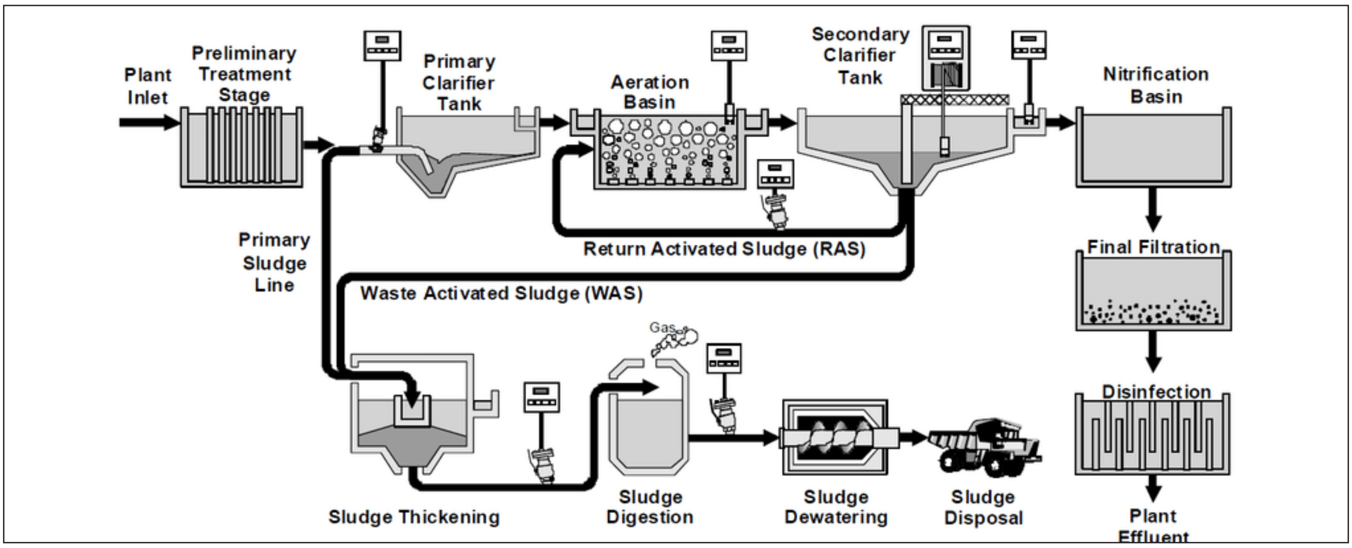

Fig. 4: Typical sewage treatment plant flow diagram.

(Diagram Source: A Review on Working, Treatment and Performance Evaluation of Sewage Treatment Plant-Scientific Figure on ResearchGate. Available from: https://www.researchgate.net/figure/Typical-sewage-treatment-plant-flow-diagram2_fig1_332440912 [accessed 9 Apr, 2022])

Primary (or Physical) Treatment:
When the sewage arrives from town at a sewage treatment plant, it is first subjected to primary (or physical) means, e.g. screening, dilution and sedimentation to remove its coarse solid materials. The sewage is passed through a series of filters or screens and then allowed to flow through sedimentation tanks. Coarse solid materials are concentrated in and collected from sedimentation tank; these particulate materials are collectively called 'sludge'.

Secondary (or Biological) Treatment:
This is a biological treatment of physically treated sewage and concerns microbial activity which biodegrades organic substrates and oxidizable inorganic compounds. This treatment accomplishes two important phases, namely, aerobic phase and anaerobic phase. The aerobic phase consists of aerobic digestion of sludge by various filters, oxidation ponds and activated sludge process. The anaerobic phase is represented by anaerobic digestion of sludge in the wastewater treatment.

Aerobic Phase of Secondary Treatment:
Aerobic Digestion in Trickling Filters: Trickling filter also known as oxidizing bed consists of generally 6-10 feet deep bed of crushed stone, gravel, slags etc. The sewage effluent received from primary treatment sprayed over the surface of the bed; the spraying saturates the effluent with oxygen. The bed surface is coated with aerobic microbial flora consisting of organic material degrading microalgae, micro-fungi, bacteria and protozoa. As the effluent percolates from oxidizing bed, the aerobic microbes degrade the organic matter. However, the treated effluent collected at the bottom of the tank is again passed through the sedimentation tank, like activated sludge process, the effluent follows tertiary treatment.

Oxidation Ponds or stabilization tank: Oxidation pond sewage-treatment is recommended for small towns where suitable and sufficient land is available. Oxidation ponds which is also called Lagoons or Stabilization Ponds are generally 2-6 feet deep shallow ponds designated to allow direct wind action and gas exchange for algal growth on the sewage effluent. Oxygen supplied from air fulfills biochemical oxygen demand (BOD) of sewage effluent and thus helps in maintaining aerobic condition in sewage effluent. In such condition the microbial growth accelerates and digests organic matter.

Activated Sludge Process: In this process, the physically treated sewage effluent is pumped into a sedimentation or settling tank wherein the sewage floes and settles out. A portion of sewage 'floe' is returned to activate a new batch of mechanically treated sewage effluent, and the rest is pumped to activate sludge digester where air is blown by artificial blowers or jets. Thus, in the presence of abundant oxygen, oxidation of sewage effluent is brought about by aerobic microorganisms which break down organic matter to CO2 and H2O. Further the effluent is passed through a sedimentation tank. Though about 90% of the organic matter of the effluent is digested via this process, the effluent still contains considerable amount of nitrate and phosphate, etc. It is, therefore, not safe to discharge effluent at this stage into a large water body both nitrate and phosphate can cause eutrophication. Now the effluent, which looks clear at this stage, is subjected to tertiary treatment for further purification.

II. Anaerobic Phase of biological Treatment (Anaerobic Digestion):
The sludge collected after primary (physical) treatment of sewage is subjected to anaerobic in absence of oxygen digestion in separate tank designed especially for the purpose. Since anaerobic condition prevails in this tank, the anaerobic microbes bring about digestion of organic matter by degrading them to soluble substances and gaseous products (methane, 60-70%; CO2, 20-30%; and smaller amounts of H2 and N2). This gas mixture can be used as a fuel for operating the sewage plant. Recently, few Municipal Corporation has started supplying this gas for cooking purposes.

Tertiary Treatment
Since the sewage-effluent treated during secondary treatment process still contains many non-biodegradable pollutants, microbial residues and mineral nutrients particularly nitrogen and phosphorus salts, it is subjected to tertiary treatment for their removal. If the effluent containing nitrogen and phosphorus salts is released in water body can cause serious eutrophication. Non-biodegradable pollutants are normally removed by using activated carbon filters whereas phosphorus and nitrogen salts by chemical treatment. Phosphorus salts are precipitated by liming and the nitrogen present mainly as ammonia is removed by volatilization at a high pH. These treatments result in a nutrient free effluent which does not cause eutrophication. The final step of tertiary treatment is disinfection which is commonly accomplished by chlorination using either sodium or calcium hypochlorite NaOCl or CaOCl2 respectively) or chlorine. Now the effluent is clean water and is considered microbiologically and chemically safe for living organisms. According to Kapoor (2009), an attitude can be defined as inclination towards some object. It is relatively permanent characteristic of human personality and is set by the essential value system, core beliefs, biological and psychological background, socialization process and environmental

experiences. Attitude is a major determinant of decision-making behavior. Many workers shave studied and design effluent treatment plant, sewage treatment plant and give their opinion and suggested for efficient working process. i.e. Joardar Souro, 2000; Zerbock Olar, 2003; Yin, 2003; Kumar and Gaikwad, 2004; Kumar Sunil, 2005; Sonawane and Thorat, 2010; Gauri Kallawar, et. al. 2018, and so on.

CONCLUSION

After reviewing all parameters our general observation is that very few cities have organized sewage treatment facility due to lack of financial and administrative capacity small and medium populated cities were always neglected in case of wastewater management. The major problem where STPs are installed sewage flow rate is much higher than the industrial effluent discharge. Steps are being made to check the sewage disposal problems. In the process, sewage treatment plants have been setup by the corporation. Data obtained from the corporations show that many STPs operate with inadequate sewage flow. It also noticed that some STPs operate with major treatment facilities, such as preliminary treatment, lagoon and oxidation ponds that are inadequate to meet the present regulatory requirement. Such STPs should be upgraded on the new technologies to meet the present regulatory requirements. ETPs operating with the new technologies may also be required to be equipped with the additional facilities to comply with the discharge limits of specific parameters such as phosphorous, nitrogen and the fecal coliform for which standards are prescribed. Some STPs have provision of by passing the untreated/partially treated sewage that is not adequate practice. The by-pass should be used judiciously wherever such arrangements are provided. The operation and maintenance of STPs need high expenses. In spite of this, the secondary by products of STPs, such as treated sewage and sludge (manure) are simply wasted, which can be viewed as the resource unutilized. Further, the methane gas a useful resource, is also flared at some STPs where gas production facility exists. The methane gas should be utilized, which would offset the operating cost of STP to a large extent. Many STPs are still without the gas production facility. Methane generation is required to be setup in STPs where UASB/sludge digesters are installed. The sludge and the treated effluent are also possible resources that could be used subject to their quality. We concluded that the each and every small or large scale municipal council should be facilitated with their own STP plants and Urban local bodies where already STPs are available they need to adopt advance technology for better performance and to treat waste water being wasted. The findings and suggestion presented in this work will serve as useful guide for improved sewage management services within the region with similar challenges in developing cities in Maharashtra.

REFERENCES

1. **Aniket R Ingole, Umer Raza Hafizullah Khan Rizvee and Bharti Changhode** (2020): Status, Difficulties and Management of Waste in Maharashtra: A Review, EC Agriculture 6.2, Pp 01-16.
2. **Central Pollution Control Board** (CPCB), 2004. Management of Municipal Solid Waste and sewage. Ministry of Environment and Forests, New Delhi, India.
3. **Central Pollution Control Board** (CPCB), 2011: Status of water quality in India (MINARS/35/ 2013-14), Central Pollution Control Board, Delhi.
4. **Central Pollution Control Board** (CPCB), 2015: National inventory of sewage treatment plants, Central Pollution Control Board, Delhi
5. **Chandrakant Yelam, Shridhar K. Jadhav, Abhijit S. Thorat and Sanjaykumar R. Thorat** (2022): Performance Evaluation to Improve the Efficiency of Effluent Treatment Plant in Automobile Industry. International E-Research Journal of Research Journey., Issue (287), February - 2022 Pp. 26-31. E-ISSN: 2348-7143.
6. **Ganpat B. More and Sanjaykumar R. Thorat** (2017): Performance Evaluation of Membrane Bioreactor Technology for Treatment of Wastewater: A Review, Global Journal of Engineering Science and Research, Vol 4 (11) Pp. 74-82.
7. **Gauri Kallawar, Rekha Tiwari, Sushen Jadhav and Mahesh Joshi.** (2018): Solid Waste management: A Case Study of Aurangabad, Maharashtra" *International J. of Sci., Engi. And Tech*., Vol. 6, Issue 4. Pp. 182-188.
8. Guidline for septage management in Maharashtra: February 2016, Swachh Maharashtra Mission (Urban), Urban Development Department, Government of Maharashtra.
9. **Joardar Souro D.** (2000): Urban Residential Solid Waste Management in India: Issues Related to Institutional Arrangements Public Works Management & Policy. 4 (4), pp 319-330.
10. **Jonnalagadda V.R. Murty** (2011:) Urban water and sanitation in Maharashtra, All India Institute for Local Self Government, Performance assessment system.
11. **Kharat D.S.** (2016) : Survey of Sewage Treatment Plants in Gujarat and Maharashtra: *Indian J. Environmental protection*, VOL.36, No. 11 Pp.957-961.
12. **Kumar Sunil** (2005): Municipal Solid Waste Management in India: Present Practices and Future Challenge. Asian Development Bank, pp 1–11. http://www.adb.org/Documents/Events/2005/Sanitation/stewaterManagement/paper kumar.pdf.

13. **Kumar, S. and Gaikwad, S. A.** (2004): Municipal Solid Waste Management in Indian Urban Centres: An Approach for Betterment, Urban Development Debates in the New Millennium, Atlantic Publishers, New Delhi, pp: 100-111.

14. **Lokhande, Singare and Pimple.** (2011): Study on Physico-Chemical Parameters of Wastewater Effluents from Taloja Industrial Area of Mumbai, India. *International Journal of Ecosystem* 2011; 1(1): Pp.1-9

15. **Lovlen Bhullar** (2013): Ensuring safe Municipal Wastewater Disposal in Urban India, *Journal of Environmental Law*, VOL. 25 No. 2 , Pp 235-260.

16. **Maharashtra Pollution Control Board** (MPCB), 2020: Annual report 19-20, Kalpataru point, sion(E) Mumbai.

17. **Pinak Ranade and Y.B. Katpatal** (2017): Estimation of waste water generation in a growing city using spatial techniques – a case study of Nagpur, Maharashtra, International Journal of Emerging Technologies in Computational and Applied Sciences (IJETCAS), 20(1)., 23-27.

18. **Raj Rajaram, SubijoyDutta and Ram Koduri:** LOW-COST WASTEWATER RECYCLING SYSTEMS CASE STUDIES FROM MAHARASHTRA AND ANDHRA PRADESH, INDIA: Rajaram, Dutta, &Koduri ©2005 92nd ISC Pp.1-10.

19. **Ramnath K. Sonawane and Sanjaykumar R. Thorat** (2010): “Studies on Municipal Solid waste management in Jalgaon city of Maharashtra: A case study”, *Bull. Of Envi. Sci.* Vol. XXVIII (1st Issue), Pp. 1-8 ISSN: 0971-1732.

20. **Sonawane Ramnath K and Sanjaykumar R. Thorat** (2010): Studies on Municipal Solid Waste Management in Jalgaon City of Maharashtra: A Case Study. *Bull. Envi. Sci.* Vol. 28 Ist Issue Pp. 1-8.

21. The Prohibition of Employment as Manual Scavengers (and their rehabilitation) Act, 2013.

22. **Velusamy and Kannan** (2016): Seasonal Variation in Physico-Chemical and Microbiological Characteristics of Sewage Water from Sewage Treatment Plants. Current World Environment Vol. 11(3), 791-799.

23. **Zerbock Olar** (2003): Urban Solid Waste Management: Waste Reduction in the Developing Nations. Michigan Technological University.

24. http://www.cee.mtu.edu/ peacecorps/ documents. july03/Waste_reduction_and_ incineration FINAL. pdf>.

www.nesa-india.org • E-mail: nesapublications@gmail.com
International Journal on Environmental Sciences

International Journal on Environmental Sciences 13 (2) Pp.66-72, ***July-December 2022***
ISSN No.: 0976-4534
https://doi.org/10.53390/ijes.v13i2.2

BIOREMEDIATION OF PAHS CONTAMINATED AGRICULTURAL SOIL-A REVIEW PAPER

Shreya Singh and Ningombam Linthoingambi Devi*

Department of Environmental Science, Central University of South Bihar
SH-7, Gaya Panchanpur, Post-Fatehpur, P.S-Tekari, District-Gaya, Bihar

Review Article

Received: **10.07.2022** Accepted: **19.07.2022** Published: **07.08.2022**

ABSTRACT

Soil is an important environmental matrix that directly or indirectly supports the life of all creatures. Despite being the ultimate sink for all contaminants, it has been neglected for a long time, resulting in poor soil quality. Due to the contamination of various toxic polycyclic aromatic compounds (PAHs) in soil, it diverts the quality of soil and impacts the soil ecosystem. Henceforth, it is necessary to identify the ecologically sustainable treatment alternatives for contaminated site cleanup. Biological treatment of PAHs contaminated soil is emerging as a promising and sustainable treatment options because they are safe, cost effective and eco-friendly treatment solutions. When it comes to pollutant degradation, microorganisms are known for their enzyme-catalyzed catabolic activity, w hich can be advantageous in the decompos ition of PAHs. There are various microbes which are extensively used for the removal of PAHs, in which *Cobetia marina, Rhodococcus soli* and *Pseudoalteromonas agarivorans* were found to be significant in degradation of PAHs. This review paper compiled a various recent in-situ and ex-situ bioremediation techniques used for the degradation and remediation of PAHs in agricultural soil.

Keywords: Polycyclic aromatic hydrocarbons, Soil, Degradation, Techniques.

INTRODUCTION

Polycyclic aromatic hydrocarbons (PAHs) are a class of chemically toxic compounds found in large quantities in agricultural soil as a result of waste water irrigation and industrial operations (Guo et al., 2017; Fernandez-Luqueno et al., 2011). PAHs pollution is a major global problem owing to its negative consequences. High persistence of polycyclic aromatic hydrocarbons (PAHs) in microbial breakdown and its negative impacts on the environment are the motivating attention to adopt various techniques for degradation and removal of PAHs in agricultural soil. Bioremediation is recognised as a relatively recent, successful technology and at the same time it is a cost-effective method for PAHs removal in contaminated site. It is a method of removing pollutants from the environment in order to restore the natural ecosystem and avoid further pollution (Sasikumar and Papinazath, 2003). Bioremediation is a method used for removal of PAHs from contaminated environment by utilising microorganisms to convert toxins to harmless products through mineralization, or by the conversion of contaminants into microbial biomass (Baggott, 1993; Mentzer and Ebere, 1996). Toxic PAHs are mineralized or bio transformed by using specific bacteria or certain enzymes in contaminated agricultural soil. Pseudomonas, Sphingomonas, Brevibacterium, Arthrobacter, Nocardioides and Mycobacterium bacteria have been used to breakdown PAHs, especially naphthalene (NAP) and phenanthrene (PHE) (Ghosal *et al*., 2016). Anaerobic biodegradation of PAHs is also extensively used for PAHs removal under denitrifying and sulphate-reducing bacteria (Lu et al., 2019). The aerobic degradation pathway is the principal oxygen-dependent pathway in surface layer soils, and it relies on genes that code for dioxygenases and monooxygenases (Yagi *et al*., 2009). There have been some advancements in

*Corresponding author: *nldevi@cub.ac.in*

bacterial remediation of contaminated soil techniques, such as inoculation with bacteria picked from PAHs-affected locations or nitrogen supplementation of contaminated soils (Cunningham *et al*., 1996; US EPA, 2000; Suthersan, 2002: Nzila, 2013). Modern biological methods have been widely employed to improve microbial PAHs degradation efficiency and clarify biodegradation metabolic pathways. Traditional ex situ approaches such as land farming, composting, and soil piles is also widely used for PAHs removal away from the contaminated site, however ex situ methods are quite expensive.

Bioremediation techniques for removal of PAHs in agricultural soil

Biological techniques have received the most attention for PAHs cleanup, followed by integrated methods, chemical oxidation, and physical procedures (Kuppusamy et al., 2017). Bioremediation is gaining acceptance as a viable alternative treatment option for PAHs contaminated soil remediation because it is regarded as a safe, effective, environmentally acceptable, and cost-effective method of eliminating organic pollutants from contaminated soil. Bioremediation of PAHs in contaminated agricultural soil is found to be a complex phenomenon because of the multi steps followed bioremediation process, and the environmental factors associated with PAHs degradation (Bosma *et al*., 1997; Tang *et al*., 2005).

Types of Bioremediations

On the basis of place where PAHs compounds are removed, there are principally two ways of bioremediation:

***In Situ* Bioremediation**

In situ bioremediation is most commonly used to remove PAHs from contaminated soils at the source point and it can frequently be done onsite, with little or no disturbance to routine operations. This also avoids the need to transfer large amounts of waste off-site, as well as the potential health and environmental risks that might occur during transit (Vidali, 2001). It is a more successful way for cleaning contaminated site, since it saves money on transportation and eliminates chemical contamination with harmless microorganisms. The procedure is also recommended since it produces the least amount of damage to the contaminated area, however it is more time-consuming than other restorative methods.

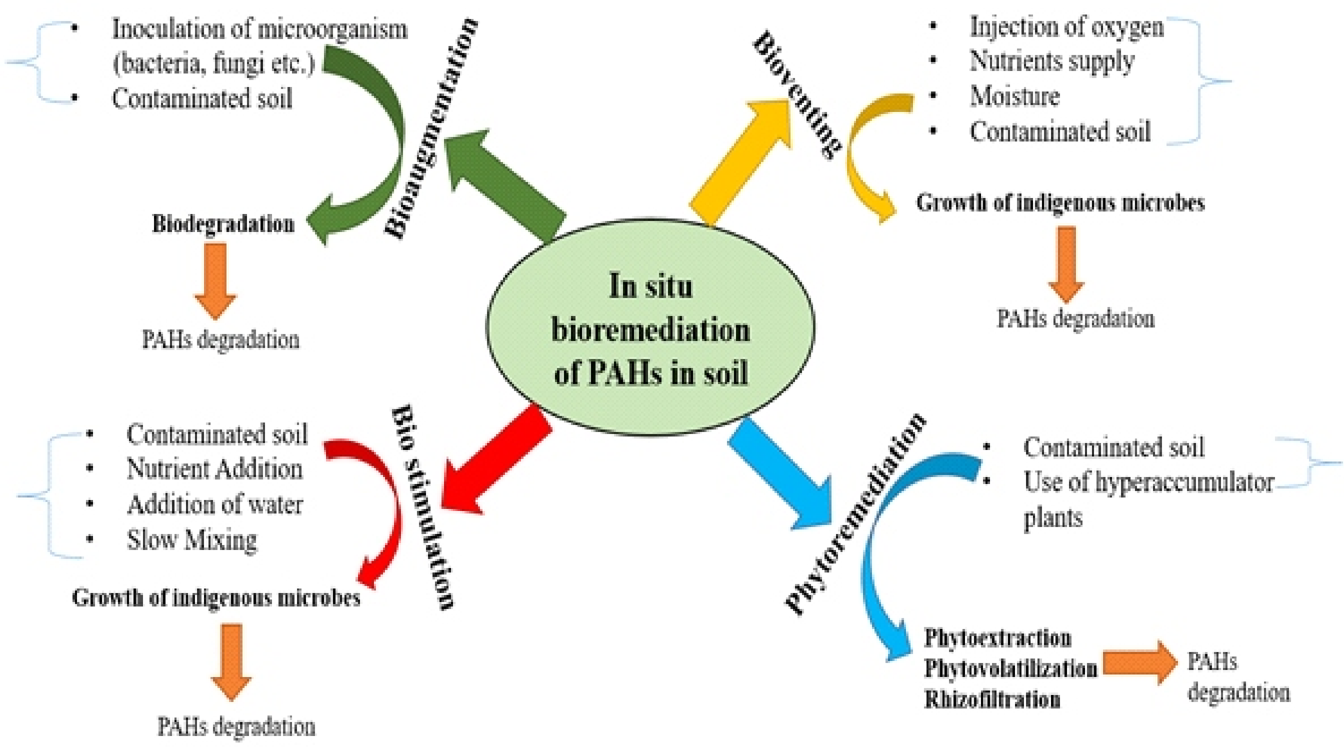

Fig. 1: In situ bioremediation techniques used for PAHs removal in agricultural soil.

Bioaugmentation

Bioaugmentation is defined as a bioremediation technique for enhancing the removal capacity of PAHs by introducing specific type of microorganisms to the polluted site for promoting biodegradation. Microbial PAHs remediation involves the application of particular microorganisms such as bacteria, archaea, fungus, and algae alone or in combination. Microbiological decontamination of PAHs contaminated soil is stated to be a more effective, cost-effective, and adaptable treatment option than physicochemical treatment (Rivas, 2006). Biodegradation of PAHs is a technique of recycling organic contaminants by employing living organisms to break down organic or inorganic matter, either in the presence of oxygen (aerobic biodegradation) or without oxygen (anaerobic biodegradation). Bioaugmentation can speed up the degradation process even in the circumstances where indigenous communities of degrading bacteria are not found (Alemzadeh, 2018; Cunningham et al., 2004). Garon et al. (2004) used fungus (Absidia cylindrospora) as a bioaugmentation supplement in contaminated soil to improve bioremediation in polluted soil, effected by fluorene. Bioaugmented microorganism also showed 70.8% and 72.2% reductions in benzo[a]pyrene and anthracene, while biostimulated and control microorganism showed substantially lower levels (Wu et al., 2008). Physical, chemical, and biological features of soils, as well as the physio-chemical characteristics of chemicals, have a significant impact on the degrading capability of naturally existing microbes for field bioremediation (Haritash and Kaushik, 2009). Bacteria have a metabolic flexibility that makes them ideal for degrading PAHs contaminants (Ma and Zhai, 2012). Unlike bacteria, archaea's degradation routes and methods for bioremediation have not been widely investigated (Khemili-Talbi et al., 2015). Mycoremediation, or fungal remediation, is a term that refers to the treatment or remediation of PAHs contaminated site, which involves a variety of fungal species. Some litter-decomposing fungi have been shown to colonise soil and degrade PAHs (Steffen et al., 2002), while native non-ligninolytic fungi isolated from soil have been found to significantly modify PAHs (D'Annibale et al., 2006; Potin et al., 2004).

Biostimulation

Biostimulation is a technique in which nutrients are added to a contaminated agricultural soil, to boost the growth of naturally occurring bacteria. It requires adding nutrients (nitrogen, phosphorus, and trace minerals) to the site, as well as adjusting the pH, soil moisture content, and aeration to encourage the proliferation of indigenous microorganisms and provide bacterial communities with a favourable environment in which they effectively degrade the PAHs (Salanitro et al., 1997). In order to boost the degrading activity of native or foreign microbes, inorganic additions of macro nutrients (N, P, K) or micro nutrients (Mg, S, Fe, Cl, Zn, Mn, Cu, Na) are needed for the recovery of contaminated agricultural soil with PAHs (Samanta et al., 2002). The addition of fertilisers has been proven to increase the number and activity of microbial communities, resulting in improved soil deterioration (Breedveld and Sparrevik, 2000; Betancur-Galvis et al., 2006; Xu and Obbard, 2003). The addition of nutrients to encourage the activity of indigenous microorganisms can aid in the degradation of PAHs based contaminants (Alexander, 1999; Samanta et al., 2002).

Bioventing

The most popular in situ therapy is bioventing, which includes providing air and nutrients to the contaminated soil with PAHs via wells in order to promote the indigenous microorganisms. To increase microbial growth and activity, oxygen is drawn through the contaminated medium. Bioventing uses low air flow rates and only supplies the quantity of oxygen required for biodegradation, reducing volatilization or pollutant release into the atmosphere. It is effective for simple hydrocarbons and can be utilised in situations where pollution is found far beneath the surface (Vidali, 2001).

Phytoremediation

Phytodegradation appears to be the most promising method for organic pollutants like polycyclic aromatic hydrocarbons (PAHs), by the use of plants to extract, sequester, and detoxify polluted agricultural soil with PAHs. Hyperaccumulator plants are used in soil to remediate PAHs contamination. Phytoremediation also known as rhizoremediation, is now regarded a viable, low-cost option for treating large areas of organic chemical pollution (Susrala et al., 2002; Parrish et al., 2005). For a small number of plants, there has been evidence of increased polycyclic aromatic hydrocarbons (PAHs) breakdown in plant rhizosphere, as a result of increased microbial activity (Spriggs et al., 2005). Phytoremediation offers the following advantages over other approaches: it prevents the natural structure and texture of the soil, uses primarily solar energy, can attain large levels of microbial biomass in the soil and it is cost effective (Huang et al., 2004). Tall fescue (Festuca arundinacea) and switchgrass (Panicum virgatum) were shown to be capable of removing all PAHs with an average of 40% effectiveness, with the exception of Indeno(1,2,3-c,d)pyrene, which had a removal efficiency of only 1.5 % (Gan et al., 2009). Lee et al. (2018) discovered that the native Korean grass species Panicum bisulcatum and Echinogalus crus-galli for phytoremediation of PAHs in contaminated soil. Gan et al. (2009) chosen five tree species (red mulberry, black willow, rooted hybrid poplar, sycamore and black locust) for phytoremediation, which have the capability of removing PAHs from soil. Liste and Alexander (2000) used three species of plant, such as jack pine (Pinus banksiana), red pine (Pinus resinosa), and white pine (Pinus strobus) for pyrene breakdown in soil. Phytoremediation has the following advantages over other approaches: it preserves the soil's natural structure and texture, greater abundance of microbial biomass in plant rhizosphere area, it is cost effective and has the potential to be rapid degradation for organic contaminants. Although there are certain advantages to utilising plants to remediate persistent toxins over other ways, there are a number of drawbacks to using this technology on a broad scale (US EPA, 2000; Suthersan, 2002). Many plant species are vulnerable to pollutants, particularly PAHs, which is a severe constraint (Huang et al., 2004; Burd et al., 1998). As a result, they grow slowly, making it difficult to produce enough biomass for effective soil remediation. Although land farming, bioremediation, and phytoremediation all have some efficacy in removing persistent PAHs from polluted soils.

Microbial Enzyme mediated Bioremediation

It is an advanced technique where isolated enzymes from fungus, bacteria, and other living organisms is used for PAHs elimination from contaminated soil for bioremediation. It performs over a wide range of temperatures and pH, henceforth the enzymatic activity is very efficient and selective. Enzymes involved for PAHs oxidation include oxygenase, dehydrogenase, lignin peroxidase, manganese peroxidase, laccases, and phenoloxidases (Mohan et al., 2006). Fungi's oxidative enzymes are less substrate-specific, so they are more efficient (Harms et al., 2011; Zhang et al., 2020). The sole disadvantage of this approach is the high cost of enzyme synthesis, extraction, and purification (Kuppusamy et al., 2017). Specifically, the bacteria use oxygenase-assisted metabolism to degrade PAHs aerobically (comprising monooxygenase and dioxygenase enzymes). PAHs breakdown is carried out by the fungus using the monooxygenase enzyme (Gupta and Pathak, 2020). Ligninolytic fungi generate enzymes including lignin peroxidase, manganese peroxidase, and laccases that oxidise PAHs (Aydin et al., 2017).

Ex Situ Bioremediation

PAHs are naturally more resistant to biodegradation and stay longer in the environment for years due to the lack of a suitable endogenous microbial population and incompatible environmental circumstances, so ex situ methods are important for the degradation of PAHs in contaminated soil. Ex situ bioremediation process takes place away from the contamination site, it necessitates the transportation of contaminated soil to the bioremediation site. Ex situ bioremediation approaches adopt the inoculation of specific foreign microorganisms like bacteria and fungus with PAHs contaminated site. This approach has more drawbacks than benefits.

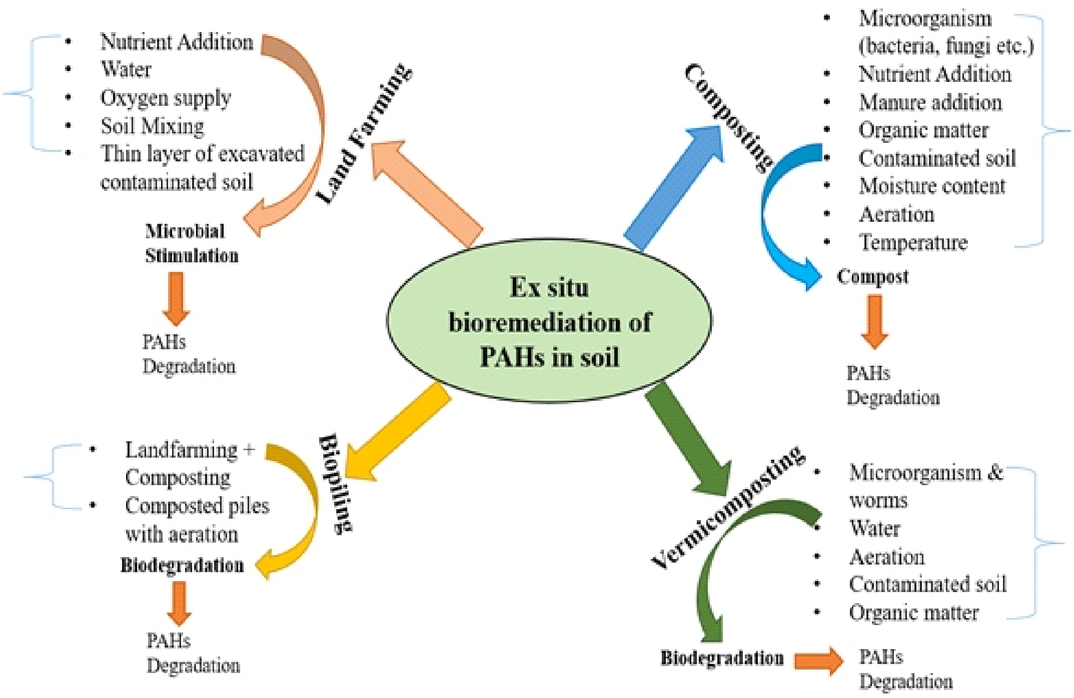

Fig. 2: Ex situ bioremediation techniques used for PAHs removal in agricultural soil.

Land farming

Land farming is a basic bioremediation approach, recently been investigated as a PAHs-remediation technology in which polluted soil is excavated and put over a prepared bed, then tilled on a regular basis to increase aeration until contaminants get degraded. The goal of this technique is to encourage indigenous bio degradative bacteria and make it easier for them to degrade pollutants aerobically. In general, the procedure is confined to treating the top 10–35 cm of soil (Vidali, 2001). Land farming will also oxygenate the soil, possibly enhancing the proliferation of aerobic soil bacteria and resulting in faster PAHs breakdown (Vidali, 2001). Land farming has a distinct advantage among other technologies for stimulating native soil microflora that are enriched in the soil by improving limiting factors such as inadequate aeration, poor microorganism contacts with the contaminants, and insufficient nutrients (Hansen et al., 2004).

Composting

Composting is the process of mixing polluted soil with non-hazardous organic additions like manure or agricultural waste. The presence of these organic materials encourages the growth of a diverse microbial population and the high temperatures associated with composting, hence promotes biodegradation of PAHs (Vidali, 2001). Temperatures in the compost range from 55 to 65 degrees Celsius. It is the decomposition of organic wastes by microbes, usually at a high temperature. Composting technology entails adding organic agents to the contaminated soil with PAHs, which increases porosity and allows for optimal air flow, optimal temperature and also providing a source of easily assimilated carbon for biomass growth (Eweis et al., 1998; Antizar-Ladislao et al., 2004). Composting technique is a successful and cost effective method for the degradation of PAHs, however it is more successful in degrading low molecular weight PAHs than high molecular weight PAHs (Cajthaml et al., 2002).

Biopiling

Land farming and composting are combined in biopiles. Engineered cells are essentially aerated with composted piles. Excavated soils are mixed with soil additives, placed on a treatment area, and bioremediated utilising forced aeration in biopile treatment, which is a full-scale technology.

Bioreactor

The polluted soil is excavated and transported to a treatment bioreactor. The bioreactor might have been built on-site or in a separate treatment facility. Ex situ method such as the use of bioreactors allow temperature and pressure control to promote PAHs breakdown in soil (Álvarez Bernal et al., 2006). Typically, the soil is slurried with water before being treated in the reactor, which improves bioremediation conditions.

CONCLUSION

Bioremediation is the most prominence and successful techniques for the degradation of PAHs from agricultural soil, as compare to other physical and chemical techniques. Various ex situ and In situ methods have been used for the removal of PAHs from contaminated soil, for a long time. In recent year researchers are most focused to develop much efficient combinations of techniques or advancement in existing techniques to achieve the removal efficiency of PAHs from contaminated soil. PAHs in agricultural soil, damage human health and soil quality, henceforth it is necessary to identify ecologically sustainable treatment alternatives for contaminated site cleanup.

REFERENCES

1. **Alemzadeh, A.** (2018). Roles of Plants and Bacteria in Bioremediation of Petroleum in Contaminated Soils. In *Phytobiont and Ecosystem Restitution* (pp. 23-44). Springer, Singapore.
2. **Alexander, M.** (1999). *Biodegradation and bioremediation*. Gulf Proional Publishing.
3. **Alvarez-Bernal, D., Garcia-Diaz, E. L., Contreras-Ramos, S. M., & Dendooven, L.** (2006). Dissipation of polycyclic aromatic hydrocarbons from soil added with manure or vermicompost. *Chemosphere*, *65*(9), 1642-1651.
4. **Antizar-Ladislao, B., Lopez-Real, J., & Beck, A.** (2004). Bioremediation of polycyclic aromatic hydrocarbon (PAH)-contaminated waste using composting approaches. *Critical Reviews in Environmental Science and Technology*, *34*(3), 249-289.
5. **Aydin, S., Karaçay, H. A., Shahi, A., Gökçe, S., Ince, B., & Ince, O.** (2017). Aerobic and anaerobic fungal metabolism and Omics insights for increasing polycyclic aromatic hydrocarbons biodegradation. *Fungal Biology Reviews*, *31*(2), 61-72.
6. **Baggott, J. E.** (1993). *Biodegradable lubricants*. Shell International Petroleum.
7. **Betancur-Galvis, L. A., Alvarez-Bernal, D., Ramos-Valdivia, A. C., & Dendooven, L.** (2006). Bioremediation of polycyclic aromatic hydrocarbon-contaminated saline–alkaline soils of the former Lake Texcoco. *Chemosphere*, *62*(11), 1749-1760.
8. **Bosma, T. N., Middeldorp, P. J., Schraa, G., & Zehnder, A. J.** (1996). Mass transfer limitation of biotransformation: quantifying bioavailability. *Environmental Science & Technology*, *31*(1), 248-252.

9. **Breedveld, G. D., & Sparrevik, M.** (2000). Nutrient-limited biodegradation of PAH in various soil strata at a creosote contaminated site. *Biodegradation*, *11*(6), 391-399.

10. **Burd, G. I., Dixon, D. G., & Glick, B. R.** (1998). A plant growth-promoting bacterium that decreases nickel toxicity in seedlings. *Applied and Environmental Microbiology*, *64*(10), 3663-3668.

11. **Cajthaml, T., Bhatt, M., Šašek, V., & Matějů, V.** (2002). Bioremediation of PAH-contaminated soil by composting: a case study. *Folia microbiologica*, *47*(6), 696-700.

12. **Cunningham, C. J., Ivshina, I. B., Lozinsky, V. I., Kuyukina, M. S., & Philp, J. C.** (2004). Bioremediation of diesel-contaminated soil by microorganisms immobilised in polyvinyl alcohol. *International Biodeterioration & Biodegradation*, *54*(2-3), 167-174.

13. **Cunningham, S. D., Anderson, T. A., Schwab, A. P., & Hsu, F. C.** (1996). Phytoremediation of soils contaminated with organic pollutants. *Advances in agronomy*, *56*(1), 55-114.

14. **D'Annibale, A., Rosetto, F., Leonardi, V., Federici, F., & Petruccioli, M.** (2006). Role of autochthonous filamentous fungi in bioremediation of a soil historically contaminated with aromatic hydrocarbons. *Applied and Environmental Microbiology*, *72*(1), 28-36.

15. **Eweis, J. B., Ergas, S. J., Chang, D. P., & Schroeder, E. D.** (1998). *Bioremediation principles*. McGraw-Hill Book Company Europe.

16. **Fernández-Luqueño, F., Valenzuela-Encinas, C., Marsch, R., Martínez-Suárez, C., Vázquez-Núñez, E., & Dendooven, L.** (2011). Microbial communities to mitigate contamination of PAHs in soil—possibilities and challenges: a review. *Environmental Science and Pollution Research*, *18*(1), 12-30.

17. **Gan, S., Lau, E. V., & Ng, H. K.** (2009). Remediation of soils contaminated with polycyclic aromatic hydrocarbons (PAHs). *Journal of hazardous materials*, *172*(2-3), 532-549.

18. **Garon, D., Sage, L., Wouessidjewe, D., & Seigle-Murandi, F.** (2004). Enhanced degradation of fluorene in soil slurry by Absidia cylindrospora and maltosyl-cyclodextrin. *Chemosphere*, *56*(2), 159-166.

19. **Ghosal, D., Ghosh, S., Dutta, T. K., & Ahn, Y.** (2016). Current state of knowledge in microbial degradation of polycyclic aromatic hydrocarbons (PAHs): a review. *Frontiers in microbiology*, 1369.

20. **Guo, G., Tian, F., Ding, K., Wang, L., Liu, T., & Yang, F.** (2017). Effect of a bacterial consortium on the degradation of polycyclic aromatic hydrocarbons and bacterial community composition in Chinese soils. *International Biodeterioration & Biodegradation*, *123*, 56-62.

21. **Gupta, S., & Pathak, B.** (2020). Bioremediation of Polycyclic Aromatic Hydrocarbons (PAHs): An Overview. *Bioremediation Technology*, 63-90.

22. **Hansen, L. D., Nestler, C., Ringelberg, D., & Bajpai, R.** (2004). Extended bioremediation of PAH/PCP contaminated soils from the POPILE wood treatment facility. *Chemosphere*, *54*(10), 1481-1493.

23. **Haritash, A. K., & Kaushik, C. P. (**2009). Biodegradation aspects of polycyclic aromatic hydrocarbons (PAHs): a review. *Journal of hazardous materials*, *169*(1-3), 1-15.

24. **Harms, H., Schlosser, D., & Wick, L. Y.** (2011). Untapped potential: exploiting fungi in bioremediation of hazardous chemicals. *Nature Reviews Microbiology*, *9*(3), 177-192.

25. **Huang, X. D., El-Alawi, Y., Penrose, D. M., Glick, B. R., & Greenberg, B. M.** (2004). A multi-process phytoremediation system for removal of polycyclic aromatic hydrocarbons from contaminated soils. *Environmental pollution*, *130*(3), 465-476.

26. **Khemili-Talbi, S., Kebbouche-Gana, S., Akmoussi-Toumi, S., Angar, Y., & Gana, M. L.** (2015). Isolation of an extremely halophilic arhaeon Natrialba sp. C21 able to degrade aromatic compounds and to produce stable biosurfactant at high salinity. *Extremophiles*, *19*(6), 1109-1120.

27. **Kuppusamy, S., Thavamani, P., Venkateswarlu, K., Lee, Y. B., Naidu, R., & Megharaj, M.** (2017). Remediation approaches for polycyclic aromatic hydrocarbons (PAHs) contaminated soils: Technological constraints, emerging trends and future directions. *Chemosphere*, *168*, 944-968.

28. **Lee, D. W., Lee, H., Lee, A. H., Kwon, B. O., Khim, J. S., Yim, U. H., ... & Kim, J. J.** (2018). Microbial community composition and PAHs removal potential of indigenous bacteria in oil contaminated sediment of Taean coast, Korea. *Environmental pollution*, *234*, 503-512.

29. **Liste, H. H., & Alexander, M.** (2000). Plant-promoted pyrene degradation in soil. *Chemosphere*, *40*(1), 7-10.

30. **Lu, H., Wang, W., Li, F., & Zhu, L.** (2019). Mixed-surfactant-enhanced phytoremediation of PAHs in soil:

bioavailability of PAHs and responses of microbial community structure. *Science of The Total Environment*, *653*, 658-666.

31. **Ma, J., & Zhai, G.** (2012). Microbial bioremediation in omics era: opportunities and challenges. *J. Bioremed. Biodeg*, *3*(e120).

32. **Mentzer, E., & Ebere, D.** (1996). Remediation of hydrocarbon of hydrocarbon contaminated sites. *Proceeding industry and the Nizena Enviornment, Nigerian National Petroleum (Corporation NNPC)*, *1*, 5-59.

33. **Mohan, S. V., Kisa, T., Ohkuma, T., Kanaly, R. A., & Shimizu, Y.** (2006). Bioremediation technologies for treatment of PAH-contaminated soil and strategies to enhance process efficiency. *Reviews in Environmental Science and Bio/Technology*, *5*(4), 347-374.

34. **Nzila, A.** (2013). Update on the cometabolism of organic pollutants by bacteria. *Environmental pollution*, *178*, 474-482.

35. **Parrish, Z. D., Banks, M. K., & Schwab, A. P.** (2005). Bioremediation and biodegradation: effect of root death and decay on dissipation of polycyclic aromatic hydrocarbons in the rhizosphere of yellow sweet clover and tall fescue. *Journal of Environmental Quality*, *34*(1), 207-216.

36. **Potin, O., Rafin, C., & Veignie, E.** (2004). Bioremediation of an aged polycyclic aromatic hydrocarbons (PAHs)-contaminated soil by filamentous fungi isolated from the soil. *International Biodeterioration & Biodegradation*, *54*(1), 45-52.

37. **Rivas, F. J.** (2006). Polycyclic aromatic hydrocarbons sorbed on soils: a short review of chemical oxidation based treatments. *Journal of Hazardous Materials*, *138*(2), 234-251.

38. **Salanitro, J. P., Dorn, P. B., Huesemann, M. H., Moore, K. O., Rhodes, I. A., Rice Jackson, L. M., ... & Wisniewski, H. L.** (1997). Crude oil hydrocarbon bioremediation and soil ecotoxicity assessment. *Environmental Science & Technology*, *31*(6), 1769-1776.

39. **Samanta, S. K., Singh, O. V., & Jain, R. K.** (2002). Polycyclic aromatic hydrocarbons: environmental pollution and bioremediation. *TRENDS in Biotechnology*, *20*(6), 243-248.

40. **Sasikumar, C. S., & Papinazath, T.** (2003, December). Environmental management: bioremediation of polluted environment. In *Proceedings of the third international conference on environment and health, Chennai, India* (pp. 15-17).

35. **Spriggs, T., Banks, M. K., & Schwab, P.** (2005). Phytoremediation of polycyclic aromatic hydrocarbons in manufactured gas plant–impacted soil. *Journal of environmental quality*, *34*(5), 1755-1762.

36. **Steffan, S., Tantucci, P., Bardi, L., & Marzona, M.** (2002). Effects of cyclodextrins on dodecane biodegradation. *Journal of inclusion phenomena and macrocyclic chemistry*, *44*(1), 407-411.

37. **Susarla, S., Medina, V. F., & McCutcheon, S. C.** (2002). Phytoremediation: an ecological solution to organic chemical contamination. *Ecological engineering*, *18*(5), 647-658.

38. **Suthersan, S. S., Lutes, C. C., Palmer, P. L., Lenzo, F., Payne, F. C., Liles, D. S., & Burdick, J.** (2002). *Technical protocol for using soluble carbohydrates to enhance reductive dechlorination of chlorinated aliphatic hydrocarbons*. ARCADIS GERAGHTY AND MILLER INC DURHAM NC.

39. **Tang, Y. J., Carpenter, S., Deming, J., & Krieger-Brockett, B.** (2005). Controlled release of nitrate and sulfate to enhance anaerobic bioremediation of phenanthrene in marine sediments. *Environmental science & technology*, *39*(9), 3368-3373.

40. United States. Environmental Protection Agency. Office of Solid Waste, & Emergency Response. (2000). *Engineered approaches to in situ bioremediation of chlorinated solvents: fundamentals and field applications*. DIANE Publishing.

41. **Vidali, M.** (2001). Bioremediation. an overview. *Pure and applied chemistry*, *73*(7), 1163-1172.

42. **Wu, Y., Luo, Y., Zou, D., Ni, J., Liu, W., Teng, Y., & Li, Z.** (2008). Bioremediation of polycyclic aromatic hydrocarbons contaminated soil with Monilinia sp.: degradation and microbial community analysis. *Biodegradation*, *19*(2), 247-257.

43. **Xu, R., Obbard, J. P., & Tay, E. T. C.** (2003). Optimization of slow-release fertilizer dosage for bioremediation of oil-contaminated beach sediment in a tropical environment. *World Journal of Microbiology and Biotechnology*, *19*(7), 719-725.

44. **Yagi, J. M., & Madsen, E. L.** (2009). Diversity, abundance, and consistency of microbial oxygenase expression and biodegradation in a shallow contaminated aquifer. *Applied and environmental microbiology*, *75*(20), 6478-6487.

45. **Zhang, H., Yuan, X., Xiong, T., Wang, H., & Jiang, L.** (2020). Bioremediation of co-contaminated soil with heavy metals and pesticides: Influence factors, mechanisms and evaluation methods. *Chemical Engineering Journal*, *398*, 125657.

www.nesa-india.org • E-mail: nesapublications@gmail.com
International Journal on Environmental Sciences

International Journal on Environmental Sciences 13 (2) Pp. 73-77, ***July-December 2022***
ISSN No.: 0976-4534
https://doi.org/10.53390/ijes.v13i2.3

RECLAMATION OF PESTICIDES CONTAMINATED SOIL AND WATER USING BIOCHAR: A REVIEW ON ADSORPTION POTENTIAL OF BIOCHAR

Akriti Ashesh and Ningombam Linthoingambi Devi*

Department of Environmental Sciences
Central University of South Bihar, SH-7 Gaya-Panchanpur Road, Gaya-824236, Bihar, India

Review Article

Received: **15.06.2022** Accepted: **22.06.2022** Published: **07.07.2022**

ABSTRACT

The application of agrochemicals into the environmental matrix has sluggishly degraded the quality of their original form. Pesticide consumption in the agricultural sector has been used for the quantity production of crops however, now considered as a culprit for the quality crops. Lands that once provided ample crops of good quality are now facing a case of severe damage impacting their crop quality. The prime need is to reclaim these contaminated matrices. For the same, an eco-friendly approach should be adopted. One such approach is the application of biochar for pesticide sorption. Biochar is a carbon-rich, stabilized product acquired when biomass undergoes pyrolysis at 200-650˚C. It is known for sequestration ability and mitigation of environmental contaminants. Its properties (surface area, pore size, ash contents, and functional groups) determine the potential for sorption. Biochar when modified is most effective for the sorption mechanism. For instance, rice straw biochar when treated with phosphoric acid (T-RSBC) showed stronger adsorption capacity for sorption in waste water effluent. Corn straw when doped with phosphorus functional groups was highly effective for adsorption of triazine pesticide from water. Other biochar that could remove pesticides are corn cob and corn starch. Activated coconut shell biochar showed the highest adsorption capacity for diazinon removal from water than other modified coconut shell biochar. Plant biochar (pine needle, oak wood, corn stover) having a high content of lignin have better properties such as large surface areas (112-642 m^2g^{-1}) and macropores (0.06-1.90 cm^3g^{-1}) that increase the sorption capacity of pesticides in soils than animal and cellulose-based biochar. This review paper aims to evaluate the role of biochar in the sorption of pesticides from soil and water.

Keywords: Biochar, Sorption potential, Pesticides, Reclamation.

INTRODUCTION

The demand for food is never going to be stabilized. It has been established that this demand is accelerating at an unprecedented rate. Recently, we have witnessed how development can turn into an uncontrollable disaster, which made us to change our lifestyle. However, one of the sectors that remained functioning was the agricultural sector. The production of food never stopped and stock of harvested crops saved our lives even in a pandemic. Pesticide managed to flourish as it offers beneficial attributes to the agricultural sector though it comes along with harmful impacts as well. Of all the pesticides available, organochlorines pose potential threat to human and ecosystem for their ability to persist, bioaccumulate, and bio-magnify in the environment (Juraske et al. 2007). The residue of pesticides in India is very high even though it consumes a lesser rate of pesticides (600g/hectare) than other developed countries (3000g/hectare) (Kumar et al. 2013). The exclusion of pesticide application from agricultural production practices will incur 50% loss of crops (Yavari et al. 2015). On the other hand, incorrect or excessive utilization will lead to substantial hazards. Pesticide contamination in soil and water happens due to surface runoff, leaching to groundwater, and air drifting (Meftaul et al. 2019). South-Asian countries like India, Pakistan, Srilanka, Nepal, & Bangladesh reported high levels of OCPs in the environmental matrix. In India, among

*Corresponding author: *nldevi@cub.ac.in*

different environmental matrices, water and soil reported most of the OCPs contamination (Ashesh et al. 2022). India marks 90000 tons of pesticide production and consumes 50000 MT. More than 98% of water resources in India are contaminated with DDT & HCH (even after the imposed ban) (Ashesh et al. 2022).

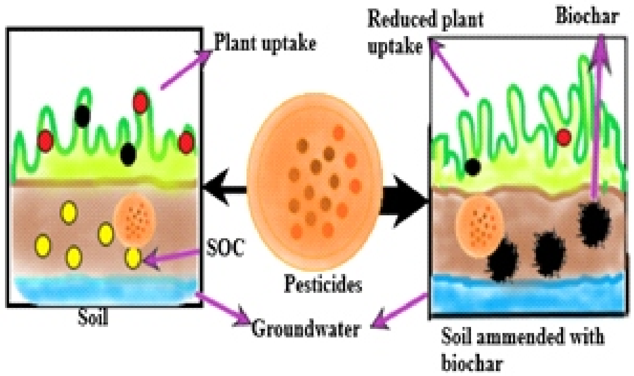

Fig. 1: Comparative diagram showing pesticide adsorption on soil amended with biochar (right) and unamended soil (left).

It is very necessary for the world to adopt strategies that are efficient in protecting the environment from pesticide's side effects (Yavari et al. 2014). Nowadays, biochar has fetched global attention as it has been reducing the bioavailability of pesticides, hence, hindering the process of bioaccumulat-ion (Yang et al. 2017). Therefore, the waste material can make all the difference. The old saying, "Lotus blooms in mud" can never go untrue. Biochar refers to carbon-rich material that is produced from pyrolysis of waste biomass (Suo et al., 2019) that can be utilized for its adsorbing properties. India generated 370 Mt of agricultural wastes per year (Ponnam et al. 2020). However, according to recent reports, it generates 500 Mt of residues annualy (Krishnaveni & Dayana 2021). Its low cost, and ability to reduce pollution makes it an efficient strategy to reduce pesticide pollution. The aim of this review is to indicate scope of the sorption potential of biochar for reclamation of pesticide contaminated soil and water.

Use of Biochar for pesticide adsorption

Burning of biomass through pyrolysis in the low/no oxygen supply in a closed system produces a by-product known as biochar. Their characteristics such as surface area, and pore volume depend upon the conditions applied during the process of pyrolysis like temperature and duration of exposure (Taha et al. 2014). Biochar is chosen for removal of pesticides because of its large surface area. Adsorption capacity of biochar is directly proportional to its surface area (Bahrum et al. 2020). However, Mondal et al. showed that biochar with lesser surface area and pore volume showed greater adsorption capacity (Mondal et al. 2017). They even treated the Rice stalk biochar (RSBC) with phosphoric acid (T-RSBC) which further reduced the surface area and pore volume resulting in increase in adsorption efficiency of atrazine and imidacloprid. Biochar possesses some of the unique properties like aromaticity, and highly carbonaceous nature. These properties together make them >2000 times effective in pesticide adsorption than soil (Kookana 2010). Biochar, when incorporated into the soil, stopped the microbial degradation of pesticides and other organic compounds. With this, it also reduces the availability to, and uptake of pesticides by plant species. Biochar prepared from agricultural wastes such as rice stalk (Liu et al. 2015; Mondal et al. 2017), corn stalk (Taha et al. 2014; Mondal et al. 2017; Suo et al. 2019), coconut shell (Baharum et al. 2020), neem waste (Ponnam et al. 2019), apricot kernel and orange peel (Abelhameed et al. 2020), wood derivatives, such as bamboo chips (Mandal et al. 2017), manures of poultry, pig, and cattle (Liu et al., 2015) have been tested for pesticide removal from water matrix in the recent past. Similarly, more examples of removal of pesticides from soil and water matrix is given in table 1.

Table 1: Adsorption percentage of biochar for pesticides.

Biochar	Pesticides	Adsorption %	Matrix	References
Coconut shell modified biochar	Diazinon	98.96	Aqueous solution of pesticides	Baharum et al. 2020
Rice straw biochar (T-RSBC)	Atrazine	58.9-89.8	Waste water	Mandal et al. 2021
	Imidacloprid	58.2-89.5		
Neem waste (Azadira-chta indica)	Bentazone	55.20	Aqueous solution of pesticides	Ponnam et al. 2019
Corn stalk biochar	Triazine	96	Polluted water	Suo et al., 2019
Wheat straw biochar	Atrazine	48	Aqueous solution of pesticides	Yang et al. 2017

Eucalyptus spp. wood chips biochar	Chlorpyrifos, Carbofuran	86-88	Soil	Yu et al. 2009
Green waste biochar (Maple, elm, oak, wood chips and barks)	Atrazine	54	Aqueous solution of pesticides	Zheng et al. 2010
Rice husk & corn stalk biochar	Phosmet	98	Water	Taha et al. 2014
	Carbaryl	90		
	Melathion	88		
Orange peel and apricot kernel biochar	Prothiofus	91.7	Water	Abelhameed et al. 2020
Pinus roxburghii/				
Fe_3O_4/ $BiVO_4$	Methylparaben	86.93	Soil	Kumar et al. 2017
Aged biochar*	Imazamox	80		Gamiz et al. 2019
	Terbuthylazine	96	Aqueous solution of pesticides	
	Picloram	83.5		

*Aged biochar- Freshly prepared biochar was kept in a mesh bag and buried in silt loam soil for 6 months prior to the experiment.

Addition of biochar in soil tend to increase the number of bacterial groups such as Alphaproteobacteria, Betaproteobacteria, Deltaproteobacteria, Gammaproteobacteria, and Rubrobacteridae (Abujabhah et al. 2016). Increase in the number of microbial communities is associated to the increase in nutrient content, organic matter, and water retention ability of the soil after ammendments (Ma et al. 2019). The microbial community present in the soil is responsible for the degradation of pesticides. The soil amended with biochar result in increased mineralization of pesticides as compared to the unamended soil (Qiu et al. 2009). Biochar addition in the soil increases the hydrolytic activity of flurorescein diacetate (FDA). The activity of FDA indicates the presence of microbial activity in soil (Chan et al. 2008). The experiment in which removal of pesticides are studied with the help biochar addition carried out in a few general steps:

- Preparation of biochar through pyrolysis.
- Examination of prepared biochar's characteristics through scanning electron microscope (SEM), BET surface area analysis, and energy dispersive X-ray.
- Examination of pesticide adsorption on biochar through batch technique.

Adsorption mechanism

Soil-pesticide adsorption occurs due to the soil organic carbon (SOC). SOC consists of soft gel like and hard parts. Soft part of the SOC is amorphous, rubber like matrix while the latter that is hard parts are condensed glass like matrix. Pesticides adsorb differently into these two matrices of SOC. The extent to which pesticides can adsorb to soil depends upon its aromaticity. Therefore, the high aromatic nature of biochar makes them stronger than soils (Figure 1) (Kookana 2010). Generally, the sorption process includes three phases. The first one is an instantaneous adsorption phase, followed by slow adsorption phase, which is then followed by the last phase known as equilibrium phase (Liu et al. 2015). In the second phase, the adsorption capacity decreases due to blocking of mesopores and micropores (Figure 2). Now, after the sorption of pesticides, it has to be desorbed to be able to attack on target pests. The further investigation on sorption-desorption of pesticides from biochar has poor evidence (Kookana 2010).

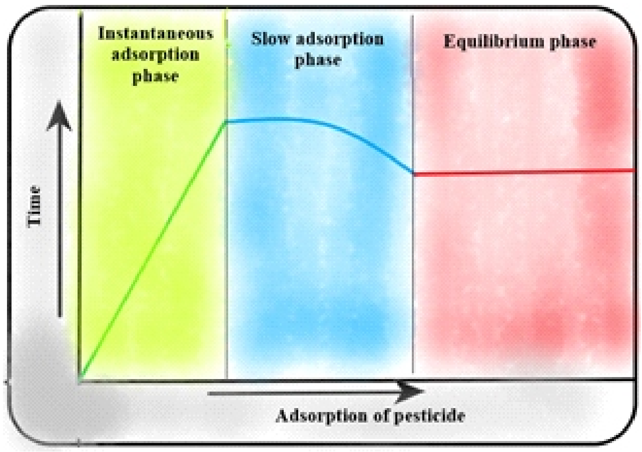

Figure 2. Graph showing phases of adsorption of pesticides on biochar surface.

Factors affecting sorption process

The process of sorption of pesticide to biochar is defined as a physico-chemical shift by which the pesticides can be shifted across solid and the aqueous phase (Yavari et al. 2015). Adsorption of pesticide to biochar is affected by factors such as biochar properties. For example, surface area, CEC, pores diameter, and attached functional groups. The other factors that affect the sorption process are pesticides' properties such as, molecular structure and their size, acidic and alkaline nature, solubility, hydrophobicity, polarity, and environmental conditions such as, moisture, pH, temperature, wind, and light (Yavari et al. 2015). Some of the chemical domains that influence sorption capacity of biochar are H-bonding, covalent bonding, and cation bridging (Gamiz et al. 2019). Apart from this, a few other factors such as aromaticity (Mandal et al. 2017), aging of biochar (Gamiz et al. 2019), sorbent dosage, and presence of other pesticides (Mandal et al. 2021). Some of the factors that affect sorption potential of biochar are:

A. **Temperature:** Adsorption of pesticide onto biochar is favorable at higher temperatures. The process of adsorption is endothermic. Increase in temperature increases the active sites and collision frequency on biochar's surface (Srivastava et al. 2011).

B. **pH:** Low pH favors the adsorption kinetics (Zheng et al. 2010). Biochar which are acidic in nature would have the higher ability to adsorb pesticides. The sorption coefficients of pesticides reduce with an increase in the value of pH. The acidic properties of media would increase the interaction between pesticides (cations) and biochar (anionic surface) through electrostatic interaction that would in turn enhance the sorption capacity of biochar for pesticides.

C. **Surface area, pore volume, and number:** In general, a large number of pores (Yang et al. 2017), larger surface areas, and higher volumes of pores (Taha et al. 2014) are evident to increase the sorption potential of biochar.

CONCLUSIONS

This review highlights the role of biochar in adsorption of pesticides from soil and water. The findings from the review shows that only little research has been conducted in the adsorption of pesticides from water and a very few were researched on soil. By altering the soil and water environment with the addition of biochar, the menace of pesticide pollution can be solved. In comparison to unamended soil, amended soil with biochar has higher potential to reduce the pesticide availability for plant uptake and prevent its bioaccumulation and toxicity in further trophic levels. Biochar application in the soil increases the diversity and number of microbial community present in the soil. The presence of microbial community felicitates biodegradation of pesticides present in soil. Many areas still have dearth of understanding and information which require more research. For instance,

1. Various types of persistent organic pollutants such as OCPs are not researched for its reduction from soil and water.
2. There is limited data available for the matrices such as water and soil.
3. Majority of the research is carried out as experiments in the confined laboratories but the data are not available for field research and still need extensive study.
4. This review indicates that most of the research were carried out for biochar prepared from corn and rice. Other biochar that can be prepared from number of agricultural wastes are needed to be explore for its potential to remove pesticides.

REFERENCES

1. **Abdelhameed, R. M., Abdel-Gawad, H., & Hegazi, B.** (2020). Effective adsorption of prothiofos (O-2, 4-dichlorophenyl O-ethyl S-propyl phosphorodithioate) from water using activated agricultural waste microstructure. *Journal of Environmental Chemical Engineering*, *8*(3), 103768.
2. **Ashesh, A., Singh, S., Devi, N.L., & Yadav, I.C.** (2022). Organochlorine pesticides in multi-environmental matrices of India: A comprehensive review on characteristics, occurrence, and analytical methods. Microchemical Journal, 177.
3. **Baharum, N. A., Nasir, H. M., Ishak, M. Y., Isa, N. M., Hassan, M. A., & Aris, A. Z.** (2020). Highly efficient removal of diazinon pesticide from aqueous solutions by using coconut shell-modified biochar. *Arabian Journal of Chemistry*, *13*(7), 6106-6121.
4. **Gámiz, B., Velarde, P., Spokas, K. A., Celis, R., & Cox, L.** (2019). Changes in sorption and bioavailability of herbicides in soil amended with fresh and aged biochar. *Geoderma*, *337*, 341-349.
5. **Juraske, R., Antón, A., Castells, F., & Huijbregts, M. A.** (2007). PestScreen: A screening approach for scoring and ranking pesticides by their environmental and toxicological concern. *Environment International*, *33*(7), 886-893.
6. **Kookana, R. S.** (2010). The role of biochar in modifying the environmental fate, bioavailability, and efficacy of pesticides in soils: a review. *Soil Research*, *48*(7), 627-637.

7. **Krishnaveni, A. S. & Dayana K.** (2021). Crop Residue Management- A Review. Int. J. Curr. Microbiol. App. Sci. 10(03): 28-33.

8. **Kumar, A., Sharma, G., Naushad, M., Kumar, A., Kalia, S., Guo, C., & Mola, G. T.** (2017). Facile hetero-assembly of superparamagnetic Fe3O4/BiVO4 stacked on biochar for solar photo-degradation of methyl paraben and pesticide removal from soil. *Journal of Photochemistry and Photobiology A: Chemistry*, *337*, 118-131.

9. **Kumar, S., Sharma, A. K., Rawat, S. S., Jain, D. K., & Ghosh, S.** (2013). Use of pesticides in agriculture and livestock animals and its impact on environment of India. *Asian Journal of Environmental Science*, *8*(1), 51-57.

10. **Liu, N., Charrua, A. B., Weng, C. H., Yuan, X., & Ding, F.** (2015). Characterization of biochars derived from agriculture wastes and their adsorptive removal of atrazine from aqueous solution: A comparative study. *Bioresource technology*, *198*, 55-62.

11. **Mandal, A., Kumar, A., & Singh, N.** (2021). Sorption mechanisms of pesticides removal from effluent matrix using biochar: Conclusions from molecular modelling studies validated by single-, binary and ternary solute experiments. *Journal of Environmental Management*, *295*, 113104.

12. **Mandal, A., Singh, N., & Purakayastha, T. J.** (2017). Characterization of pesticide sorption behaviour of slow pyrolysis biochars as low cost adsorbent for atrazine and imidacloprid removal. *Science of the Total Environment*, *577*, 376-385.

13. **Meftaul, I. M., Venkateswarlu, K., Dharmarajan, R., Annamalai, P., & Megharaj, M.** (2020). Pesticides in the urban environment: A potential threat that knocks at the door. *Science of the Total Environment*, *711*, 134612.

14. **Ponnam, V., Katari, N. K., Mandapati, R. N., Nannapaneni, S., Tondepu, S., & Jonnalagadda, S. B.** (2020). Efficacy of biochar in removal of organic pesticide, Bentazone from watershed systems. *Journal of Environmental Science and Health, Part B*, *55*(4), 396-405.

15. **Srivastava, V., Weng, C. H., Singh, V. K., & Sharma, Y. C.** (2011). Adsorption of nickel ions from aqueous solutions by nano alumina: kinetic, mass transfer, and equilibrium studies. *Journal of Chemical & Engineering Data*, *56*(4), 1414-1422.

16. **Suo, F., You, X., Ma, Y., & Li, Y.** (2019). Rapid removal of triazine pesticides by P doped biochar and the adsorption mechanism. *Chemosphere*, *235*, 918-925.

17. **Taha, S. M., Amer, M. E., Elmarsafy, A. E., & Elkady, M. Y.** (2014). Adsorption of 15 different pesticides on untreated and phosphoric acid treated biochar and charcoal from water. *Journal of Environmental Chemical Engineering*, *2*(4), 2013-2025.

18. **Yang, F., Sun, L., Xie, W., Jiang, Q., Gao, Y., Zhang, W., & Zhang, Y.** (2017). Nitrogen-functionalization biochars derived from wheat straws via molten salt synthesis: An efficient adsorbent for atrazine removal. *Science of the Total Environment*, *607*, 1391-1399.

19. **Yang, F., Sun, L., Xie, W., Jiang, Q., Gao, Y., Zhang, W., & Zhang, Y.** (2017). Nitrogen-functionalization biochars derived from wheat straws via molten salt synthesis: An efficient adsorbent for atrazine removal. *Science of the Total Environment*, *607*, 1391-1399.

20. **Yavari, S., Malakahmad, A., & Sapari, N. B.** (2015). Biochar efficiency in pesticides sorption as a function of production variables—a review. *Environmental Science and Pollution Research*, *22*(18), 13824-13841.

21. **Yu, X. Y., Ying, G. G., & Kookana, R. S.** (2009). Reduced plant uptake of pesticides with biochar additions to soil. *Chemosphere*, *76*(5), 665-671.

22. **Zheng, W., Guo, M., Chow, T., Bennett, D. N., & Rajagopalan, N.** (2010). Sorption properties of greenwaste biochar for two triazine pesticides. *Journal of hazardous materials*, *181*(1-3), 121-126.

23. **Chan, Y.K., Van, Z. L., Meszaros, I., Downie, A., & Joseph, S.** (2008). Using poultry litter biochars as soil amendments. *Aust J Soil Res* 46:437–444

24. **Abujabhah, I.S., Bound, S.A., Doyle, R., Bowman, J.P.** (2016). Effects of biochar and compost amendments on soil physico-chemical properties and the total community within a temperate agricultural soil. *Appl Soil Ecol* 98:243–253.

25. **Ma, H., Egamberdieva, D., Wirth, S., Li, Q., Omari, R. A., Hou, M., & Bellingrath-Kimura, S. D.** (2019). Effect of biochar and irrigation on the interrelationships among soybean growth, root nodulation, plant P uptake, and soil nutrients in a sandy feld. Sustainability 11(23):6542.

26. **Qiu, Y., Pang, H., Zhou, Z., Zhang, P., Feng, & Sheng, D.G.** (2009). Competitive biodegrada-tion of dichlobenil and atrazine coexisting in soil amended with a char and citrate. *Environ Pollut* 157:2964–2969.

www.nesa-india.org • E-mail: nesapublications@gmail.com
International Journal on Environmental Sciences

International Journal on Environmental Sciences 13 (2) Pp. 78-88, ***July-December 2022***
ISSN No.: 0976-4534
https://doi.org/10.53390/ijes.v13i2.4

A COMPARATIVE ANALYSIS OF REVENUE-BASED LAND INFORMATION SYSTEM INTEGRATING SENTINEL-2 AND PLANET IMAGERY FOR CROP CLASSIFICATION

Kusum[1], Sumit Kumar[1], Reenu Sharma[1], Syed Shabih Hassan[2] and Brijendra Pateriya[1]

[1]Punjab Remote Sensing Centre, Ludhiana-141004 (Punjab) India
[2]Guru Angad Dev Veterinary and Animal Sciences University, Ludhiana-141004 (Punjab) India

Review Article

Received: **20.06.2022** Accepted: **28.06.2022** Published: **14.07.2022**

ABSTRACT

The study presents a revenue-based land information system integrated with the crop information. In this study, Sentinel-2 and Planet imagery have been used for crop classification using supervised classification. The accuracy attained from the Planet image was 90.67% and 82% for Sentinel 2, respectively. The study finds that the rice crop was grown a significant portion in the study area. The result shows the Murabba and Khasra based information of the existing Land use and Land cover information and Planet data provides better adjustment with the cadastral data. This integration includes essential information for identifying crops at the Khasra level and revenue base estimation of crop yield for the particular land parcel.

Keywords: Cadastral Map, GIS, NDVI, Time Series, Land Information, Land Management.

INTRODUCTION

Climate change becomes a unique challenge to the world's food security and nutrition needs (Schmidhuber & Tubiello 2007). Food systems are highly vulnerable to climate change. According to the United Nations' most recent estimate, the world's population is 7.3 billion, with a potential of 9.7 billion by 2050 (Roser et al., 2013). This increase in global food demand and limited land resources and decreased water availability were likely to pose a substantial threat to achieving food security (Misra 2014). Geospatial technology for crop monitoring and mapping becomes a pivotal solution to counter the present challenge (Singh et al., 2021). New sensors have been launched in past years, such as Sentinel and Planet, providing higher resolution datasets with near real-time data. Multi-temporal, Multi-spectral based remote sensing provides field-level information of crop type and crop health (Saini & Ghosh 2019). The time-series analysis provides critical phenological information to extract specific crops. The crop classification becomes essential to study the crop diversity and effect of environmental factors in the particular area. Apart from the conventional methods, remote sensing data has increased for estimating the crop acreage, crop health and crop patterns. The advanced classification techniques have provided enormous opportunities for crop monitoring and improved feature selection, contributing to improved map accuracy and computing efficiency (Griffiths et al., 2019).

Crop mapping at the cadastral level provides valuable information for Government Agencies and Insurance Companies for crop insurance and yield estimation (Aggarwal et al., 2016). The cadastral-based map provides the dissemination of individual agricultural plots. A cadastral map includes detailed information about land records information within a defined area (Williamson & Enemark 1996). Multipurpose cadastral provides a framework for recording, storing, and providing comprehensive land information at the parcel level and allowing users to share parcel data (Demir et al., 2003). Mondal et al., 2014 generated digital maps from cadastral data integrated with satellite-

*Corresponding author: *Skumar1@ce.iitr.ac.in, Sumit.civil18@gmail.com*

based LULC and also developed a land parcel information system. Park & Song (2020) analysed the use of UAV data to identify the inconsistency in the land parcels for updating the land use category in the Cadastral Map. There are a few more studies conducted in which cadastral data has been used for land cover updating. However, a survey regarding cadastral data for crop monitoring is very few. This study provides a detailed analysis regarding the accuracy of two different resolution satellite data for crop mapping with respect to cadastral level information. The study was initiated with the following objectives: (i) Crop classification using Sentinel and Planet data. (ii) Conversion of hard copy cadastral data into the Geo-referenced vector data. (iii) To integrate the cadastral information with a crop type map.

MATERIAL AND METHODS

Study Area

Figure 1 shows the study area of Malakapur village situated in the District Ludhiana, Punjab. The village lies in the 30.9289° N 75.7392°E. The Köppen-Geiger climatic classification for this location is Cwa.

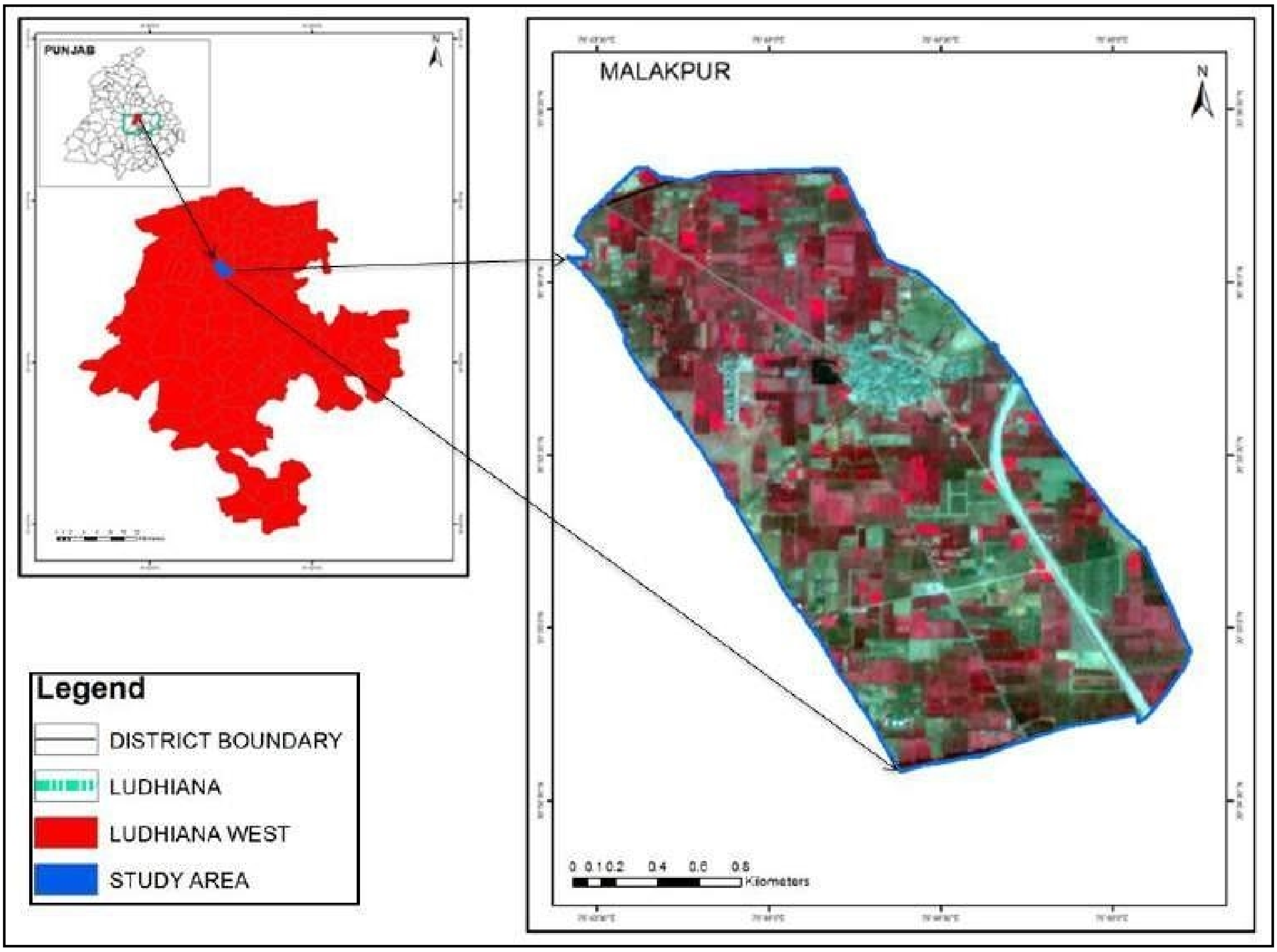

Figure 1: Map showing the Location of Study Area.

Field data collection

The data collection was conducted on October 9, 2021, using MAPinr mobile application. This application allows marking the polygon on a particular field using Google Earth imagery in the background and will enable us to take photographs of that field. The study area consists of three land-use classes, i.e., Cropland, built-up land and vacant land. Three crops were found in this village: rice, maize and vegetables. For the data collection, as shown in Figure 2 random sampling has been done for data collection, and a minimum of 20 samples have been taken of individual land-use classes.

Figure 2: Field locations of the selected study area

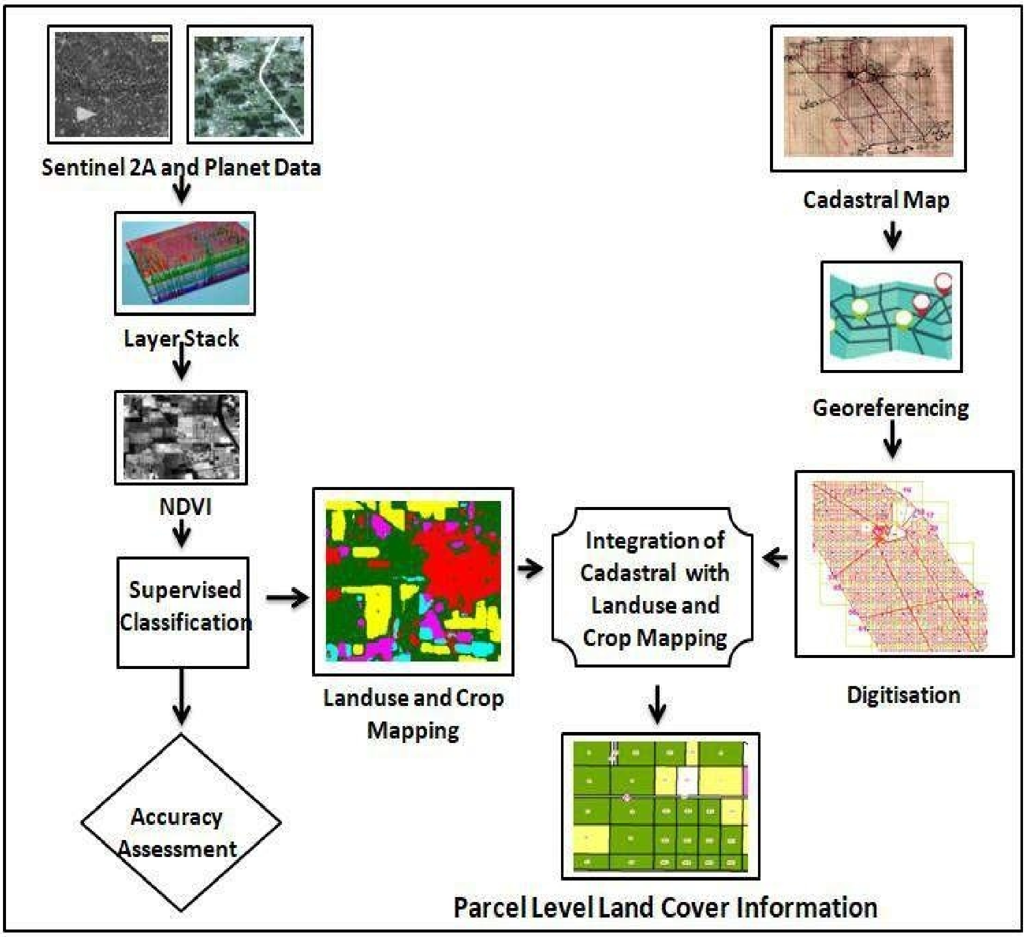

Figure 3: Flowchart showing Methodology.

Satellite Data used

Sentinel 2 is a wide-swath, medium resolution with a high spectral imaging mission. Sentinel 2 is equipped with a multispectral sensor that gives data in 13 spectral bands with a spatial resolution of 10 meters in the visible and near-infrared regions (Table 1). There are two sentinel satellite constellations: Sentinel2A (launched June 2015) and Sentinel 2B (launched March 2017) with a revisit period of 10 days. However, two satellites reduce the revisit time to 5 days, making them ideal for crop monitoring. Planet Scope, a constellation of about 130 satellites operated by Planet, is capable of imaging the whole land surface of the Earth every day. The Planet Scope satellite constellation is made up of multiple Dove satellites. The Planet data have a spectral resolution of 4 bands and provide a spatial resolution of about 3 meters (Table 1). The images were atmospherically corrected to BOA reflectance, which improves consistency across time and site localized atmospheric conditions while reducing spectral response uncertainty (Planet Team, 2017). The Planet data is ideal for crop monitoring due to its daily revisit and provides high-resolution imagery. Detail methodology in the form of flow chart is furnished in Figure 3.

Table 1: Spectral Bands, spatial resolution and wavelength of the Sentinel-2 and PlanetScope image.

SENTINEL 2			PLANET SCOPE	
Spectral Bands	**Spatial Resolution (m)**	**Wavelength (nm)**	**Spectral Bands**	**Wavelength (nm)**
B1	60	443	Blue	455 – 515
B2	10	490	Green	500 – 590
B3	10	560	Red	590 – 670
B4	10	665	NIR	780 – 860
B5	20	705		
B6	20	740		
B7	20	783		
B8	10	842		
B8A	20	865		
B9	60	945		
B10	60	1375		
B11	20	1610		

Image Classification

Normalized Difference Vegetation Index (NDVI)

The NDVI is a vegetation index that uses the reflectance qualities of healthy vegetation to distinguish vegetated from non-vegetated areas and evaluate the current vegetation's health. It shows the spectral characteristic of vegetation that can be used to classify crops based on their physical features. This is accomplished by computing the Normalized Difference between the Near Infrared and the Red bands. The NDVI value ranges from -1 to +1. Early techniques based on the normalized difference vegetation index (NDVI) were created in the 1970s (Rouse et al., 1973) and were widely used for vegetation monitoring (Stone et al., 1996). As a result, the NDVI time series was used as the classifying feature. A time series has been used to identify the changing patterns of vegetation around the year.

The NDVI is calculated by: $\text{NDVI} = \frac{\text{NIR-RED}}{\text{NIR-RED}}$

Supervised classification

The supervised classification method was used for the land use land cover classification. The classification method allows the image analyst to monitor the pixel categorization process. In supervised classification, the computer algorithms classify according to the selected signature by the analyst. The selection of samples or training fields is vital for accurate classification results. Maximum likelihood classifier is a popular method in supervised classification techniques. It calculates the relevant statistics (mean and variance-covariance) and a probability function using input for classes defined from training site data (Ford et al., 2008). The probability of a pixel belonging to each of the classifications evaluated is calculated.

For the image classification, the time series NDVI images were first generated for both the satellite data. Then NDVI images are stacked in a single raster file in ERDAS Imagine 2014 software. The training samples collected from fields were used as input signatures for the classification. The maximum likelihood classifier was used for supervised classification and the classification accuracy was evaluated using the overall accuracy. For the classification, five land-use classes were selected, and the following classes have been generated (i) Built-up, (ii) rice, (iii) maize, (iv) vegetables and (v) Others (includes Vacant land for urban development).

Accuracy Assessment

In order to assess the accuracy of LULC maps, the Kappa coefficient and Overall accuracy were calculated using randomly selected sample ground control locations for both maps. The assessment of accuracy was evaluated by comparing the classified image and referencing Google earth image and field collection points. For the assessment of crop type field data were used and evaluation of built-up area and another class was validated by Google earth imagery. The overall accuracy, user and producer accuracy were computed from the confusion matrix (Congalton and Green. 2019). The kappa coefficient was also calculated for the assessment of results.

Cadastral Mapping

The cadastral map of Malakpur village was received from the Department of Revenue, Rehabilitation and Disaster Management, Punjab. The village data was converted from hard copy to digital copy using a scanner. The scanned cadastral map of the village was then Geo-referenced and digitized. The point, line and polygon vector layers with attribute information were generated. The UTM 43N projection system in the WGS84 datum has been selected.

The vector layers were topologically corrected and null and duplicate errors were also removed. The village was divided in Murabba and Khasra and one Murabba contains 25 Khasra and one Khasra represents 4046.8m^2. The vector layers generated based on the character of the feature as per the cadastral records are as follows: (i) Murabba line, (ii) Murabba number, (iii) Khasra line, (iv) Khasra number, as shown in Figure 3. All the features on the cadastral map, like roads, canals, Khasra and Murabba are demarcated in a vector layer--the digitized cadastral map of Malakpur village shown in Figure 4. The digital cadastral layer overlaid on satellite imagery is shown in Figure 5.

(a) **(b)**

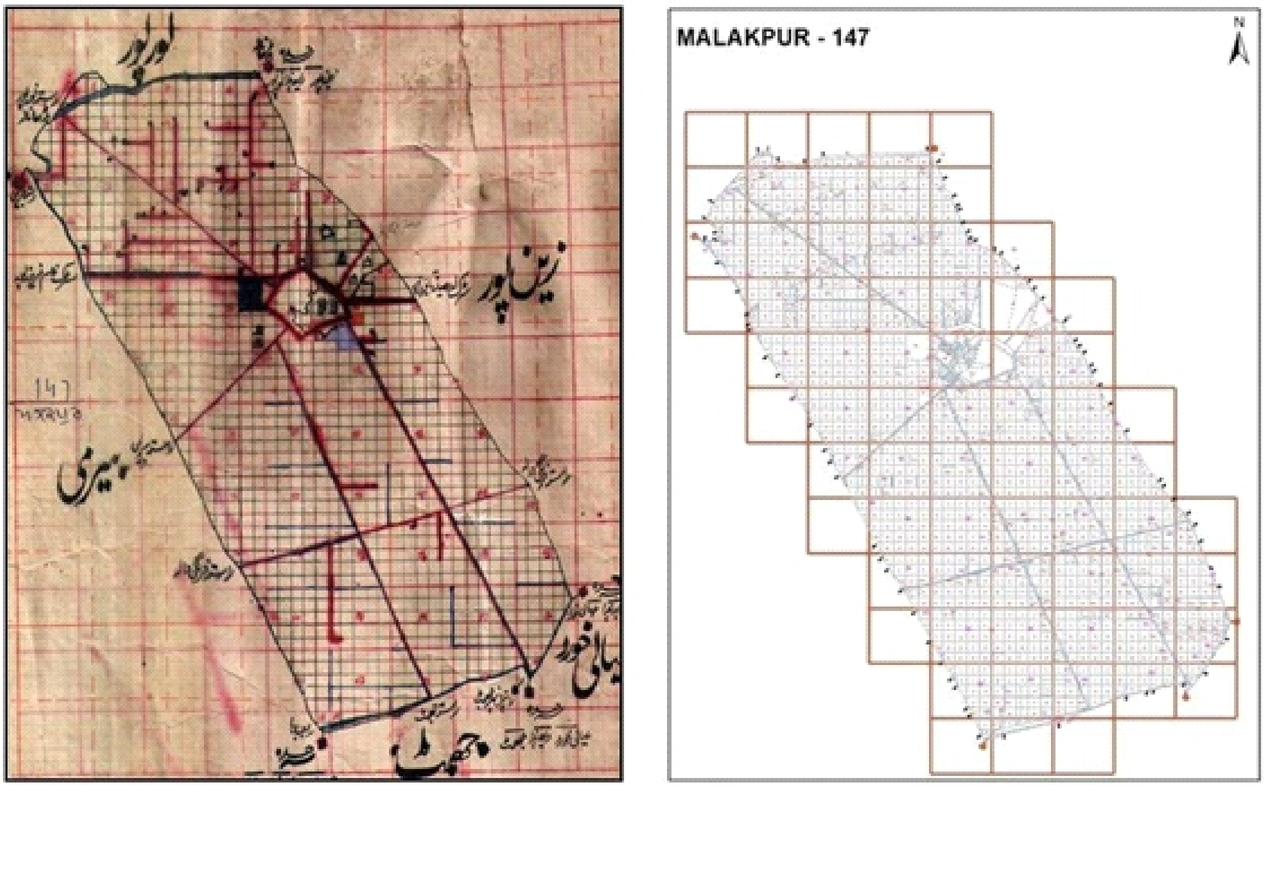

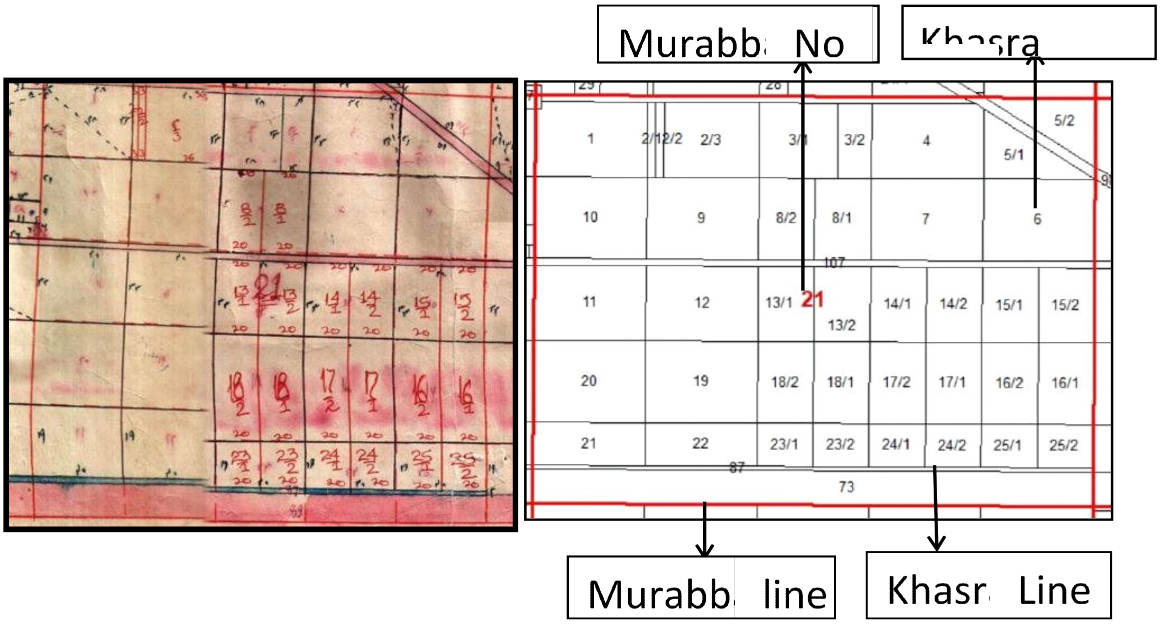

Figure 4: (a) Scanned Mussavi (b) Digitized Cadastral Map of Malakpur (c) Enhanced part of the village.

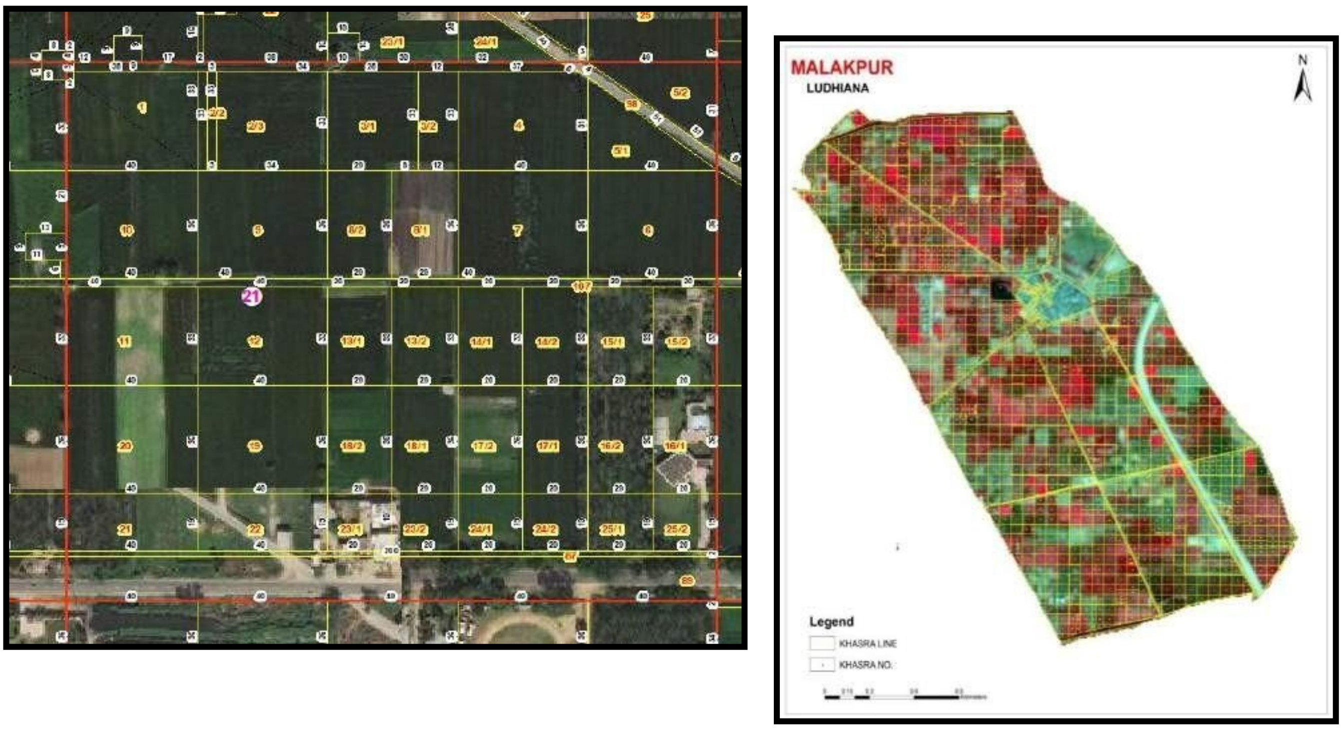

Figure 5: (a) Georeferenced Cadastral Map and (b) Enhanced section of the Georeferenced Cadastral Map.

Parcel Identifier

A unique identifier should be assigned to each parcel polygon. The parcel identifier provides a common index for all property records. Each parcel should have a unique identification or code that connects the cadastral layer to files that contain information like ownership, building and land value, usage, and zoning. Unique Identification was assigned to each feature in the GIS database, which might be numeric (Figure 6). This unique id linked all attribute data relating to the part was attached to raster data.

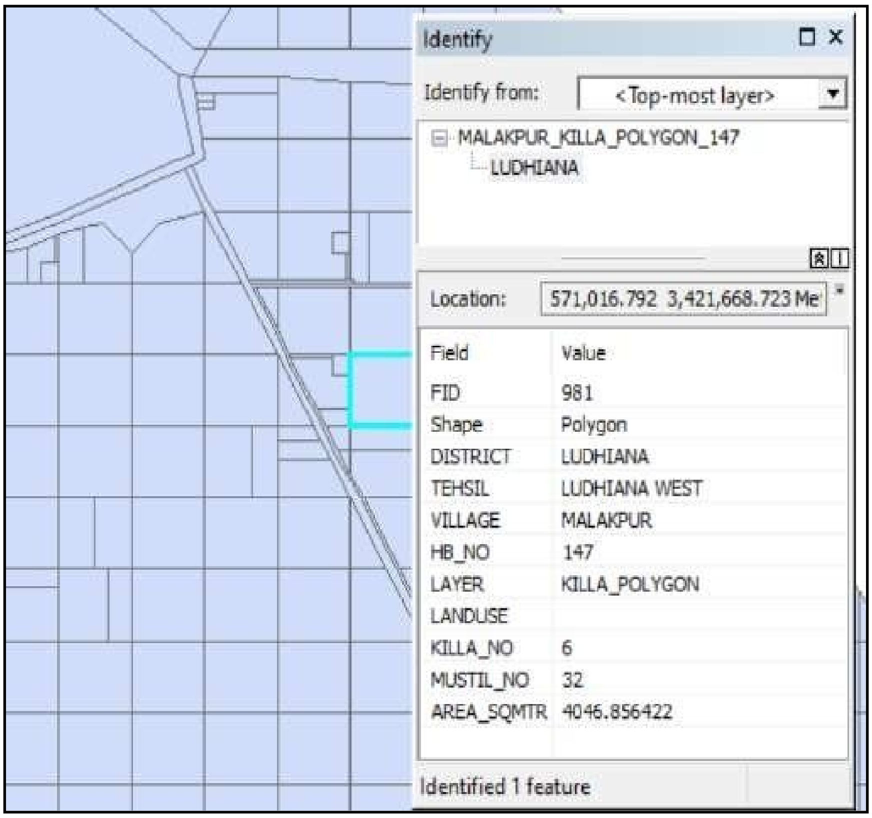

Figure 6: Parcel Information

RESULTS AND DISCUSSIONS

Phenological characteristics of different crop

Figure 7 shows the phenology curve for the land use classes in both datasets. The analysis has been carried out for the Kharif season (June to October). The NDVI value of Planet Scope and Sentinel 2 peaks in September for Rice crop. However, the NDVI value peaks in the maize crop in July and August. The vegetable class shows the two peaks, which show two crops grown in the same area. The phenological curves demonstrate a typical pattern for every crop and provide separation in the classes for accurate classification.

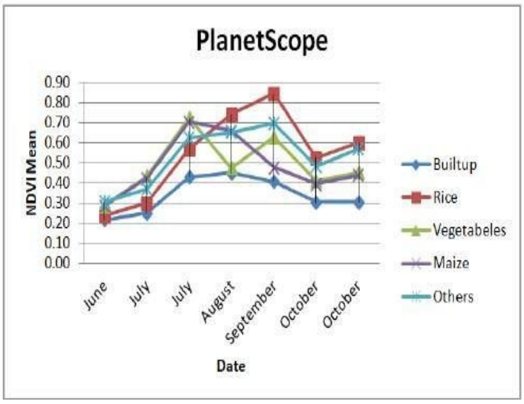

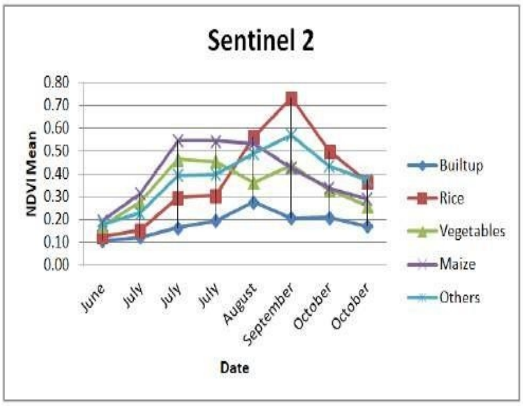

Fig. 7: NDVI curves of crops growing and other classes.

value, usage, and zoning. Unique Identification was assigned to each feature in the GIS database, which might be numeric (Figure 6). This unique id linked all attribute data relating to the part was attached to raster data.

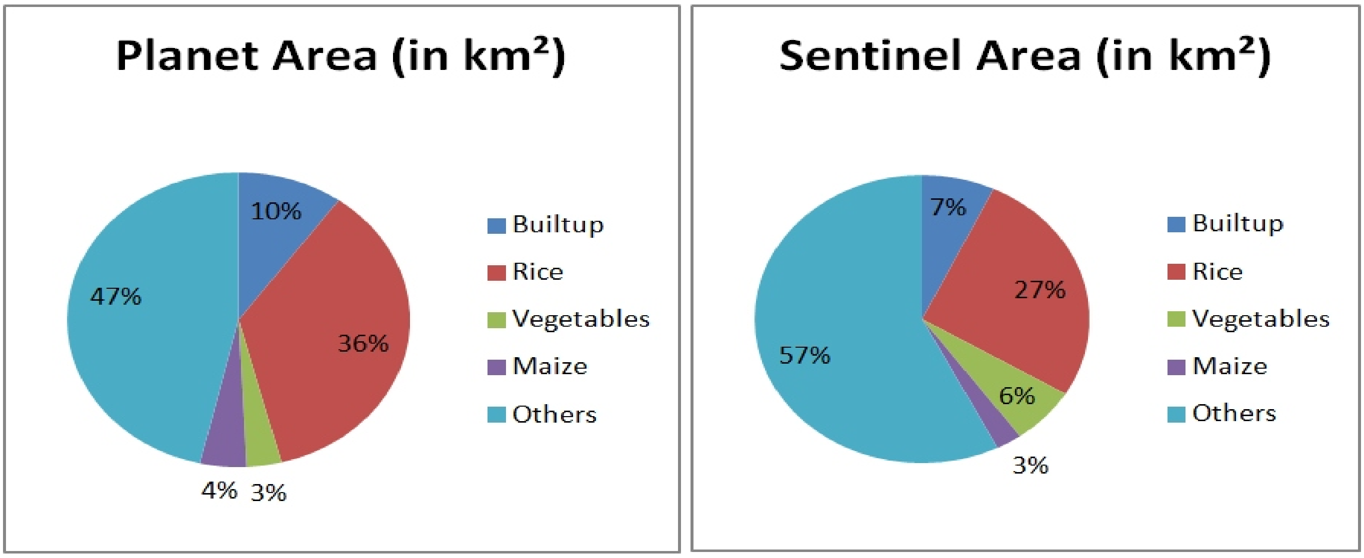

Fig. 8: Area of different classes in percentage.

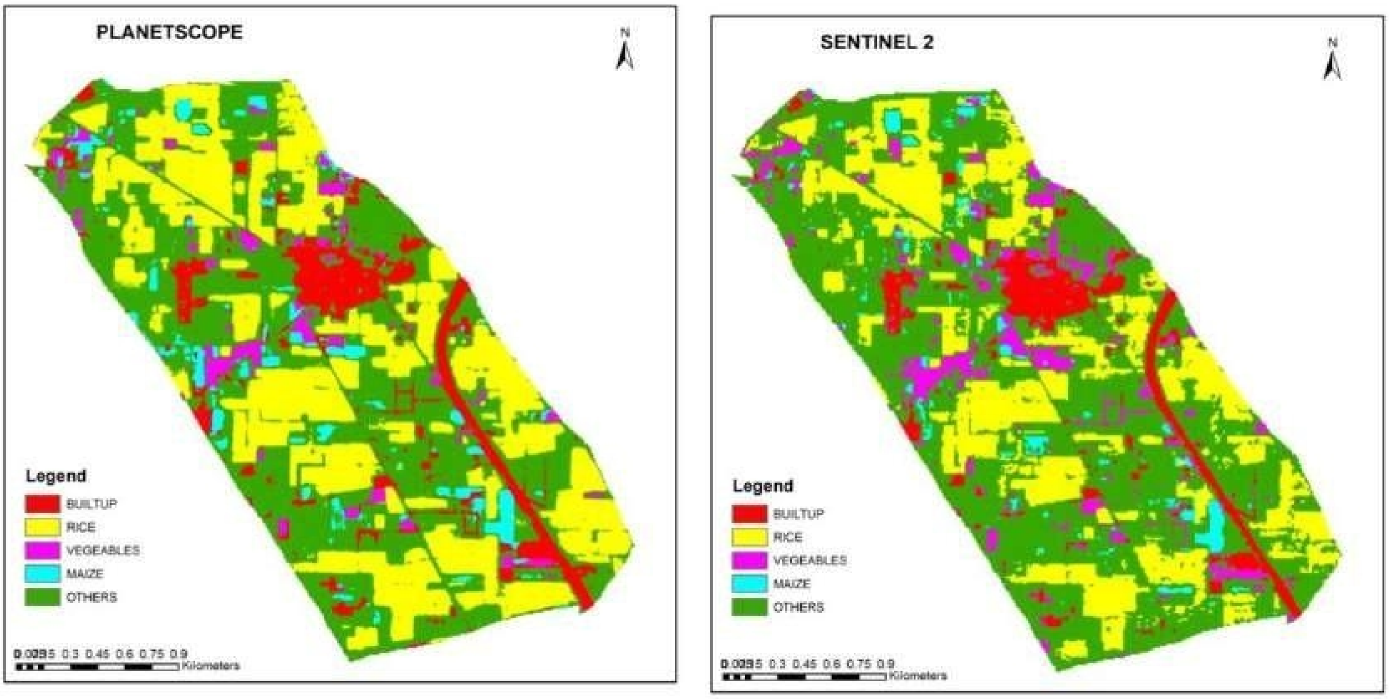

Figure 9: Supervised Classification of PlanetScope and Sentinel 2.

Parcel Based Analysis

The integration of digital cadastral data provides crop information at the Khasra level. This gives us an understanding of the spatial extent of different crops at the Khasra Level. Figure 10 shows number of Khasra containing the particular land use. The classified map from Planet data shows a better representation of classes than Sentinel data. It was observed that Planet data provide accurate class information at cadastral level data, whereas the sentinel data shows the mixing of classes at the Khasra level (Figure 11).

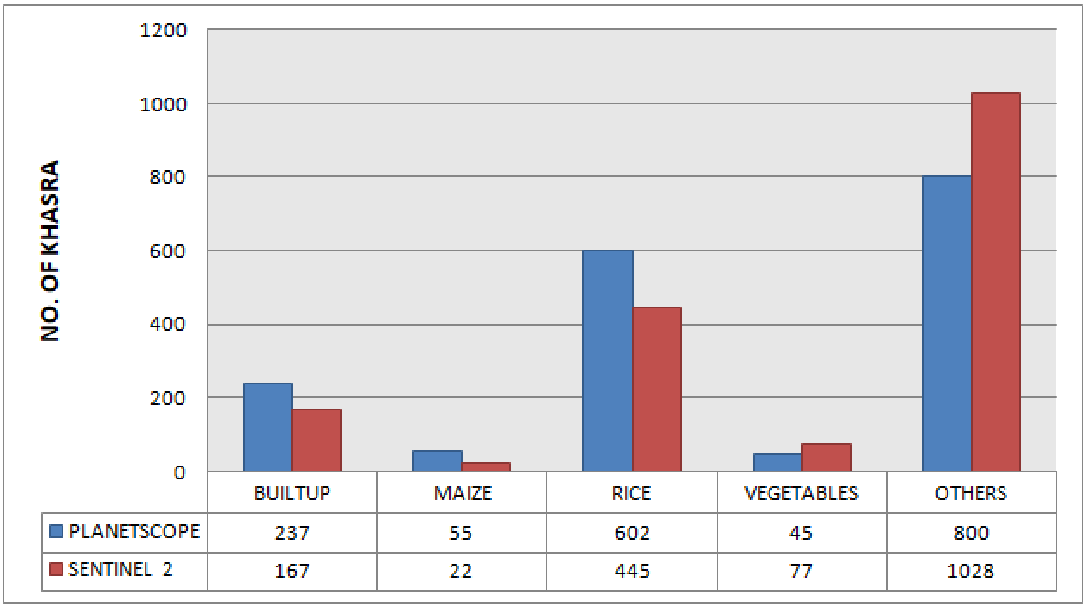

	BUILTUP	MAIZE	RICE	VEGETABLES	OTHERS
PLANETSCOPE	237	55	602	45	800
SENTINEL 2	167	22	445	77	1028

Figure 10: Khasra wise class information.

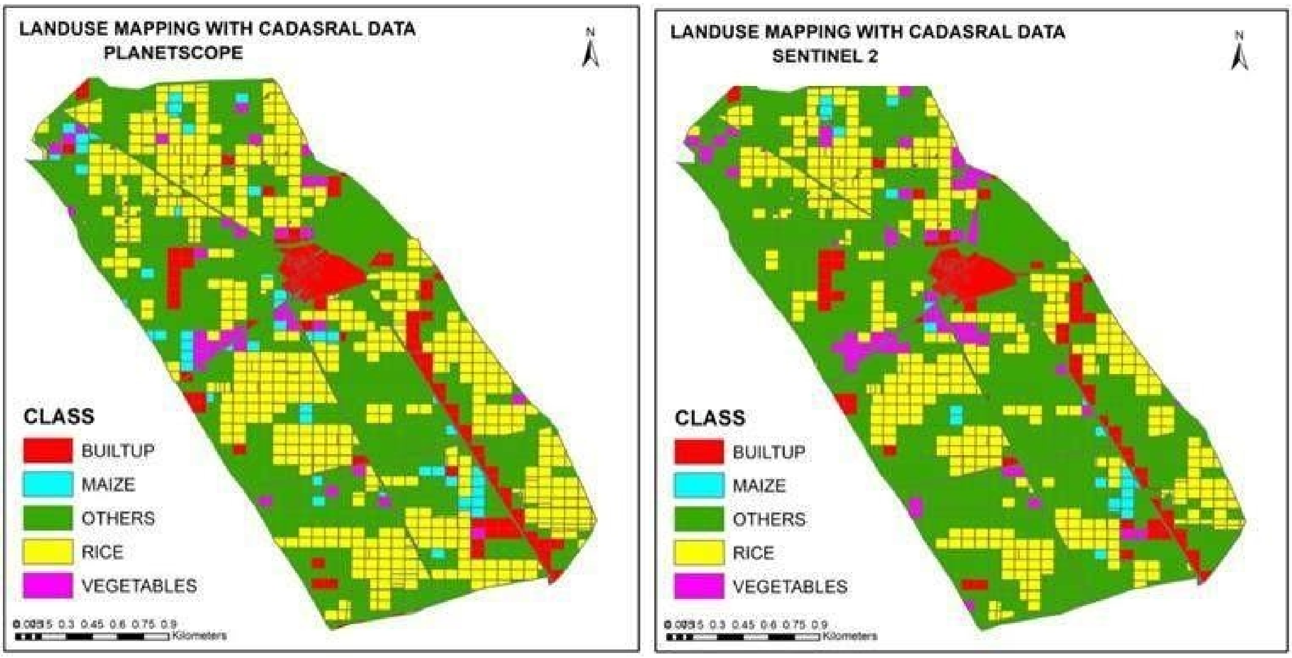

Figure 11: Khasra wise classified map PlanetScope and Sentinel 2.

This study provides a comparative analysis of two different satellite data and offers the compatibility of these data with the cadastral data. This study develops a cadastral information system using remote sensing and GIS to better the village-level land management system. The map was generated using remote sensing and overlay in GIS with the parcel boundaries map to illustrate that the satellite images correlate with Khasra. The present study provides cadastral-based crop classification analysis. The results find that the rice crop was grown significantly in the study area. The use of Planet data for crop classification on Field level will provide more accurate results. The Khasra wise crop information will help estimate the crop yield estimation at the field level. Cadastral-based information helps government and private agencies for better crop management and crop insurance.

Acknowledgement
We gratefully acknowledge the ESA for providing open access Sentinel data and authors thankful to the Department of Revenue, Rehabilitation and Disaster Management, Punjab for providing Cadastral Data.

Declaration of Conflicting Interests
The authors declared no potential conflicts of interest with respect to the research, authorship and publication of this article.

REFERENCE

1. **Aggarwal, P. K., Chand, R., Bhutani, A., Kumar, V., Goel, S. K., Rao, K. N., & Lochan, R.** (2016). Report of the Task Force on Enhancing technology use in agriculture insurance.
2. **Congalton, R. G., & Green, K.** (2019). Assessing the accuracy of remotely sensed data: principles and practices. CRC press.
3. **Demir, O., Nişanci, R., Atasoy, M., & Aydin, C.** (2003). Forming the digital cadastral maps from current cadastral data: the importance of the geodetic control points. In 2nd FIG regional conference, Marrakech, Morocco, December (pp. 2-5).
4. **Ford, K., Harris, J., Shives, R., Carson, J., & Buckle, J.** (2008). Remote predictive mapping 2. Gamma-ray spectrometry: A tool for mapping Canada's North. *Geoscience Canada*, *35*(3-4), 109-126.
5. **Griffiths, P., Nendel, C., & Hostert, P.** (2019). Intra-annual reflectance composites from Sentinel-2 and Landsat for national-scale crop and land cover mapping. *Remote Sensing of Environment*, 220, 135-151.
6. **Makkar, A., Chatli, A. S., Sharma, A., Kaur, P., Kaur, N., & Goswami, E.** (2018). Analysis of Soil Samples from Various Areas of Punjab. *International Journal of Research in Engineering, Science and Management.* 11(1), 496-498.
7. **Misra, A. K.** (2014). Climate change and challenges of water and food security. *International Journal of Sustainable Built Environment*, 3(1), 153-165.
8. **Mondal, M. S., Chakravatry, D., & Bandayopadhyay, J.** (2014). Cadastral Maps for Socio-Economic Data Visualization and Integration for Land Use in Raniganj Mining Areas. *International Refereed Journal of Engineering and Science (IRJES)*, *3*, 55-63.
9. **Park, S., & Song, A.** (2020). Discrepancy analysis for detecting candidate parcels requiring update of land category in cadastral map using hyperspectral UAV Images: A case study in Jeonju, South Korea. *Remote Sensing*, *12*(3), 354.
10. **Planet Team** (2017). Planet Application Program Interface: In Space for Life on Earth. San Francisco, CA. https://api.planet.com
11. **Roser, M., Ritchie, H., & Ortiz-Ospina, E.** (2013). World population growth. Our world in data.
12. **Rouse, J.W., Haas, R.H., Schell, J.A., and Deering, D.W.** (1973). Monitoring vegetation systems in the Great Plains with ERTS, p. 309–317. In: 3rd ERTS Symp. NASA AP-351. vol. 1. NASA, Wash., D.C.
13. **Saini, R., & Ghosh, S. K.** (2019). Analyzing the impact of red-edge band on land use land cover classification using multispectral RapidEye imagery and machine learning techniques. *Journal of Applied Remote Sensing*, 13(4), 044511.
14. **Schmidhuber, J., & Tubiello, F. N.** (2007). Global food security under climate change. Proceedings of the National Academy of Sciences, 104(50), 19703-19708.
15. **Singh, R. K., Kumar, P., Mukherjee, S., Suman, S., Pandey, V., & Srivastava, P. K.** (2021). Application of geospatial technology in agricultural water management. In Agricultural Water Management (pp. 31-45). *Academic Press.*
16. **Stone, M.L., Solie, J.B., Raun, W.R., Whitney, R.W., Taylor, S.L., and Ringer, J.D.** (1996). Use of spectral radiance for correcting in-season fertilizer nitrogen deficiencies in winter wheat. *Trans. ASAE*. 39(5):1623–1631.
17. **Williamson, I., & Enemark, S.** (1996). Understanding cadastral maps. *Australian Surveyor*, 41(1), 38-52.

Abbreviations Used

1. GIS - Geographic Information System
2. NDVI - Normalized Difference Vegetation Index
3. UTM - Universal Transverse Mercator
4. WGS84 - World Geodetic System 1984
5. LULC - Land Use and Land Cover
6. ERDAS - Earth Resource Data Analysis System
7. UAV - Unmanned Aerial Vehicle

www.nesa-india.org • E-mail: nesapublications@gmail.com
International Journal on Environmental Sciences

International Journal on Environmental Sciences 13 (2) Pp. 89-98, ***July-December 2022***
ISSN No.: 0976-4534
https://doi.org/10.53390/ijes.v13i2.5

MONITORING AND SIMULATING LAND USE/COVER CHANGES USING OPEN SOURCE MOLUSCE FOR LUDHIANA, PUNJAB, INDIA

Prince Dhiman*[1], Harpinder Singh[1], Nilesh Biwalkar[2], Syed Shabih Hassan[3]

*Remote Sensing & Geographic Information System, PAU, Ludhiana-141004, Punjab, India.
[1]Scientist, Punjab Remote Sensing Centre, Ludhiana-141004.
[2]Department of Soil and Water Engineering, PAU, Ludhiana-141004, Punjab, India.
[3]College of Fisheries, Guru Angad Dev Veterinary and Animal Sciences University, Ludhiana-141004, Punjab, India

Research Article

Received: **22.07.2022** Accepted: **08.08.2022** Published: **24.09.2022**

ABSTRACT

Accurate information on land use/land cover dynamics is needed for the selection and implementation of land use programs to meet the rising demands of basic human requirements and wellbeing. Land use land cover transition analysis is a rigorous approach that helps to understand physical and human involvement in the natural environment as well as sustainable development. Thus, the study aims to predict the land use/land cover of Ludhiana, Punjab state, for the year 2033 using the MOLUSCE plugin. Classified land use/land cover maps for the years 2009, 2015, and 2020 were prepared in the Google Earth Engine platform. The prediction model used these prepared classified maps along with four generated spatial variables maps i.e. slope, elevation, distance from road, and distance from water maps. According to the study, the built-up area might grow by 85.79 sq. km between 2020 and 2033. Forecasted reductions in vegetation, bare soil, and water class cover could total 23,91, 49,02, and 12,87 square kilometers, respectively. The results may help policymakers create the best land use strategies and improved management practices of natural resources.

Keywords: Land use, Land cover, Google Earth Engine, MOLUSCE.

INTRODUCTION

Land features on the earth's surface are referred to as land use and land cover, or LULC. Land use refers to how the land is used for various purposes, such as agricultural, industrial, and residential. In contrast, land cover refers to the primary forms of land, such as towns and built-up regions, forests, water bodies, and grasslands (Meyer et al. (13)). Natural land cover has evolved into man-made land cover due to human activities to gain the essentials of everyday existence. Humans have transformed the earth's surface for several centuries, but the land cover dynamics have changed significantly with the development of new machines and techniques (Hamad et al. (6)).

Land use applications involve baseline mapping and ongoing monitoring since timely information is needed to understand how much land is now used for what purposes and to track changes in land use over time. A few instances of how human exploitation of the environment explicitly impacts the regional ecosystem are urbanization, division of agricultural land, and elimination of green spaces. This pattern of changes in LULC mainly depends on the degree of urbanization. It is crucial to identify, delineate, and map the land cover for planning, resource management, and monitoring studies.

For decision-makers and planners, understanding urban land transformation is crucial. Developing nations usually lack this information as they use conventional survey and mapping procedures that are expensive and time-consuming to estimate urban expansion. Given its affordability and technological superiority, Remote Sensing (RS) is being utilized more frequently to monitor and analyses urban

*Corresponding author: *dhimanprince.hp17@gmail.com*

growth. While using satellite image data, RS has the potential to extract information about LULC in a given area (Yuan et al. (14)).

For the design and implementation of land-use policies, information about land use and land cover dynamics is necessary to meet the growing demands of human requirements and well-being. Modelling is a solution that may be used to handle the issue of conversion and modification of LULC classes. LULC transition models often try to predict the timing and frequency of these changes. Many land cover prediction studies have been done using various statistical and analytical models. Jayasinghe et al. (7) conducted a comparative study for available urban growth prediction models. For the study, three freely available models MOLUSCE (Modules for Land Use Change Simulations), SLEUTH (Slope, Land use, Exclusion, Urban, Transport and Hillshade), and FUTURES (FUTure Urban-Regional Environment Simulation) were compared based on their prediction results for Colombo. According to their study, the FUTURES model is considered the best to simulate future urban growth. Although there are many proprietary software for LULC modelling, MOLUSCE is the most popular free and open-source option (https://github.com/nextgis/molusce). MOLUSCE combines well-known methods that can be utilized in forestry applications, urban analysis, and land use/cover change analysis. It is well suited to analyze changes in land use and forest cover over time, model possible changes in land use in at-risk areas, and simulate future changes in land use and forest cover.

Saputra et al. (10) utilized MOLUSCE module for ANN-CA (Artificial Neural Network model-based cellular automata) modeling in their study to predict LULC in North Sumatra, Indonesia. The model used five factors, including soil type, aspect, altitude, distance from the road, and slope, for the training process to examine their effects on LULC changes between 1990 and 2000, and the model predicted maps for the years 2050 and 2070. The predicted maps showed increase of about 4 percent in plantation area. By 2050, it was anticipated that the area used for farming and forests will decline by 1.2 and 1.6 percent, respectively. Kamaraj et al. (9) identified the changes in land cover in the Bhavani basin, Tamil Nadu, between 2005 and 2015. They forecasted the possible land use map for 2025 and 2030 using the MOLUSCE plugin in QGIS software. They revealed an increase of 20 km2 and 10 km2, in farmland and built-up areas, respectively. Guidigan et al. (4) aimed to examine the LULC patterns for the Benin region using MOLUSCE. They obtained land cover maps and made a simulated map for the years 2025 and 2037. The findings of this study showed a significant decrease in Savannah land and a rapid growth in agriculture and forestland.

Abbas et al. (1) used satellite imagery from 1980 to 2020, regularly at a 10-year time gap. They also used many spatial factors like distance from the road, DEM, and distance from water for integration in the MOLUSCE plugin of QGIS software to predict and analyze the simulated map of the Greater Bay Area. The study's results showed significant urban growth from 4.75 per cent to 14.75 per cent over the past 40 years. Forests regions reduced from 53.49 per cent to 50.57 per cent, farmlands areas reduced from 21.85 per cent to 16.04 per cent, and grasslands reduced from 13.89 per cent to 12.05 per cent. Alrubkhi et al. (2) aimed to see how QGIS software combined with GIS methodologies may be used to identify, assess, and analyze LULC change between 2000 and 2010, as well as predict the future of LULC. MOLUSCE plugin was used to create area change maps and to prepare a simulated future map for 2025 using cellular automata simulation. The study's results revealed a growth in the urban area but a decrease in agricultural land. The forecast also suggested that agriculture would shrink by 1.49 percent by 2025.

Nugroho et al. (8) aimed this research to map out Malang City's urban growth over 24 years and to forecast the city's future development using an ANN model and the MOLUSCE QGIS plugin for the year 2027. Maps of land information for 2003, 2009, and 2015 were classified from Landsat ETM+ and OLI. The overall accuracy of classification and kappa coefficient was about 85% and 0.76, respectively, for all obtained maps. As per the predicted map of 2027, around 1049.58 hectares of farmland and 241.29 hectares of bare land in 2015 will be converted into built-up areas accounting for an increase in the urban area of 11.79 per cent.

According to the literature study, few studies have been done on measuring and analyzing LULC of the entire Ludhiana district of Punjab state. The district has experienced significant urbanization, industrialization, and population growth during the previous few decades. Therefore, the study's objective was a) classify the satellite imagery to generate the LULC maps of 2009, 2015 and 2020 b) analyze the LULC changes and c) prepare the simulated LULC map of 2033 for the Ludhiana district.

Study area and datasets

Study Area

The district of Ludhiana is situated in the central region of Punjab state (fig. 1). The area is bounded by latitudes of 30° 33' and 31° 01' North and longitudes of 75° 25' and 76° 27' East, respectively, and is on an average 244m above mean sea level. The district's geographic area is about 3706 square kilometers. The river Sutlej forms the district's northern boundary with the districts of Jalandhar and Hoshiarpur. The districts of Fatehgarh Sahib and Sangrur delineate the eastern and southern boundaries. In the west of the region is the district of Moga. According to the 2011 census, it has a population of around 3,498,739, making it the most populous district in the state.

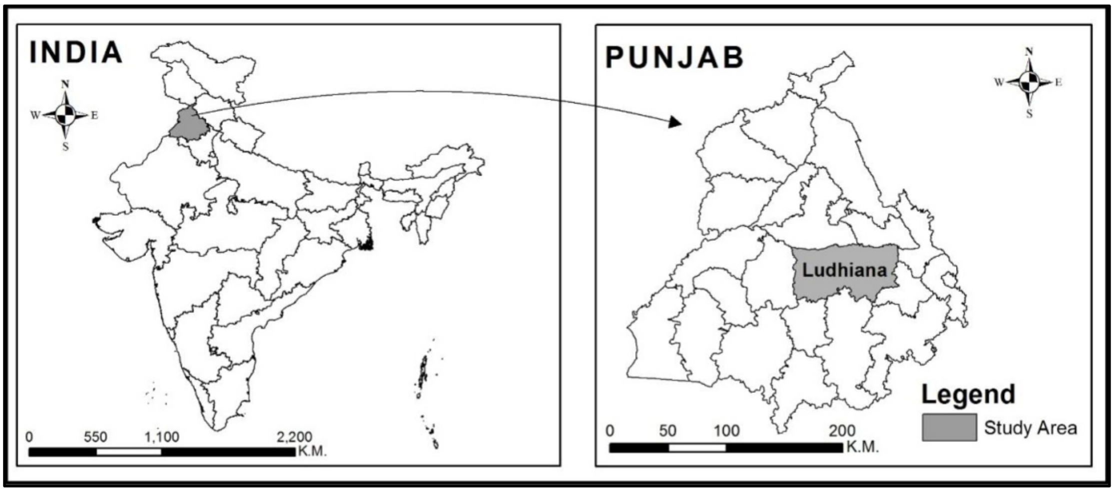

Fig. 1 Study area

Data

The atmospherically corrected surface reflectance Landsat 5 and 8 data was used for the preparation of the LULC maps of 2009, 2015 and 2020. The Landsat images courtesy of the U.S. Geological Survey, were obtained from Operational Land Imager/Thermal Infrared Sensors. These images contain five visible and near-infrared (VNIR) bands and two short-wave infrared (SWIR) bands processed to orthorectified surface reflectance, and two thermal infrared (TIR) bands processed to orthorectified brightness temperature.

The Japan Aerospace Exploration Agency (JAXA)'s free elevation dataset collection called the Advanced Land Observing Satellite (ALOS) (Tadono et al. (12)) World 3D-30m was used for the generation of slope and elevation maps. The slope, elevation, and Landsat imagery were obtained and processed in the cloud-based Google Earth Engine (GEE) platform.

Datasets regarding the major roads and water bodies (Canal network and Drainage) were sourced from the open street map (Haklay et al. (5)). These datasets were used to prepare the distance from the road, and distance from water maps. The distance from roads and water maps were processed in ArcGIS 10.4 software using the Euclidean distance tool.

Methodology

This section describes the methodology of the research work. The first step includes processing the satellite imagery and its classification for the LULC map preparation, while the second step includes the simulation and validation. GEE has been used for the first step, and QGIS and the MOLUSE plugin have been used for the second. The complete methodology of the research is presented in Figure 2.

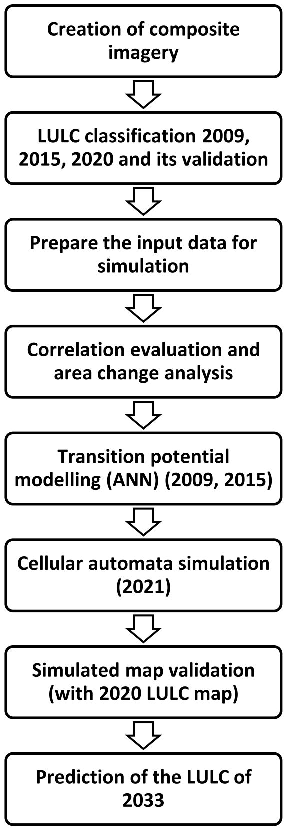

Fig. 2 Methodology

LULC Classification

Creation of composite imagery

Landsat imagery was selected for 2009, 2015, and 2020. The study used a Tier 1 surface reflectance Landsat dataset from the GEE repository. The period for filtering the imagery was selected as mid of January to the middle of February. This was done because the wheat crop was the greenest, and there was no inter-mixing of land classes during the classification. A median best composite image for a particular year was created, keeping the cloud cover percentage as low as possible. The image was further clipped for the area of interest (Fig 3).

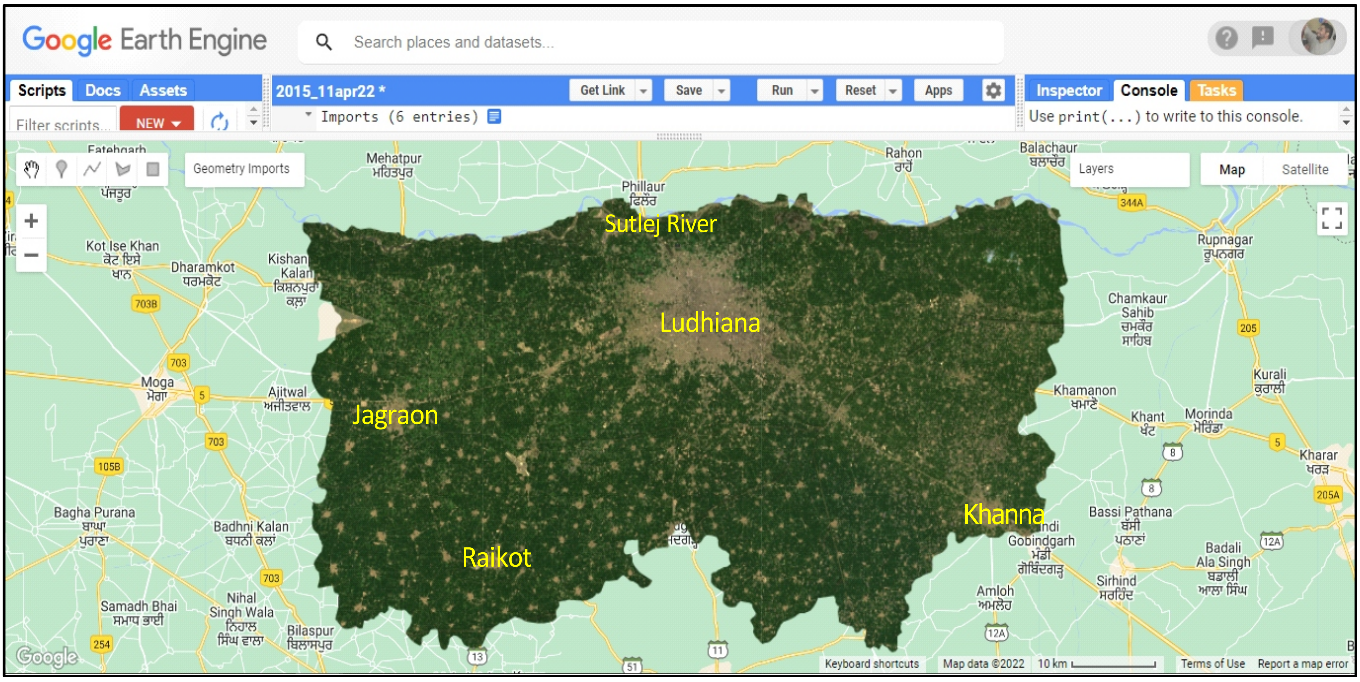

Fig 3: True Color Composite image (2015).

LULC Classification and Validation

The LULC classification was attempted on the composite imagery. LULC maps were prepared for 2009, 2015, 2020. A random forest algorithm was used for this purpose. For the classification, the imagery was categorized into four major classes (Table 1). For the preparation of the training and validation dataset for the classifier, manually ground control points (GCP) to the satellite imagery were marked for each class for various periods. Figure 4 shows various marked GCPs for the year 2015. Table 2 shows the number of GCPs marked for each imagery. The points were marked based on local knowledge and using Google Earth Pro software's time-series image visualization option. Eighty per cent of the total market points were used for the training and the remaining 20 per cent for validation purposes.

Accuracy assessment of the classified maps was done by creating a confusion matrix. The confusion matrix shows the number of pixels that were correctly or incorrectly categorized into each class. The confusion matrix was used to construct several metrics, including producer's accuracy (PA), user's accuracy (UA), overall accuracy (OA), and kappa coefficient (K). These indicators make it easier to assess the LULC classification's correctness objectively.

Table 1: LULC classification scheme.

LULC types	Description and color tone
Built-up	All infrastructures- houses, buildings, stadiums, sheds, warehouses, roads, etc. (red tone)
Vegetation	All agricultural land, forests, horticultural land, and plantations (green tone)
Bare Soil	All barren lands, vacant plots covered with shrubs, and playground grounds (yellow tone)
Water	All water bodies like rivers, canals and ponds (blue tone)

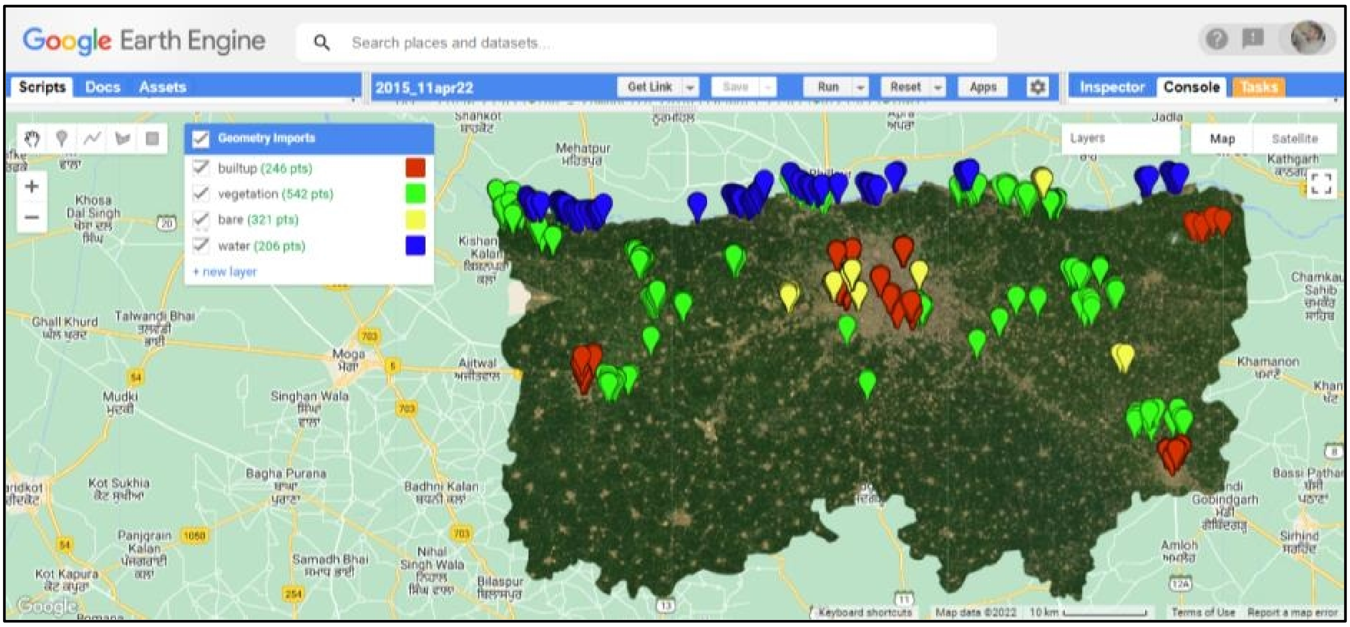

Fig 4: Marked training/validation dataset (2015).

Table 2: Number of marked training and validation GCPs

	2009	2015	2020
Built-up	238	246	463
Vegetation	432	542	526
Bare Soil	297	321	348
Water	202	206	324

Simulation

MOLUSCE plugin of QGIS software was used for the work of LULC simulation and prediction.

Input data preparation

The first step includes the input of the LULC maps for the starting year and the ending year, i.e. 2009 and 2015, respectively. Four spatial variable elements were also added: elevation map, slope map, distance from the road, and distance from water areas. The properties of the spatial variables were matched with the LULC maps before adding to the plugin. A summary of the explanatory data used in the study is shown in Table 3.

Table 3: Summary of the explanatory data used in the study.

Data	Criteria	Purpose	Source	Description
DEM	Slope	Explanatory map	ALOS JAXA	30m spatial resolution
	Elevation	Explanatory map	ALOS JAXA	30m spatial resolution
Road Map	Distance from the road	Explanatory map	OpenStreetMap	The road map of Ludhiana district
Water bodies map	Distance from the water body (Canal, Drain)	Explanatory map	OpenStreetMap	The water map of Ludhiana district

Correlation evaluation and area change analysis

Pearson's correlation was calculated to assess the geographic variable correlation among the two LULC maps and the spatial variables.

The area change analysis was done to analyze the LULC changes in the area between the initial (2009) and the final year (2015). The area change map was also generated along with the transition matrix, which shows the percentage of pixels switching between LULC classes.

Transition potential modelling

The transition probability for various classes is modelled in this stage using available methods. There are several ways to compute probable transition maps. MOLUSCE plugin offers the Artificial Neural Network (ANN), Weights of Evidence (WoE), Logistic Regression (LR), and Multi-Criteria Evaluation (MCE) approaches. Each method uses LULC change data and spatial variables as inputs for calibrating and modelling LULC changes. In this study, ANN was used to model the transition probability.

ANN algorithm works on a back-propagating learning-based iterative neural network. The neural network structure comprises three layers the input, hidden, and output. Each neuron in the output layer produces a transition probability from one form of land use to another at each cycle. By comparing the transition probability values, it is possible to predict how LULC will change from one type to another, with the highest transition probability being the new type. The corresponding cell's state is unaffected if the same type of LULC has the highest transition probability (Saputra et al. (10)).

$$P(k,t,l) = \sum_j w_{j,l} \frac{1}{1+e^{-net_j(k,t)}},$$

ANN follows the below equation to calculate the transition probability:

Where wj, l is the weight between the hidden and the output layers and P(k, t, l) is the probability of conversion from the current to the lth kind of LULC for the k-th cell at time t.

ANN model used in this study had a learning rate of 0.1, number of samples of 1000, maximum iterations of 1000 and momentum of 0.05. The optimal neural network gets stored in the memory after the learning algorithm analyses the achieved accuracy on training and validation sets of samples. Training is supposed to be completed when the highest accuracy is attained.

Cellular automata simulation

Once the transition probability has been determined, the Cellular Automata (CA) simulates the LULC. The CA simulation module provided a simulated map based on the number of iteration/s. The number of simulations should be 1 to get a simulated 2021 LULC map.

Based on four key components, the CA simulates the LULC for 2021. The components are C, n, K, and R, where C stands for pixels, n for the number of classes, K for the size of the Moore neighbourhood, and R for the transition potential maps (TPMs) (Aneesha et al. (3). In this step, the CA model identifies the 2009 and 2015 pixels with the highest TPMs values produced by transition potential modelling. This step and the transition potential modelling step are related to each other. The simulated LULC classes are created using a black box approach. The simulation resulted in a LULC map for 2021 showing the defined classes.

Validation

The MOLUSE's validation module was finally used to check and validate the simulated image of 2021. It was done using a map comparison with the classified 2020 LULC. The overall accuracy (% of correctness), kappa (overall), kappa (histo) and kappa (loc) were calculated in the end.

Once satisfactory accuracy was achieved, the simulation step of the cellular automaton to forecast future LULC was re-executed. The prediction year is determined by multiplying the iterations by the second year minus the first year. The iteration values in this study were taken as 3 for simulating the LULC of 2033.

RESULTS AND DISCUSSION

Classified LULC maps and validation

The LULC maps were prepared by classifying the Landsat satellite imagery. This study produced three 30m LULC maps of the Ludhiana district for 2009, 2015, and 2020 (Fig 4a, 4b, and 4c, respectively). Further, the confusion matrix for the classified maps was generated to validate the classified maps (Table 4). The overall accuracies of 2009, 2015, and 2020 classified maps were found to be 99.5%, 96.1%, and 95%, respectively. The kappa coefficient was also calculated for 2009 (0.994), 2015 (0.945), and 2020 (0.933). The results show that the 2009 LULC was classified with the best accuracy.

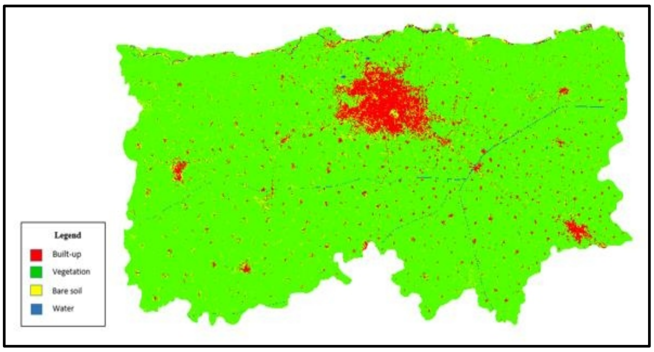

Fig. 4(a): Classified Image of 2009.

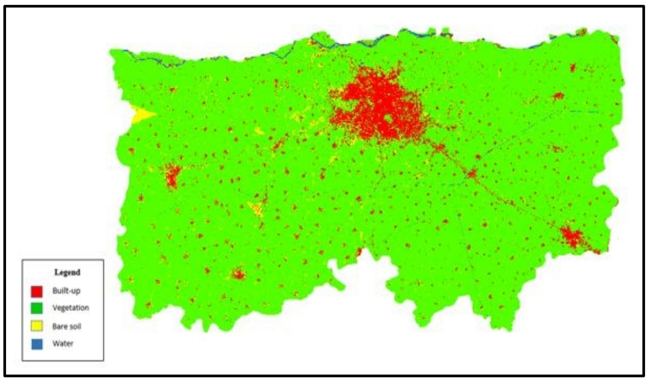

Fig. 4(b): Classified Image of 2015.

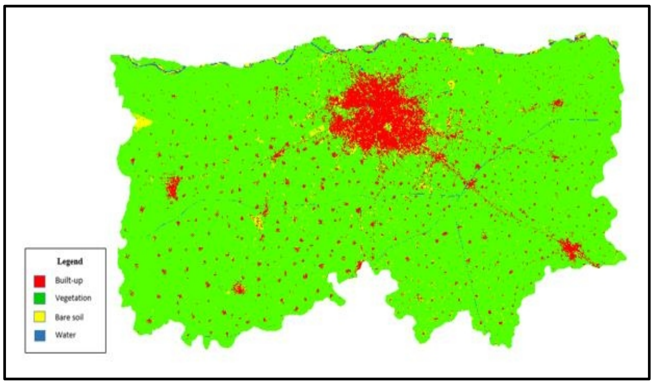

Fig. 4c : Classified Image of 2020.

Table 4 Accuracy assessment results

Year	Predicted class					PA	Overall accuracy	Kappa
	True class	Built-up	Vegetation	Bare Soil	Water			
2009	Built-up	50	0	0	0	1	0.995	0.994
	Vegetation	0	80	0	0	1		
	Bare Soil	0	1	55	0	0.982		
	Water	0	0	0	49	1		
	UA	1	0.98	1	1	-		
2015	Built-up	48	2	0	0	0.96	0.961	0.945
	Vegetation	2	100	3	0	0.952		
	Bare Soil	2	0	45	0	0.957		
	Water	0	0	0	34	1		
	UA	0.923	0.98	0.937	1	-		
2020	Built-up	92	0	2	0	0.978	0.95	0.933
	Vegetation	5	96	2	3	0.905		
	Bare Soil	1	2	63	0	0.954		
	Water	0	1	0	59	0.983		
	UA	0.938	0.969	0.940	0.951	-		

Spatial variables

Euclidean distance tool helped create distance from road and water bodies maps. Slope and elevation maps were generated from the DEM dataset in the GEE database. These spatial variables maps (Fig 5) significantly impacted the simulation model.

Area change statistics

A summary of the LULC change trend from 2009 to 2020 for each class is shown in Table 5. The increase in built-up land is noticeable and indicates an increasing trend. According to classed maps, only 196.84 sq. km., or 5.31% of the entire study region, was built-up land in 2009. 91.43% of the area was seen covered with vegetation class (3389.28 sq. km). Bare soil and water cover correspond to about the remaining 2.83% and 0.43%, respectively. In 2015, an increase of 50.64 sq. km was seen in the built-up class, accounting for 247.49 sq. km (6.67% of total area) and a decrease of 34.29 sq. km in the vegetation land (3355sq. km). Bare soil and water cover were noticed to be decreasing (Table 5). However, compared to 2015, water cover grew by 5.61 sq. km in 2020 (19.98 sq. km in total). The built-up area reached 269.37 sq. km, and vegetative land decreased to 3343.54 sq. km.

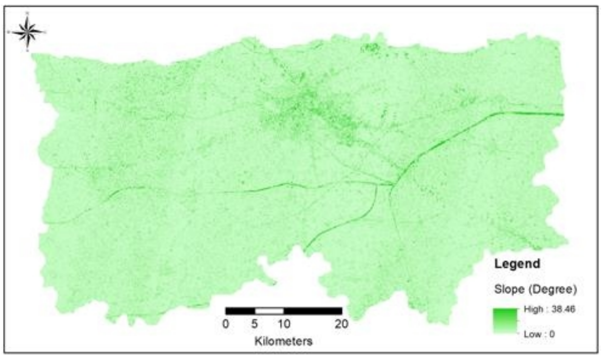

(a)

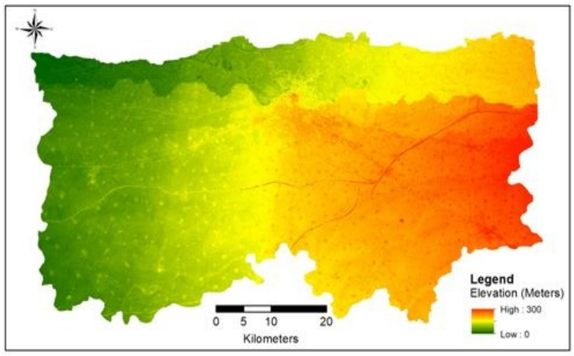

(b)

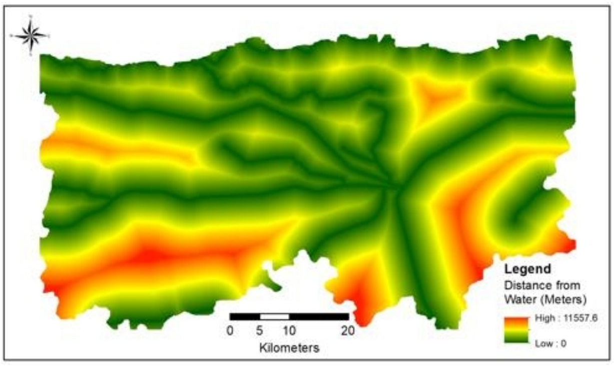

(c)

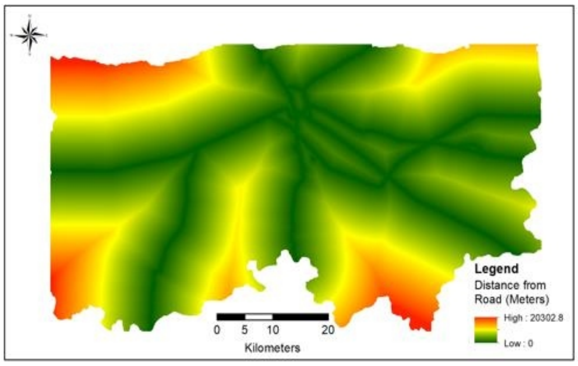

(d)

Fig. 5: Spatial variables maps (a) slope (b) elevation (c) distance from water (d) distance from road.

Table 5: LULC analysis from 2009 to 2020.

LULC Classes	2009		2015		2020	
	Area in km^2	% area covered	Area in km^2	% area covered	Area in km^2	% area covered
Built-up	196.84	5.31	247.48	6.67	269.37	7.27
Vegetation	3389.28	91.43	3355.00	90.5	3343.54	90.19
Bare Soil	104.86	2.83	90.24	2.44	74.20	2.0
Water	16.11	0.43	14.37	0.39	19.98	0.54

Simulation and its validation

With the spatial variables and the input 2009 and 2015 LULC maps, the MOLUSCE plugin's CA provided a 2021 simulated map. The simulated 2021 map was compared with the classified 2020 map to validate the CA model. The validation results showed 93.76 per cent of correctness (Fig 6) with a kappa value of 0.63. The validation results were considered good, and with the same CA model, the simulated 2033 map was generated by giving three iterations in the cellular automata simulation step. Figure 7 shows the predicted 2033 LULC map.

Fig. 6: Validation results.

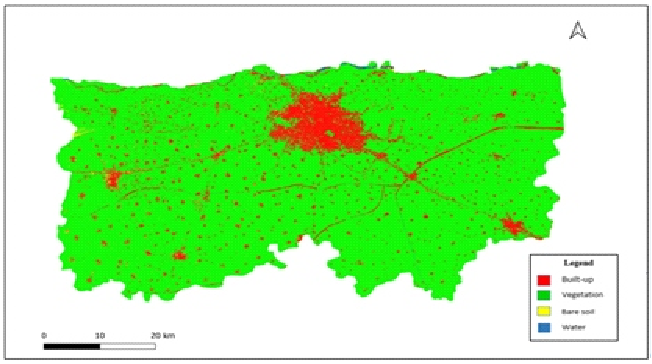

Fig. 7: Predicted LULC map (2033).

The changes in land cover classes between 2020 and predicted 2033 are presented in Table 6. Area change among the total land area was also analysed. A positive change value indicates an increase in area, whereas a negative value indicates that it has reduced. The study finds that the built-up area might increase by 85.79 sq. km in 2033 compared to 2020. The forecasted vegetation, bare soil and water class cover may reduce by 23.91 sq. km, 49.02 sq. km and 12.87 sq. km, respectively.

The study analysis revealed that generally, when one classification's area grows, the areas of other classes decrease and vice versa.

Table 6: Change in land classes between 2020 and predicted 2033.

	Class	2020	2033	Δ	2020%	2033%	Δ %
1	Built-up	269.37 sq. km.	355.16 sq. km.	85.79 sq. km.	7.26	9.58	2.31
2	Vegetation	3343.54 sq. km.	3319.63 sq. km.	-23.91 sq. km.	90.19	89.54	-0.64
3	Bare Soil	74.20 sq. km.	25.19 sq. km.	-49.02 sq. km.	2.00	0.67	-1.32
4	Water	19.98 sq. km.	7.11 sq. km.	-12.87 sq. km.	0.53	0.19	-0.34

Kalota (2015) made an effort to use landscape metrics to evaluate urban sprawl in the Ludhiana city. From 1955 to 2009, built-up areas were seen to have excessive and unplanned growth. According to the study, the city has grown rapidly due to the lack of planning and the unexpected influx of migrant labourers during the period. Most of the city's urban growth was centred in the southwest corner. According to the results, the urban area has grown dramatically and haphazardly from 1955 to 2009.

For the years 1955, 1979, 1989, 1999, 2009, and 2015, (Singh et al. (11)) calculated the annual percentage growth rates of the built class and population for the Ludhiana district. They examined that the percentage of growth rate in built-up regions was ten or more between 1955 and 1979, which fell to 6% and 4% between 1989 and 1999. The average growth rate of populated areas was noticed to be 8% overall per year.

The following studies have been conducted for Ludhiana city. Our study is for the whole district, and according to our results also, the built-up is increasing rapidly, and maximum built-up growth has been witnessed in and around Ludhiana city. A similar trend is also seen for the future.

The study's findings can be utilized as a preliminary s tep by government officials, city planners, and all other decision-makers involved in the process of preparing urban spatial planning and environmental sustainability.

CONCLUSION

Information about land use and land cover dynamics is required for the design and implementation of land-use policies in order to meet the rising demands of human needs and well-being. The prediction of LULC crucially influences plans for balancing pressures from development, conflicting users, and conservation. Thus, the ANN-CA model in the MOLUSCE plugin of QGIS software was utilized to predict the LULC map for the Ludhiana district. Firstly, the GEE cloud platform was used to prepare the LULC maps for 2009, 2015, and 2020. The LULC maps showed good classification accuracy, with the kappa ranging from 0.93 to 0.95. The classified maps, along with spatial variables maps viz. slope, elevation, distance from the road, and distance from water bodies, were used in the ANN-CA simulation model. The model gave 93.76 per cent of correctness results on validation. The model used 2009 and 2015 maps for predicting the 2033 LULC map. The study concludes that, compared to 2020, the built-up area might rise by 85.79 sq. km in 2033. Vegetation, bare soil, and water class cover may decrease by 23.91 sq. km, 49.02 sq. km, and 12.87 sq. km, respectively.

This type of research helps us identify specific land-use changes and predict which land use will be impacted in the future to understand potential ecological risks and biodiversity loss. However, this study does not consider other factors affecting LULC changes, such as climate, policy, regulation, or human development. Therefore, incorporating those characteristics in future research will improve the results.

Conflict of interest: The authors declare that they have no competing interests.

Acknowledgement: The authors would like to thank Punjab Remote Sensing Centre, Ludhiana, along with Punjab Agricultural University, Ludhiana for their support in this research and useful discussions.

REFERENCES

1. **Abbas Z, Yang G, Zhong Y, Zhao Y.** Spatiotemporal Change Analysis and Future Scenario of LULC Using the CA-ANN Approach: A Case Study of the Greater Bay Area, China. *Land*. 2021 Jun;10(6):584.
2. **Al-Rubkhi AN, Talal AA, Mohammed AB.** Land Use Change Analysis and Modeling Using Open Source (QGis)-Case Study: Boasher Willayat. Muscat: College of Arts and Social Science, Department of Geography, Sultan Qaboos University. 2017.
3. **Aneesha Satya B, Shashi M, Deva P.** Future land use land cover scenario simulation using open source GIS for the city of Warangal, Telangana, India. *Applied Geomatics*. 2020 Sep;12(3):281-90.
4. **Guidigan ML, Sanou CL, Ragatoa DS, Fafa CO, Mishra VN.** Assessing land use/land cover dynamic and its impact in Benin Republic using land change model and CCI-LC products. *Earth Systems and Environment*. 2019 Apr;3(1):127-37.
5. **Haklay M, Weber P.** Openstreetmap: User-generated street maps. IEEE Pervasive computing. 2008 Oct 17;7(4):12-8.
6. **Hamad R, Kolo K, Balzter H.** Land cover changes induced by demining operations in Halgurd-Sakran National Park in the Kurdistan Region of Iraq. *Sustainability*. 2018 Jul 11;10(7):2422.
7. **Jayasinghe P, Kantakumar LN, Raghavan V, Yonezawa G.** Comparative Evaluation of Open Source Urban Simulation Models Applied to Colombo City and Environs in Sri Lanka. *International Journal of Geoinformatics*. 2021 Jun 1;17(3).
8. **Nugroho AB, Hasyim AW, Usman F.** Urban growth modelling of Malang city using artificial neural network based on multi-temporal remote sensing. *Civil and Environmental Science Journal* (CIVENSE). 2018 Oct 2;1(2):52-61.
9. **Kamaraj M, Rangarajan S.** Predicting the future land use and land cover changes for Bhavani basin, Tamil Nadu, India, using QGIS MOLUSCE plugin. *Environmental Science and Pollution Research*. 2022 Feb 3:1-2.
10. **Saputra MH, Lee HS.** Prediction of land use and land cover changes for north sumatra, indonesia, using an artificial-neural-network-based cellular automaton. *Sustainability*. 2019 May 28;11(11):3024.
11. **Singh R, Kalota D.** Urban sprawl and its impact on generation of urban heat island: A case study of Ludhiana city. *Journal of the Indian Society of Remote Sensing*. 2019 Sep;47(9):1567-76.
12. **Tadono T, Ishida H, Oda F, Naito S, Minakawa K, Iwamoto H.** Precise global DEM generation by ALOS PRISM. *ISPRS Annals of the Photogrammetry, Remote Sensing and Spatial Information Sciences*. 2014;2(4):71.
13. **Meyer WB, Turner BL.** Land-use/land-cover change: challenges for geographers. *GeoJournal*. 1996 Jul;39(3):237-40.
14. **Yuan F, Sawaya KE, Loeffelholz BC, Bauer ME.** Land cover classification and change analysis of the Twin Cities (Minnesota) Metropolitan Area by multitemporal Landsat remote sensing. *Remote sensing of Environment*. 2005 Oct 15;98(2-3):317-28.

www.nesa-india.org • E-mail: nesapublications@gmail.com
International Journal on Environmental Sciences

International Journal on Environmental Sciences 13 (2) Pp. 99-106, ***July-December 2022***
ISSN No.: 0976-4534
https://doi.org/10.53390/ijes.v13i2.6

ANALYZING THE IMPACT OF BUILT UP AND GREEN SPACES ON LANDSURFACE TEMPERATURE WITH SATELLITE IMAGES IN JALANDHAR SMART CITY

Yukti Prashar[1], Reenu Sharma[1], Sumit Kumar[1], Syed Shabih Hassan[2] and Brijendra Pateriya[1]

[1]Punjab Remote Sensing Centre, Ludhiana-141004 (Punjab) India
[2]College of Fisheries, Guru Angad Dev Veterinary and Animal Sciences University
Ludhiana-141004 (Punjab) India

Research Article

Received: **10.09.2022** Accepted: **22.09.2022** Published: **02.10.2022**

ABSTRACT

Land use in developing nations is shifting as a result of rapid urbanisation. The ecosystem is being harmed by the unplanned, urban development of cities. Utilizing data from Landsat, the present research examined the spatiotemporal urban growth in Jalandhar City and its impact on variations in land surface temperature (LST). The results indicate that urban regions have increased while urban green spaces have shrunk (UGS). UGS and LST have been found to be inversely correlated. Where there was a low percentage of urban areas and a high percentage of accessible green spaces, it was observed that the LST decreased. The link between spectral variability and changes in vegetation growth rate was studied using the NDVI (Normalized Difference Vegetation Index). It works on tracking the growth of green vegetation and spotting variations in the amount of greenery. Where NDVI value was low, the scatter plots indicate higher surface temperatures. The dense urban regions with little available vegetation cover were linked to the low NDVI number and the NDVI is negative in the urban area of Jalandhar. High NDVI values indicate regions with dense vegetation and low surface temperatures. The research findings of present study could be applied to urban administration, planning, management and research projects.

Keywords: LST, NDVI, Urban Expansion, Urban Green Spaces, Urban Heat Island, Landsat.

INTRODUCTION

On a global scale, urban regions currently reside 56.2 percent of the population. According to the UN-Habitat World Cities study, the future population growth will be concentrated in cities. From 2018 to 2050, about 35% of predicted urban population growth will be centered in India, China, and Nigeria – In India, the metropolitan cities, urban centers, and expanding urban infrastructures are increasingly subject to aggressive urbanization . This increasing urban area in the cities can be defined as Urban Sprawl ' . It is characterized by single-use, scattered low-density residential areas due to planned or unplanned urban development. The unplanned urban sprawl leads to high carbon emissions, reduction in green spaces and poor infrastructural development — . These expanding urban zones are responsible for transforming natural surfaces into urban areas, affecting evapo-transpiration, albedo, surface emissivity; anthropogenic heat flow, wind speed, and air pollution, among other physical and biophysical features – . Changes in these characteristics can change the local and regional climate in the long run .

Urban Heat Islands (UHI) are the most visible example of local climate alteration caused by urbanization ' . Urban areas have higher temperatures than non-urban areas. This phenomenon leads to the difference between urban and rural temperatures. The intensity of UHI is primarily determined

*Corresponding author: *reenusharma30@gmail.com; reenusharma@prsc.gov.in*

by the urban geometry and the capacity of the urban fabric to absorb heat . UHI occurs when natural green areas are replaced with grey surfaces (concrete). The impervious and concrete surface absorbs incoming solar radiation and increases the surface temperature . This UHI can directly impact city dwellers' thermal comfort and health. Additionally, UHI has been linked to increased energy demand for cooling, increased day and night temperature, and heat-related mortality and sickness. Remote sensing data has been extensively used to analyze LST in relation to green spaces and built-up areas. Landsat data has been widely used for the retrieval of LST due to its long time series archive ' . The Landsat data provides high-resolution thermal data making it fit for analyzing local or city level studies '—' . This study aims to use remote sensing data to examine urban expansion and its effects on surface temperature. The objectives of this study were (i) Time Series land use land cover analysis of Jalandhar city from 2000 to 2020. (ii) Spatial pattern and correlation of NDVI and LST.

1. MATERIAL AND METHODS

2.1. Study area

Jalandhar city lies in the north-eastern part of Punjab (India), located between 35°59´ and 31°37´ N latitudes and 75°04´ and 75°57´E longitudes and it covers area around 99.79 km² in (Fig.1).The city is part of the Trans-Indian Ganges Plain, the terrain is almost flat, and the area's soil is very fertile. The climate of Jalandhar can be classified as tropical and dry sub-humid. The maximum temperature varies from 19.4°C in January and 40°C May and June. The average annual rainfall in the area was about 569 mm. Maximum precipitations is obtained from the southwest monsoon.The Jalandhar city is developing as important industrial and commercial hub in India . The detailed methodology chart has been shown in (Fig. 2).

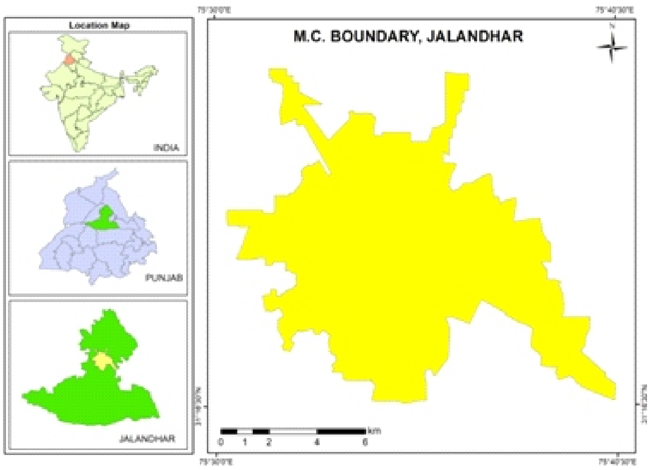

Fig. 1:Study area map of Jalandhar city.

2.2. Satellite data and image pre-processing

The Landsat data were was used in this study, including Landsat 5 Thematic Mapper (TM) and Landsat 8 Operational Land Imager (OLI) satellite images. These images were downloaded from the United States Geological Survey (USGS) Earth Explorer site of 2000, 2010 and 2020. Landsat 5 (TM) provides spectral information in seven bands: band 1, 2 and 3 (blue, green and red) obtained in the visible range, band 4 in the Near Infrared (NIR) and band 6 is a thermal infrared band (TIR) with 120 m spatial resolution. Landsat 8 (OLI) acquires the images in 11 spectral bands: band 2, 3 and 4 (blue, green and red) in visible range, band 5(NIR) and 10 and 11 (TIRS) thermal infrared bands) with 100 m spatial resolution while other bands with 30m spatial resolution. The remote sensing images were first pre-processed for atmospheric correction. There after Layers stacking, and image subset were undertaken.

2.3. Land Use Land Cover Classification and Change Analysis

Many Studies reviewed to select the best and most appropriate classification method in which supervised classification methods have been widely used —— (Adam et al., 2014; Bokaie et al., 2016; Kaul & Sopan, 2012; Shahtahmassebi et al., 2021; Talukdar et al., 2020).The pre-processed images were used as inputs in image classification. The maximum likelihood classifier has been used for the land use land cover classification. The training sample collected for the classification were spread around the whole image and pure classes were selected. These training samples provides variability within the class and between the other classes. In the classification, two classes' i.e.,built-up and non-built-up or green spaces were selected for LULC classification. The output results land cover changes and time series variations were studied for Jalandhar.

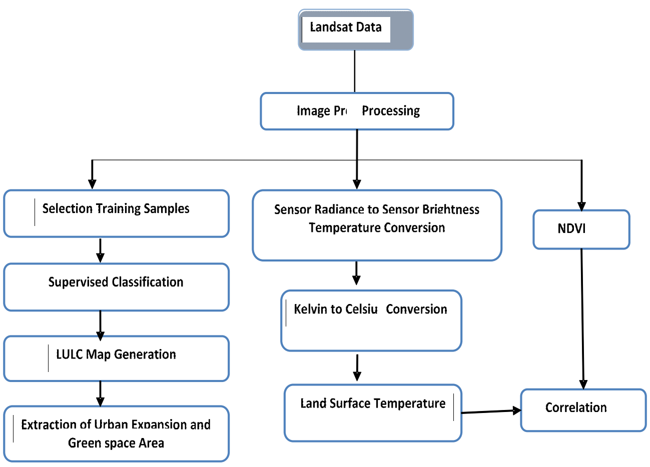

Fig. 2: Methodological approach used in this study

2.4. Derivation of Land Surface Temperature

The Landsat 5(TM) band 6 and Landsat 8 (OLI) band 10 were used to retrieve Land surface temperature.

LST estimation for Landsat 5:

For the mapping of land surface temperature from Landsat 5 data following steps were followed: (1) conversion of Digital number into the spectral radiance (2) converting the spectral radiance to temperature (Kelvin scale) image; and (3) converting the temperature in Kelvin to degree Celsius.

Step 1: Covert top of Atmospheric digital number to spectral radiance calculation formula for Landsat 5 data:

(1) $$L(\lambda) = Lmin(\lambda) + \frac{(Lmax(\lambda) - Lmin(\lambda))Qdn}{Qmax}$$

Where: L(λ) spectral radiance, Lmin (λ) minimum spectral radiance, L max (λ) maximum spectral radiance, Q dn= gray level of the TM image (DN= 0), Qmax=maximum numerical value of the TM image (Q max= 255) equation (1).

Step2: Conversion of spectral radiance to Temperature in Kelvin

(2) $$TB = K2/\{\left(\frac{K1}{L\lambda}\right) + 1\}$$

(Alhawiti & Mitsova et al., 2016) provides the formula to converts the spectral radiance to at satellite brightness temperature equation (2), where:

TB is the satellite brightness temperature in degree Kelvin; K1 and K2 are the pre-calibration constants of thermal band from the metadata file (Downloaded from USGS), the value of K1 = 607.76 and K2 = 1260.56 for Landsat 5 thermal band.

Step 3: Conversion of Kelvin to Celsius

$$TB = TB - 273 \quad (3)$$

LST estimation for Landsat 8:

For the mapping of land surface temperature from Landsat 8 data following steps were followed: (1) conversion of Digital number into the spectral radiance (2) converting the spectral radiance to temperature (Kelvin scale) image; and (3) NDVI Calculation (4) Emissivity Calculation (5) Derivation of LST.

The brightness temperature Tb is determined using radiative transfer equations, which estimate top of the atmosphere (TOA) radiances and use Planck's law to calculate blackbody temperatures equation (1).Landsat 8 has two thermal bands (band 10 and 11), but the only band 10 is used in the LST calculation due to uncertainty in the bands 11 .

Step 1: Covert top of Atmospheric digital number to spectral radiance calculation formula for Landsat 8 data:

(1) $$L(\lambda) = \mathrm{ML} * \mathrm{QCAL} + \mathrm{AL}$$

Where:

L (λ) = Top-of-Atmosphere (TOA) spectral radiance in W/(m2.sr.mm), ML = Band-specific multivariate rescaling factor from the metadata, AL = band-specific additive rescaling factor from the metadata, Qcali= Calibrated standard product pixel value (DN) Oi: i= Offset used for the calibration of Landsat 8 TIRS band.

Step 2: The next step was to convert the spectral radiance into brightness temperature.

The satellite brightness temperature TB in degree Kelvin; K1 and K2 are the pre-calibration constants of thermal band from the metadata file (Downloaded from USGS), the value of K1 = 774.8853 and K2 = 1321.0789 for Landsat 8, band 10 equation (2).

$$TB = \frac{K2}{\{\left(\frac{K1}{L1}\right)+1\}} - 273.15 \quad (2)$$

Step 3: NDVI calculation

Emissivity is calculated using the NDVI threshold approach, which used OLI bands 4 and 5.

The NDVI is a useful indication of vegetative stress, health, greenness, andbiomass. NDVI values ranged from - 1 to + 1 and positive values indicated vegetation, while negative values represented barren areas containing no vegetative cover equation (3).

The Normalized Difference Vegetation Index (NDVI) calculation formula:

$$\mathrm{NDVI} = (\mathrm{NIR} - \mathrm{RED}) / (\mathrm{NIR} + \mathrm{RED})$$

Step 4: Emissivity Calculation

In this study, for estimation of LST, we have used the method (Dar et al., 2019) that considered variance (m), alongside soil and vegetation emissivity (n), and the proportion of vegetation (PV) as calculated from equations (4),(5) and (6).Obtain the land surface emissivity (e) from equation (7).

$$m = (\varepsilon v - \epsilon s) - (1 - \epsilon s)F\varepsilon v \quad (4)$$

$$n = \epsilon s(1 - \epsilon s)F\varepsilon v \quad (5)$$

$$Pv = \left(\frac{NDVImin}{NDVImax} - NDVImin\right)^2 \quad (6)$$

$$\varepsilon = mPv + n \quad (7)$$

Where, $\in$ Sand εv are the soil and vegetation emissivity, F=0.55 (shape factor and it considering different geometric distribution ' We have considered m= 0.004 and n=0.986 these findings of ' .

Step 5: Derivation of LST

Finally, LST were calculated from Landsat 8 TIRS band 10 using equation (8), at satellite brightness temperature (TB) obtained from equation (3) and the corrected for surface emissivity (e) from equation (7)and in last temperature converted to degree Celsius (°C) equation (8).

$$\mathrm{LST} = \mathrm{TB} =/ \left(1 + (\lambda \mathrm{TB}/\rho)\ln \varepsilon\right) \quad (8)$$

Where (λ) wavelength of emitted radiance (λ=10.8 m) for band 10 of Landsat 8 (Dar et al., 2019).

$$\rho = h * c/\sigma(1.438 * 1010^{-2}\mathrm{mk})$$
$$\sigma = \text{Boltzmann constant } (1.38*10^{-23}\mathrm{J/K})$$
$$h = \text{Planck's constant } (6.625 * 10^{-34}\mathrm{Js})$$
$$c = \text{ velocity of light } (2.998 * 10^{8}\mathrm{m/s})$$
$$\varepsilon = \text{ land surface emissivity}$$

2.5. Statistical analysis and spatial analysis

Pearson's correlation coefficient was used to analyze the linear correlation between LST and NDVI. The correlation coefficient was used to measure the relationship. The statistical method depends on the properties of the variable or the scale of the variable. There is a medium to high relationship if the correlation coefficient value is 1 or close to 1. Conversely, if the value is close to 0, there is a medium-low relationship or no relationship. In addition, the positive or negative sign in mathematics indicates the direction of the relationship. The plus sign represents the value of the positive relationship and the minus sign represents the value of the negative relationship in equation (9).

$$r_{xy=}\sum_{i=1}^{n}\frac{(xi - x)(yi - y)}{\sqrt{\sum_{i=1}^{n}(xi - x)^2}\sqrt{\sum_{i=1}^{n}(yi - y)^2}} \quad (9)$$

The correlation analysis has been carried out to understand the relationship between of LST and NDVI. The scatter plots of LST and NDVI have been generated to draw the trend line and statistically analyses of the degree of effect and relationship, R^2 values were calculated.

3. RESULTS AND DISCUSSION

3.1. Land Use Land Cover changes in 2000, 2010 and 2020

The results show that Jalandhar city has experienced rising urbanizations from 2000 to 2020 (Fig. 3, 4, 5 and Table 1). The LULC classification shows a substantial change in the urban area. The total built-up area in 2000 was 73.38 km², it increased to 78.92 km² by 2010 and finally reached 87.21 km² in 2020. It was observed that from 2000 to 2020, the transition takes place in which a large quantity of fallow land and empty land was converted into an urban area and followed by plantation, cropland and vegetation. The amount of this conversion was high for the sites that contain green cover. The change of fallow land and empty regions to urban areas increased considerably.

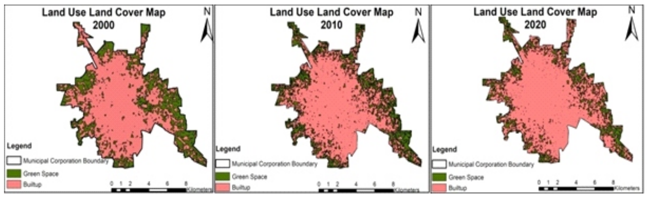

Fig.3 : LULC Maps of Jalandhar City during 2000, 2010 and 2020.

The results demonstrate that a significant area of 28.76 km² (2000), 20.35 km² (2010) and 14.40 km²of cropland have been converted to urban space. The change in land use/cover was mostly caused by over exploitation of land for built-up purposes and to raise real estate value.

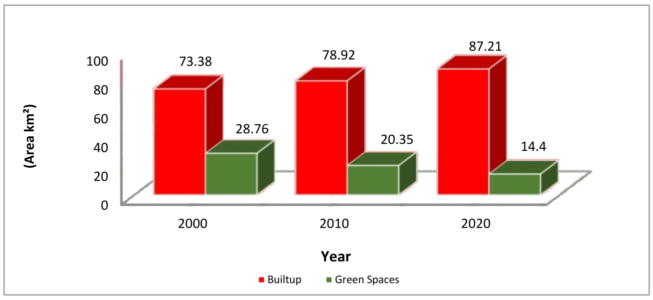

Fig. 4 : Area statistics analysis of urban expansion and urban green spaces.

Table 1: Urban growth and green spaces statistics of Jalandhar city during 2000 to 2020.

Year	Increase in Built-up area (km²)	Decrease in green spaces area (km²)
2000 -2010	5.54	8.41
2010- 2020	8.29	5.95

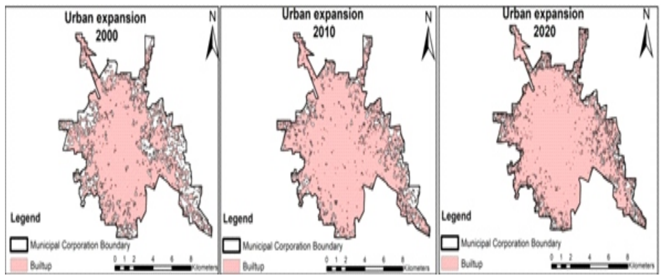

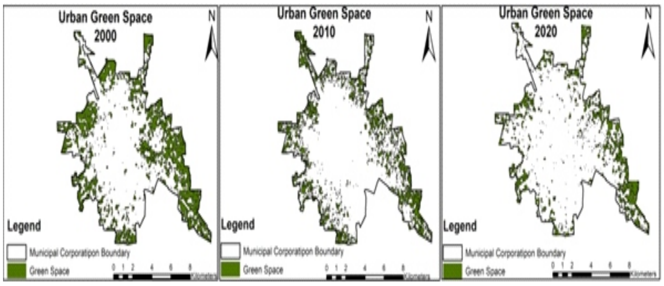

Fig. 5: Spatial temporal changes in urban expansion and urban green spaces during 2000, 2010 and 2020.

3.2. Spatial Pattern of Normalized Difference Vegetation Index

The NDVI have been broadly used to study the relationship between spectral variability and changes in vegetation growth rate. It is also effective for determining the development of green vegetation and detecting changes in green cover. For the respective years in NDVI most remarkable change was found. NDVI in Jalandhar city varies the range of NDVI values in 2000 from -0.14 to 0.51, in 2010 -0.11 to 0.49 and in 2020 image from -0.02 to 0.56 (Fig.6). The positive NDVI value shows the high green cover, while lower NDVI value shows the barren and urban areas. The green areas in Jalandhar are situated in the north and west direction of the city. The NDVI value was highest in the dense vegetation area of the outer edge. Furthermore, in 2000 and 2010, the NDVI values ranges are higher than 2020, which shows that the density of vegetation in Jalandhar has been more than in 2020.The NDVI is mostly negative in the urban area.

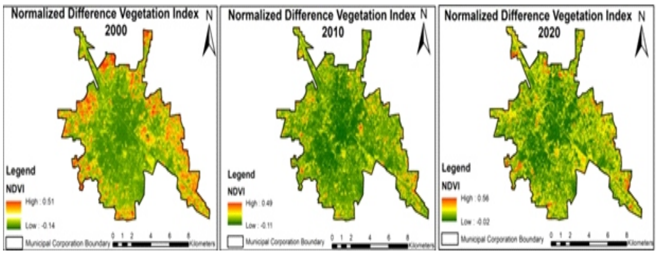

Fig.6 : Normalized difference vegetation index (NDVI) of Jalandhar City 2000, 2010 and 2020.

3.3. Spatial Pattern of Land Surface Temperature

The distribution of LST shows that the city has more temperature inside than its outskirts (Fig.7). The LST distribution in Jalandhar city depicts a change in the surface temperatures in time series. The temperature varies from of 36.05 °C (May) in the year 2000, followed by 42.96 °C (June) in 2010, and then, it was 49.39 °C (June) in 2020, whereas the minimum temperature was observed to be 20.64 °C in 2000, 30.42 ° in 2010 and 33.12 ° in 2020 and the average LST in the study area was 28.20°C, 37.82°C and 43.03°C in from 2000 to 2020 (Table 2).

Table 2: The statistical information of the land surface temperature.

Date	Minimum temperature	Average temperature	Maximum temperature
May 2000	21.64	28.20	34.52
June 2010	32.05	37.82	42.58
June 2020	33.73	43.03	48.25

The 30 years trend shows that LST is increasing which may cause of UHI effects. LST increases especially in the North and Northwestern part of the study area. This area consists of industrial center, center of economic and transportation. The distribution of LST can be influenced by the composition and structure of urban green spaces. The central part of the city consists of high-density residential area causing high surface temperature. The result showed that in 2000, 2010 and 2020 LST is increased.

Fig.7 : LST variation in Jalandhar City 2000, 2010 and 2020.

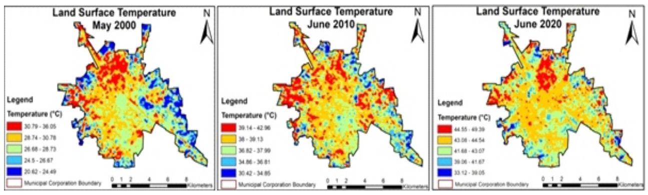

3.4. Correlation between Land Surface Temperature and Urban Green Spaces

The mean LST and NDVI shown negative correlation (Fig.8) respectively. The scatter plots shows higher surface temperature, where value of NDVI was low. The low value of NDVI was associated with the dense urban areas containing very low vegetation cover available. High value of NDVI shows high vegetative cover and these areas shows low surface temperature.

Fig.8: Correlation between LST and NDVI during 2000, 2010 and 2020.

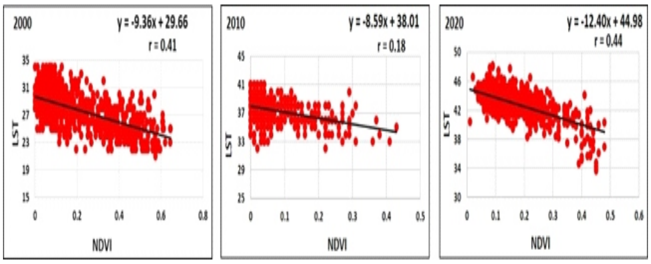

CONCLUSION

This study provides an analysis of LST in Jalandhar City using Landsat 5 TM and Landsat 8 OLI data from 2000 to 2020. The relationship between built-up area and Urban Green Space was studied, and their impact on Land Surface temperature was analyzed. The results clearly indicate that the Land surface temperature rises as the percentage of built-up land increases. The green cover in the city negatively impacts the Land surface temperature. The study suggested that the sustainable development of a city requires an adequate green surface, which helps to dissipate the solar energy into the environment and helps the urban areas reduce the temperature gradient. For the already developed regions, the use of trace gardening and a green roof will help to reduce the effect of the urban heat island. This study demonstrates that green spaces are essential for the urban environment to reduce negative impacts of urban sprawl.

ACKNOWLEDGEMENT

We gratefully acknowledge the United States Geological Survey Earth Explorer (USGS) and National Aeronautics and Space Administration (NASA) for providing open access Landsat data.

DECLARATION OF CONFLICTING INTERESTS

The authors declared no potential conflicts of interest with respect to the research, authorship and publication of this article.

REFERENCES

1. **Adam, G., Hermawan, R., Prasetyo, L. B., Rosli, A. Z., Reba, N. M., Roslan, N., & Room, M. H. M.** (2014). IOP Conference Series: Earth and Environmental Science Sustainable Urban Forestry Potential Based Quantitative And Qualitative Measurement Using Geospatial Technique You may also like Use of Geographical Information System (GIS) and remote sensing in development of urban forest types and shapes in Tangerang Selatan City Sustainable Urban Forestry Potential Based Quantitative And Qualitative Measurement Using Geospatial Technique. IOP Conf. Ser.: Earth Environ. Sci, 18, 12021. https://doi.org/10.1088/1755-1315/18/1/012021.
2. **Alhawiti, R.H. and Mitsova, D.** (2016). Using Landsat-8 Data to Explore the Correlation Between Urban Heat Island and Urban Land Uses. IJRET: International Journal of Research in Engineering and Technology, 5(3), pp.457-466.
3. **Beamish, A., Raynolds, M. K., Epstein, H., Frost, G. V., Macander, M. J., Bergstedt, H., Bartsch, A., Kruse, S., Miles, V., Tanis, C. M., Heim, B., Fuchs, M., Chabrillat, S., Shevtsova, I., Verdonen, M., & Wagner, J.** (2020). Recent Trends and Remaining Challenges for Optical Remote Sensing of Arctic Tundra Vegetation: A Review and Outlook. *Remote Sensing of Environment*, 246(March), 111872. https://doi.org/10.1016/j.rse.2020.111872.
4. **Bokaie, M., Zarkesh, M. K., Arasteh, P. D., & Hosseini, A.** (2016). Assessment of Urban Heat Island Based on the Relationship between Land Surface Temperature and Land Use/ Land Cover in Tehran. *Sustainable Cities and Society*, 23, 94–104. https://doi.org/10.1016/j.scs.2016.03.009.
5. **Dar, I., Qadir, J., & Shukla, A.** (2019). Estimation of LST from Multi-Sensor Thermal Remote Sensing Data and Evaluating the Influence of Sensor Characteristics. *Annals of GIS*, 25(3), 263–281. https://doi.org/10.1080/19475683.2019.1623318.
6. **Fuladlu, K., Riza, M., & Ilkan, M.** (2021). Monitoring Urban Sprawl Using Time-Series Data: Famagusta Region of Northern Cyprus. SAGE Open, 11(2). https://doi.org/10.1177/21582440211007465.
7. **Guan, K.** (2011). Surface and Ambient Air Temperatures Associated with Different Ground Material: A Case Study at the University of California, Berkeley. Surface and Air Temperatures of Ground Material, 14. http://nature.berkeley.edu/ classes/es196/projects/2011final/GuanK_2011.pdf.
8. **Guo, J., Ren, H., Zheng, Y., Lu, S., & Dong, J.** (2020). Evaluation of Land Surface Temperature Retrieval from Landsat 8/TIRS Images Before and After Stray Light Correction Using the SURFRAD dataset. *Remote Sensing*, 12(6). https://doi.org/10.3390/rs12061023.
9. **He, X., Wang, J., Feng, J., Yan, Z., Miao, S., Zhang, Y., & Xia, J.** (2020). Observational and Modeling Study of Interactions between Urban Heat Island and Heatwave in Beijing. *Journal of Cleaner Production*, 247, 119169. https://doi.org/10.1016/j.jclepro.2019.119169.
10. **Kaul, H. a, & Sopan, I.** (2012). Land Use Land Cover Classification and Change Detection Using High Resolution Temporal Satellite Data. *Journal of Environment*, 01(04), 146–152.
11. **Khamchiangta, D., & Dhakal, S.** (2020). Time Series Analysis of Land Use and Land Cover Changes Related to Urban Heat Island Intensity: Case of Bangkok Metropolitan Area in Thailand. *Journal of Urban Management*, 9(4), 383–395. https://doi.org/10.1016/j.jum.2020.09.001.

12. **Kumar, R., Mishra, V., Buzan, J., Kumar, R., Shindell, D., & Huber, M.** (2017). Dominant control of Agriculture and Irrigation on Urban Heat Island in India. Scientific Reports, 7(1), 1–10. https://doi.org/10.1038/s41598-017-14213-2.

14. **Kurihara, Y., Murakami, H., Ogata, K., & Kachi, M.** (2021). A Quasi-physical Sea Surface Temperature Method for the Split-window Data from the Second-Generation Global Imager (SGLI) Onboard the Global Change Observation Mission-Climate (GCOM-C) Satellite. Remote Sensing of Environment, 257(January), 112347. https://doi.org/ 10.1016/ j.rse.2021.112347.

15. **Piyoosh, A. K., & Ghosh, S. K.** (2022). Analysis of Land Use Land Cover Change using a New and Existing Spectral Indices and its Impact on Normalized Land Surface Temperature. Geocarto International, 37(8), 2137–2159. https://doi.org/10.1080/ 10106049. 2020.1815863.

16. **Rahman, M. H., Islam, M. H., & Neema, M. N.** (2022). GIS-based Compactness Measurement of Urban form at Neighborhood Scale: The Case of Dhaka, Bangladesh. *Journal of Urban Management*, 11(1), 6–22. https://doi.org/10.1016/j.jum.2021.08.005.

17. **Ryu, Y. H., & Baik, J. J.** (2012). Quantitative Analysis of Factors Contributing to Urban Heat Island Intensity. *Journal of Applied Meteorology and Climatology*, 51(5), 842–854. https://doi.org/10.1175/JAMC-D-11-098.1.

18. **Salathé, E. P., Leung, L. R., Qian, Y., & Zhang, Y.** (2010). Regional Climate Model Projections for the State of Washington. *Climatic Change*, 102(1–2), 51–75. https://doi.org/10.1007/s10584-010-9849-y.

19. **Shahtahmassebi, A. R., Li, C., Fan, Y., Wu, Y., Lin, Y., Gan, M., Wang, K., Malik, A., & Blackburn, G. A.** (2021). Remote Sensing of Urban Green Spaces: A Review. *Urban Forestry & Urban Greening*, 57, 126946. https://doi.org/10.1016/j.ufug.2020.126946.

20. **Sholihah, R. I., & Shibata, S.** (2019). Retrieving Spatial Variation of Land Surface Temperature Based on Landsat OLI/TIRS: A Case of Southern Part of Jember, Java, Indonesia. IOP Conference Series: Earth and Environmental Science, 362(1). https://doi.org/ 10.1088/1755-1315/362/1/012125.

21. **Singh, H., Suryawanshi, S., & Planner, U.** (2019). Directional Change Detection of Urban Sprawling in Jalandhar City. *Global Journal of Engineering Science and Researches*., 6(May), 481–504.

22. **Singh, R., & Kalota, D.** (2019). Urban Sprawl and Its Impact on Generation of Urban Heat Island: A Case Study of Ludhiana City. *Journal of the Indian Society of Remote Sensing*, 47(9), 1567–1576. https://doi.org/ 10.1007/s12524-019-00994-8.

23. **Sun, L., Chen, J., Li, Q., & Huang, D.** (2020). Dramatic Uneven Urbanization of Large Cities Throughout the World in Recent Decades. *Nature Communications*, 11(1). https://doi.org/10.1038/s41467-020-19158-1.

24. **Sun, X., Liu, Y., Sun, T., Yu, S., Li, C., & Zhai, L.** (2021). Land Cover Changes and Urban Expansion in Chongqing, China: A Study Based on Remote Sensing Images. *Environment and Urbanization ASIA*, 12(1_suppl), S39–S58. https://doi.org/ 10.1177/0975425321998035.

25. **Talukdar, S., Singha, P., Mahato, S., Shahfahad, Pal, S., Liou, Y.-A., & Rahman, A.** (2020). Land-Use Land-Cover Classification by Machine Learning Classifiers for Satellite Observations—A Review. Remote Sensing, 12(7), 1135. https://doi.org/10.3390/rs12071135.

26. **Vinayak, B., Lee, H. S., Gedam, S., & Latha, R.** (2022). Impacts of Future Urbanization on Urban Microclimate and Thermal Comfort Over the Mumbai Metropolitan Region, India. *Sustainable Cities and Society*, 79(April 2021), 103703. https://doi.org/ 10.1016/j.scs.2022.103703.

27. **Vivekananda, G. N., Swathi, R., & Sujith, A. V. L. N.** (2021). Multi-Temporal Image Analysis for LULC Classification and Change Detection. *European Journal of Remote Sensing*, 54(sup2), 189–199. https://doi.org/10.1080/22797254.2020.1771215.

28. **Wamukoya, M., Kadengye, D. T., Iddi, S., & Chikozho, C.** (2020). The Nairobi Urban Health and Demographic Surveillance of Slum Dwellers, 2002–2019: Value, Processes, and Challenges. *Global Epidemiology*, 2, 100024. https://doi.org/ 10.1016/j.gloepi.2020.100024.

29. **Wang, J., Huang, B., Fu, D., Atkinson, P. M., & Zhang, X.** (2016). Response of Urban Heat Island to Future Urban Expansion Over the Beijing-Tianjin-Hebei Metropolitan Area. *Applied Geography*, 70, 26–36. https://doi.org/10.1016/j.apgeog.2016.02.010.

30. **Zhang, X. Q.** (2016). The Trends, Promises and Challenges of Urbanisation in the World. *Habitat International*, 54, 241–252. https://doi.org/ 10.1016/J.HABITATINT.2015.11.018.

Abbrevation Used

1. LST: Land Surface Temperature
2. TOA: Top of the Atmosphere
3. TB: Brightness Temperature
4. NDVI: Normalized Difference Vegetation Index
5. OLI: Operational Land Imager
6. PV: Proportion of Vegetation

7. UGS: Urban Green Space
8. UHI: Urban Heat Island
9. TIR: Thermal Infrared Band
10. USGS: United States Geological Survey
11. LULC: Land Use Land Cover
12. TM: Thematic Mapper

www.nesa-india.org • E-mail: nesapublications@gmail.com
International Journal on Environmental Sciences

International Journal on Environmental Sciences 13 (2) Pp. 107-113, ***July-December 2022***
ISSN No.: 0976-4534
https://doi.org/10.53390/ijes.v13i2.7

DIVERSITY OF FUNGI FROM DIFFERENT TYPES OF VEGETABLES IN THE MUMBAI METROPOLITAN REGION

Rafi Ahmed* and Afiya Shaikh

Department of Botany
Maharashtra College of Arts, Science & Commerce, Mumbai (M.S.), India.

Research Article

Received: **20.09.2022** Accepted: **29.09.2022** Published: **12.10.2022**

ABSTRACT

The present study was performed at exceptional markets in Mumbai for isolation, characterization and identity of fungi inflicting the degradation and deterioration of vegetable like Potato *(Solanum tuberosum*), Onion *(Allium cepa*), Eggplant (*Solanum melanogenic*), Cabbage (*Brassica oleracea*), Cucumber (*Cucumis sativus* L.), Tomato (*Solanum lycopersicum*), Pea (*Pisum sativum*), Lemon (*Citrus limon*), Capsicum (*Capsicum annum*), Spinach (*Spinacia oleracea* L.), Cauliflower (*Brassica oleracea*), Garlic (*Allium sativum*) and Carrot (*Daucus carota*) had been selected from 4 markets in Mumbai. Both healthful and diseased samples were gathered. Eleven fungal species: *Fusarium oxysporium*, *Aspergillus niger*, *Penicillium* sp*, Alternaria* sp*, Aspergillus flavus, Colletotrichum* sp*, Aspergillus fumigatus, Rhizopus stolonifer, Sclerotinia sclerotiorum*, *Cladosporium* sp. and *Geotrichum candidum* had been isolated at the duration of the research.

Keywords: Degradation, Vegetables, Deterioration, Fungi.

INTRODUCTION

Vegetable products have dramatically increased in India by more than 40% during the past few decades. About 30% of all vegetables are lost due to spoilage (Elufer, 2019). Vegetables are vital sources of nutrients for human beings. They are the fresh and edible portions of herbaceous plants. They are essential food, highly beneficial for maintaining health and are valued mainly for their high carbohydrate, vitamin and mineral contents (Nareen *et al*., 2017). Associated with disease prevention by improvement of good vision and gastrointestinal health and decrease the risk of chronic and degenerative diseases like diabetes, certain cancers, cardiovascular diseases, rheumatoid arthritis and obesity (João, 2012) are of the utmost importance.

Fungi play a substantial role in the spoilage of vegetables because of their pathogenicity to the harvested products. However, during the various stages of pathogenesis, most of these fungi may generate different mycotoxins, which can be harmful to humans and animals that consume them. In recent decades, various vegetables that form part of our daily diet have been added to the list of products exposed to mycotoxin contamination (Hero *et al.*, 2017). The contamination of vegetables by fungi could also be a result of poor handling of vegetable supply, Storage conditions, distribution, marketing practices and Transportation (Elufer, 2019). Fungi are increasingly implicated as the agent of spoilage of economically essential vegetables such as *Alternaria, Aspergillus, Fusarium, Mucor*, *Penicillium, Rhizopus* and *Trichoderma species*. (Nareen *et al.,* 2017). The dumped plant material and debris present in market places acts reservoirs of the plant pathogen and for the growth of different fungi, which carries biodegradation and deterioration due to the presence of nutrients like carbon and nitrogen etc. (Umesh *et al.*, 2012)

It has been an increase in the need to isolate the pathogenic fungi associated with the spoilage of vegetables. Due to which

*Corresponding author: *rafiahmed12@rediffmail.com*

food becomes less palatable or even toxic, these changes may be accompanied by taste, smell, appearance or texture alternations (Benita B.R. *et. al.*, 2019). Therefore, this study was undertaken to isolate fungi associated with spoilt vegetables commonly sold in the Mumbai market. No systematic studies have been published on the incidence of plant pathogenic fungi from vegetables in the Mumbai market. However, such information is needed to evaluate diseases of vegetables due to pathogenic fungi, which can cause health effects. Hence, the present study was undertaken in four major vegetable markets in Mumbai city to investigate and isolate other pathogenic fungi from vegetables.

The selected vegetables in this paper are, Potato (*Solanum tuberosum*) belongs to the family Solanaceae, is the most commonly cultivated tuber and The fourth most important tuber crop, after wheat, rice and maize (Reddy *et al.*, 2018). India is the fourth biggest producer in Asia as well as Onion has been one of the necessary cash crops grown in India during the last 5000 years and throughout the tropical and sub-tropical countries of the world (Vaijayanthi *et al.*, 2019). Brinjal (*Solanum melongena L*), it is a non-tuberous vegetable crop from the *Solanaceae* family. It is a low-calorie vegetable, a great source of protein, vitamins, fibre, minerals, and antioxidants and contains anticancerous compounds (Damini *et al.*, 2021). Cauliflower (*Brassica oleracea variety botrytis*) is a vegetable that belongs to the family of *Cruciferous* and is characterized by its broad leaves and fleshy stem. They have compounds called isothiocyanates, which activate enzymes (substances that speed up chemical reactions) that reduce the activity of carcinogens (substances that promote the mutation of cells) (Supriya *et al.*, 2017). Also, Cabbage (*Brassica oleracea)* belongs to the same Genus and is an excellent source of vitamin C. In addition, it contains some B vitamins, and cabbage supplies potassium and calcium to the diet (Astrit, 2014). Carrot (*Daucus Carota L.*) is an important crop that refers to the Umbelliferae family. They are a great source of nutritional fibre and whit mineral molybdenum which are rarely found in many vegetables. It is a rich source of magnesium and manganese, which are needed for bone and protein, activating vitamin B, creating new cells, ergonomic muscles, nerves, and energy production (Moayad, 2018). The cucumber (*Cucumis sativus L.*) is one of the most essential vegetables which belong to the *cucurbit* family and has great economic importance.

Cucumbers are high in vitamins A, B, and C and contain almost (96%) water, (3%) carbohydrates, and (1%) protein, as well as minerals like manganese, copper, iron, calcium, and potassium (Ali et al., 2020). Tomato (Solanum lycopersicum) belongs to the family Solanaceae. Tomato is a widely grown and versatile vegetable worldwide for taste, colour, high nutritive value, and diversified use (Varinder et al., 2017) are rich in vitamins, minerals and lycopene, an excellent antioxidant (Khatoon et al., 2016). Pea (Pisum sativum L.) comes under Leguminoceae family. The second largest producer of green peas is India which ranks in the 10th position among vegetable crops (Junghare et al., 2014). It also has an important ecological advantage for its contributions to developing low-input farming systems by fixing atmospheric nitrogen (Mahmoud et al., 2018). Lemon (Citrus limon) belongs to the family Rutaceae. High juice contents, nutritional values and distinct taste have made the Citrus fruit unique among all other fruits with a great source of vitamin C (Anam et al., 2014). In high quantities, they contain essential natural compounds containing ascorbic acid, citric acid, minerals, essential oils, and flavonoids. Lemon shows antibacterial and anticancer activity due to alkaloid constituents in different parts of the lemon (Yahaya et al., 2016).

The *Capsicum* genus, which also includes more than 30 species of flowering pepper plants, belongs to one of the essential families known as Solanaceae. They are rich in fibre, capsicum is also rich in micronutrients and is hugely beneficial to body functions, and Bell peppers are rich in vitamin C, and they help in many functions like wound healing, immune function and collagen synthesis. With vitamin C, *capsicum* it is also high in vitamin A. Vitamin A is necessary for the immune system and reproductio*n.* Cabbage (*Brassica oleracea*) is an excellent and rich source of vitamin C. In addition, it contains some B vitamins, and cabbage supplies potassium and calcium to the diet. (Astrit, 2014). Spinach (*Spinacia oleracea* L.), family Chenopodiaceae, is native to central and south western Asia. They are a source of vitamins A, B2, B6, B9, C, E and K. Spinach and other green leafy vegetables are huge sources of iron. Spinach also has high calcium content (Marraiki *et al.*, 2012).

Garlic is a crop of great importance worldwide and is more valued for its culinary and medicinal properties. Secondary metabolites have been shown to positively affect health and prevent many common human diseases, particularly through their antioxidant, anti-inflammatory, and lipid-lowering effects (Laura *et al*., 2021). Diversity of flora and fauna indicate a good ecosystem. Biodiversity is important for ecological balance, sustainable development and human survival (Ashok, 2017, 2018; Verma, 2019), however climate change and anthropogenic activities badly influence the biodiversity (Verma, 2021; Prakash and Verma, 2022). In the present exploration, diversity of fungi from different types of vegetables in the Mumbai metropolitan region is taken into consideration.

MATERIAL AND METHODS

Survey and Sample Collection : Four markets in Mumbai region Maharashtra state: Byculla, Kurla, Thane and Mumbra markets were surveyed with diseased and healthy vegetables of Potato (*Solanum tuberosum*), Onion (*Allium cepa*), Eggplant (*Solanum melanogenic)*, Cabbage (*Brassica oleracea*), Cucumber (*Cucumis sativus* L.), Tomato (*Solanum lycopersicum*), Pea (*Pisum sativum*), Lemon (*Citrus limon*),

Fig: Map Mumbai showing different markets.

Sr. No.	Market	CO-ORDINATE
1	BYCULLA	18.9750° N, 72.8295° E
2	KURLA	19.0726° N, 72.8845° E
3	THANE	19.2183° N, 72.9781° E
4	MUMBRA	19.1761° N, 73.0229° E

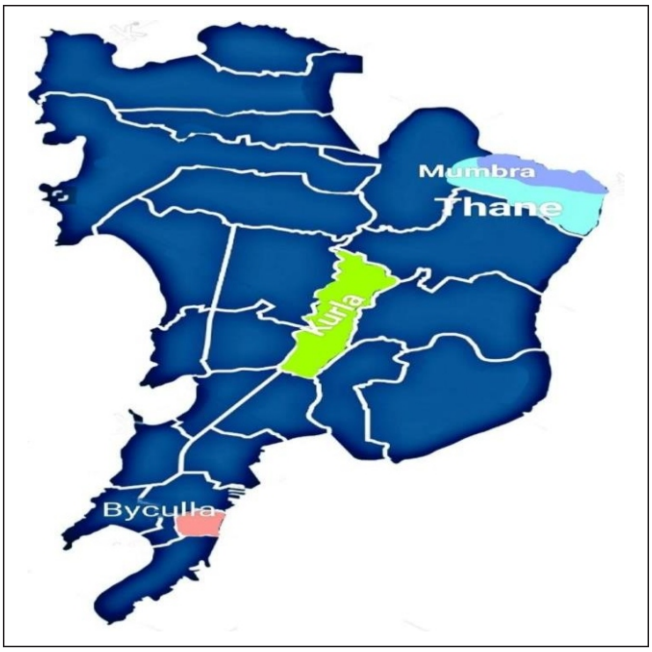

Isolation and Identification of Fungi

The infected parts were put in 6% of sodium hypochlorite solution for 1-2 minutes, rinsed twice in sterilized water to remove the toxic material, and then the pieces were transferred by using forceps to a Petri dish containing solidified potato dextrose agar containing streptomycin to prevent the growth of bacteria, was conducted in laminar flow, then incubates for 5-7 days at 25ºC±2. After seven days of incubation, a small portion of mycelium from each fungal colony is transferred aseptically into fresh plates containing the medium. Purification of fungi is done by repeated sub-culturing. Identification of fungi was carried out by doing pure culture of the isolated fungi using a Microscope and studying different characteristics of fungi according to their shape, size, colours, and mycelia textures of the fungi and making reference to standard literature (Ainsworth, et al., 1972; Barnett, 1960; Ellis,1971; Ingold,1974; Gilman,1957; Smith, 1969), The percentage frequency was calculated by the following formula:

$$\text{Percentage frequency} = \frac{\text{Total number of observations}}{\text{Number of observations in which a species appeared}} \times 100$$

Table 1: Percentage Frequency of Fungal Isolate from Different locations.

Location	Vegetable sample	Isolated fungal species	Percentage Frequency (%)
Byculla	Potato (*Solanum tuberosum*)	*Fusarium oxysporium* *Aspergillus niger*	70% 90%
	Onion (*Allium cepa*)	*Aspergillus niger* *Penicillium* sp.	80% 35%
	Egg plant (Solanum melanogenic)	*Alternaria* sp. *Aspergillus flavus* *Colletotrichum* sp.	50% 60% 45%
	Cabbage (*Brassica oleracea*)	*Aspergillus niger* *Alternaria* sp.	70% 60%
Kurla	Cucumber (*Cucumis sativus* L.)	*Fusarium* sp. *Aspergillus fumigatus*	75% 55%

	Tomato (*Solanum lycopersicum*)	*Fusarium oxysporium* *Alternaria alternata* *Rhizopus stolonifer*	65% 50% 30%
	Potato (*Solanum tuberosum*)	*Aspergillus niger* *Fusarium* sp.	65% 70%
	Pea (*Pisum sativum*)	*Sclerotinia sclerotiorum*	45%
Thane	Lemon (*Citrus limon*)	*Alternaria* spp. *Aspergillus niger*	50% 80%
	Capsicum (*Capsicum annum*)	Aspergillus niger *Fusarium solani* Alternaria sp.	85% 70%
	Spinach (*Spinacia oleracea* L.)	*Fusarium* sp. *Cladosporium* sp.	55% 35%
	Cauliflower (*Brassica oleracea*)	*Aspergillus* spp. *Alternaria* sp.	60% 55%
Mumbra	Cauliflower (*Brassica oleracea* var. botrytis)	*Aspergillus flavus* *Alternaria alternata*	75% 60%
	Tomato (*Solanum lycopersicum*)	*Fusarium oxysporum* *Alternaria* sp. *Aspergillus flavus*	65% 50% 60%
	Garlic (*Allium sativum*)	*Aspergillus niger* *Fusarium* spp. *Alternaria* sp.	80% 65% 55%
	Carrot (*Daucus carota*)	Geotrichum candidum *Fusarium* sp. *Alternaria* sp.	40% 65% 30%

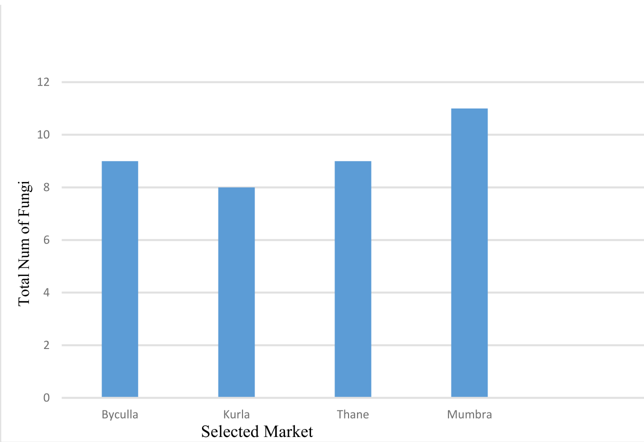

Fig: 1 Total number of Fungal species associated with Vegetable samples collected from four different markets

Potato (*Solanum tuberosum*)

Egg plant (*Solanum melongena*)

Fig. 1: Collection of infected vegetables from markets of Mumbai.

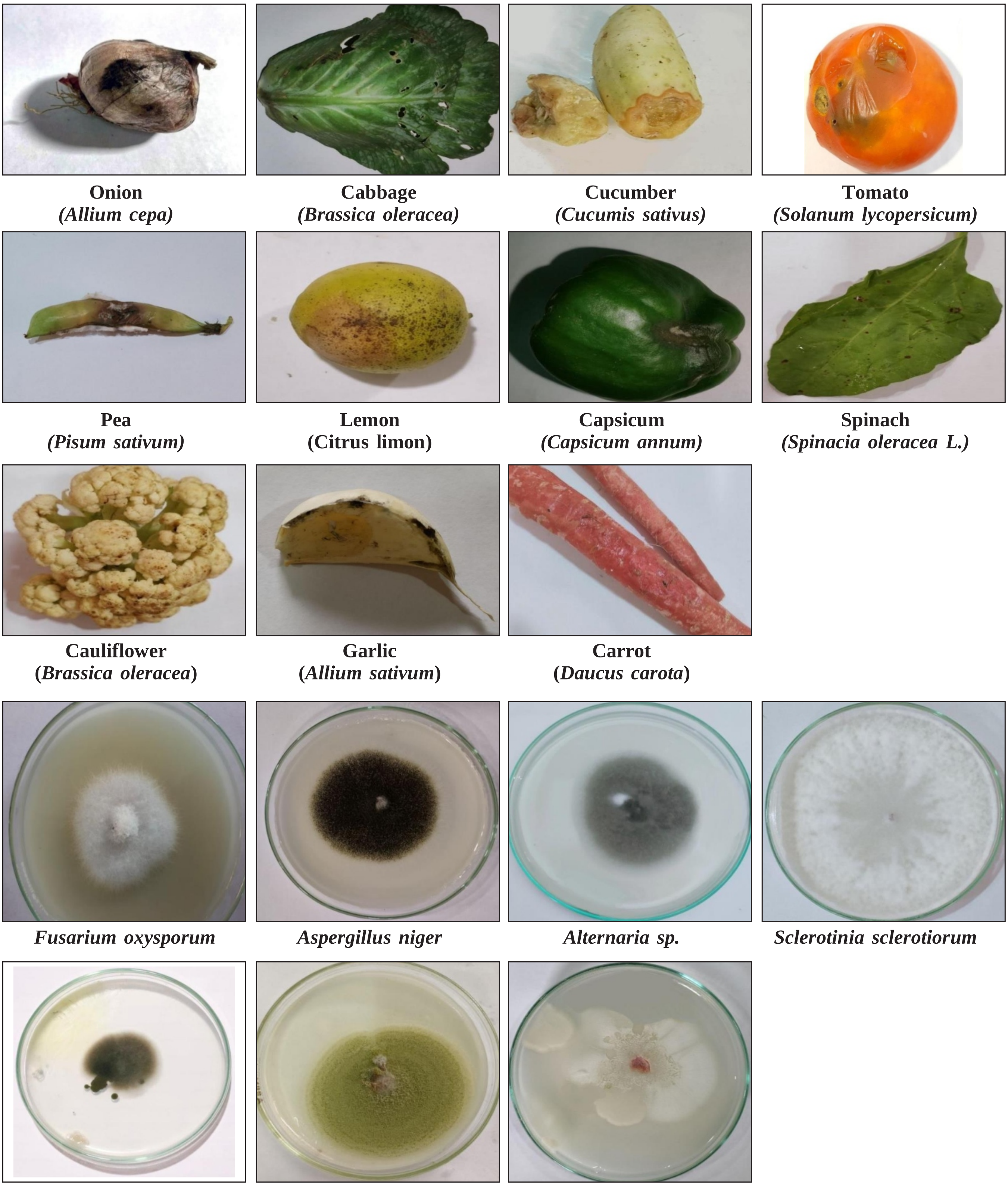

Figure 2: Growth of different species fungal culture on PDA.

RESULT AND DISCUSSION

Fungi were isolated from vegetables, namely Potato *(Solanum tuberosum)*, Onion *(Allium cepa)*, Eggplant *(Solanum melanogenic*), Cabbage *(Brassica oleracea*), Cucumber (*Cucumis sativus L.)*, Tomato *(Solanum lycopersicum*), Pea (*Pisum sativum*), Lemon (*Citrus limon*), Capsicum (*Capsicum annum*), Spinach (*Spinacia oleracea L*.), Cauliflower (*Brassica oleracea*), Garlic (*Allium sativum)* and Carrot (*Daucus carota*) which were collected from Four different markets of Mumbai, i.e. Byculla, Kurla, Thane & Mumbra markets. The occurrence and distribution of fungi are present in Table 1 and Fig-1. All total fungi were isolated. *Aspergillus niger, Aspergillus flavus, Fusarium oxysporum* and *Alternaria* sp. were predominant in all four markets of the Mumbai region. The common fungi found are opportunistic and grow on rotten vegetables, thrown away material and produce spores enormously. The present study revealed that the vegetables marketed in the different markets of Mumbai are contaminated by several fungal pathogens and opportunistic Fungi. The market values of vegetables are reduced as a result of pathogen infection. Their presence in these food products also constitutes health risks.

ACKNOWLEDGEMENT

Gratefully Acknowledge a deep gratitude to Dr. Sirajuddin Chougle principal Maharashtra College of Arts, Science & Commerce Mumbai, for providing necessary facilities and encouragement.

REFERENCES

1. **Ainsworth, G. C., Sparrow, F.K., Sussman, A.S**. (1973)., The Fungi. An Advanced Treatise. Vol:(4) B: A Taxonomic Review with Keys: Basidiomycetes and Lower Fungi. XXII, 504 S., 85 Abb. 1 Tafel. New York—London 1973: Academic Press.
2. **Barnett, H. I**. (1960)., Illustrated Genera of Imperfect Fungi. Burgess Publishing Co. Minneapolis.
3. **Ellis, M. B.** (1971)., Dematiaceous hyphomycetes. Publisher Common wealth Agricultural Bureaux. Common wealth Mycological Institute. Kew, Surrey (Uk).
4. **Ingold, C. T.** (1974)., Fungus Spores: Their Liberation and Dispersal. Publisher: Clarendon Press, Oxford.
5. **Gilman, J. C.** (1957)., "A manual of soil fungi" (II Ed.) The Iowa State Univ. Press. Ames, Iowa, 450.
6. **Smith, G**. (1969)., An Introduction to Industrial Mycology. Edward Arnold Ltd, London.
7. **Narin Q. F. A. and Shrihan R. M**. (2016)., Isolation and Identification of Fungi from different Types of Vegetables. In Erbil Local Market. *ZANCO Journal of Pure and Applied Sciences*. Vol:28(6), pp.81-89.
8. **João S. D**. (2012)., Nutritional Quality and Effect on Disease Prevention of Vegetables Food and Nutrition Sciences. (10) 369-402.
9. **Elufer A**. (2019)., Isolation, Identification and characterization of Fungi from stored vegetables.
10. **Hero F., Ghafur, S. R. and Narin Q**. (2017)., Isolation and Identification of Fungi from Different Types of Vegetables In Erbil Local Market. ZANCO Journal of Pure and Applied Sciences. Vol:28 (6) pp.81-89.
11. **Umesh B k and Hemalata U. k.** (2012)., Seasonal variation of fungal propagules in a fruit market environment, Nagpur (India). Acta Bot. Croat. 71 (1), 147–157.
12. **Benita B.R and Umesh B. K** (2019). Post-harvest fungi associated with *Solanum lycopersicum* (Tomato) fruits collected from different markets of Mumbai. *Online International Interdisciplinary Research Journal*, {Bi-Monthly}, ISSN 2249-9598, Volume:09 (1).
13. **Khatoon A, Mohapatra A, Satapathy K.B.** (2016). Studies on Fungi Associated with Storage Rot of Carrot (*Daucus carota* L.) and Radish (Raphanussativas L.) in Odisha.
14. https://www.semanticscholar.org/paper/Studies-on-Fungi-Associated-with-Storage-Rot-of-%28-L-Akhtari-Ashirbad/531a513813ba36f 248d54d7 e5657c54f23bf7cb9.
14. **Junghare A., Nasare P. N. and Mousmi B**. (2014)., Fungal Diversity in Vegetables, *Int. J. of Life Sciences*, Special Issue A2:25.
15. **Yahaya S. M., Fagwalawa L. D., Ali M. U., Lawan M. and Mahmud S**. (2016)., On Identification of Pathogenic Fungi Causing Deterioration of Lettuce Plant *(Lactuca sativa)* A Case Study of Yankaba and Sharada Vegetables Markets.J Plant Sci Res. 3(1): 141.
16. **Reddy B. J., Mandal R., Chakroborty M., Hijam L., and Dutta P.** A review on Potato (*Solanum tuberosum L*.) and its genetic diversity. International Journal of Genetics, ISSN: 0975- 2862.
17. **Vaijayanthiand R., Vijayakumar** (2019)., Isolation and identification of fungal pathogens from onion crop cultivatedinPerambalur District, South India.J. Sci. Trans. Environ. Technov. 12(3).
18. **Damini M. and Anita S**. (2021)., Identification of fungal pathogens associated with fruit rot of Solanum melongena L. in Pantnagar (Uttarakhand). Pharma Innovation 10(7):05-09.

18. **Astrit B., (2014)**., Cabbage. Handbook of Vegetables Vol:(3)

19. **Anam R., Iram Z., Shazia I**., (2014)., Isolation and Characterization of Post-Harvest Fungal Pathogens of Citrus Varieties From The Domestic Markets of Rawalpindi And Islamabad. *International Journal of Scientific & Engineering Research*, Volume:5(10) ISSN 2229-5518.

20. **Supriya K., Vijay R., Pramod R., Rubina L., and Harison M**., (2017)., Isolation and Characterization of Potassium and Phosphorus Solubilising Bacteria and Fungus (KSB, PSB, KSF, PSF) and its Effect on Cauliflower. *Int.J.Curr.Microbiol.App.Sci.* 6(4): 987-1006.

21. **Moayad S. H**., (2018)., Survey of the Fungi that Infect Imported Carrot (*Daucus Carota L.*) in the Areas of Baghdad. Al-Mustansiriyah Journal of Science 29(4):38.

22. **Mahmoud A. A., Youssef, A. Z., Aly, M. R. A., Tohamy and M. I. Ghonim** (2018)., Studies on Fungi associated with Pea seeds and their effect on germination and some seed characters. Zagazig Journal of Agricultural Research 45(4):1291-1308.

23. **Ali A. A., and Hurria Al-Juboory**., (2020)., Isolation of the Fungus *fusarium solani* causing cucumber root rot disease and it's Morphological and molecular identification. *Int. J. Agricult. Stat. Sci.* Vol:16 (1). pp. 1959-1966.

24. **Marraiki, I., Siddiqui, H., Rizwanaand A., Javaid** (2012)., First report of *Alternaria Alternata* leaf spots on spinach in Saudi Arabian. *The Journal of Animal & Plant Sciences*.22(1).

25. **Laura G., and Daniel P**., (2021)., Incidence and Etiology of Postharvest Fungal Diseases Associated with Bulb Rot in Garlic (*Alllium sativum*) in Spain. Foods :Multidisciplinary Digital Publishing Institute (MDPI)..